International Journal of Photoenergy

Photobiomodulation 2014

Guest Editors: Timon Cheng-Yi Liu, Quan-Guang Zhang, and Lutz Wilden

Photobiomodulation 2014

International Journal of Photoenergy

Photobiomodulation 2014

Guest Editors: Timon Cheng-Yi Liu, Quan-Guang Zhang, and Lutz Wilden

Editorial Board

Contents

Hindawi Publishing Corporation
International Journal of Photoenergy
Volume 2014, Article ID 520501, 2 pages
http://dx.doi.org/10.1155/2014/520501

Editorial
Photobiomodulation 2014

Timon Cheng-Yi Liu,[1] Quan-Guang Zhang,[2] and Lutz Wilden[3]

[1] *Laboratory of Laser Sports Medicine, South China Normal University, Guangzhou 510006, China*
[2] *Institute of Molecular Medicine and Genetics, Medical College of Georgia, Georgia Regents University, Augusta, GA 30912, USA*
[3] *Privatpraxis für Hochdosierte Low Level Lasertherapie, Wilden, L. Kuralle 16, 94072 Bad Füssing, Germany*

Correspondence should be addressed to Timon Cheng-Yi Liu; liutcy@scnu.edu.cn

Received 30 September 2014; Accepted 30 September 2014; Published 9 November 2014

It is our great pleasure to present this special issue of this journal. The stories of photobiomodulation (PBM) of a low level laser irradiation or monochromatic light (LLL) continued in this issue since its first annual issue published in 2012. We have selected eleven papers: two review papers making progress in understanding PBM mechanism, four original papers about cellular PBM, one original paper about clinical PBM, three original papers about photodynamic therapy, and one original paper about visual imagine operation of athletes. These eleven articles offered advancements in both understanding and optimizing potential new technologies.

Among these eleven articles, the cross-talking between the negative feedback and functions is very interesting. As T. C.-Y. Liu et al. have pointed out, there is a function-specific homeostasis (FSH), a negative feedback mechanism for a function to be perfectly performed. A function can be finely classified into a normal function in its FSH and a dysfunctional function far from its FSH. A PBM can be then finely classified into a direct PBM (dPBM) to modulate a dysfunctional function and an indirect PBM (iPBM) to upgrade a normal function. With its negative feedback mechanism, a normal function can resist external disturbance under its threshold so that it resists a dPBM. Far from its negative feedback mechanism, a dysfunctional function is sensitive to its external disturbance so that a LLL may self-adaptively modulate it until it becomes a normal function in a dPBM way. A cell responds to an external signal with its intracellular signal transduction pathways. A cellular normal function not only can resist its external disturbance, but also can resist the activation of other signal transduction pathways to maintain the full activation of its specific signal transduction pathways (normal function-specific signal transduction pathways, NSPs) so that it does not respond to some external signals under their respective thresholds. However, almost all the signal transduction pathways are partially activated for a cellular dysfunctional function so that the cell can respond to any external signals. A normal function may have n NSPs which are called redundant pathways with one another, and the normal function maintained by the synergistic activation of n NSPs is called the nth-order normal function. In other words, the NSPs maintaining a normal function are very sparse, but the signal transduction pathways maintaining a dysfunctional function are extraordinarily dense. The activation of each signal transduction pathway needs adenosine-5′-triphosphate (ATP). This is why the ATP level of a cell with its dysfunctional function is lower than the one of the same cell with a normal function. A cellular dPBM may promote the microenvironment-allowed activation of a partially activated NSP of a dysfunctional function until it is fully activated and then the normalization of the dysfunctional function so that it may also increase the ATP level. A cellular iPBM may promote the microenvironment-allowed activation of partially activated redundant NSPs of a normal function until they are fully activated so that the normal function is upgraded. Whether a cellular function is a normal or dysfunctional function and the activation of which partially activated NSPs is promoted by a PBM depend on the cellular microenvironment which then depends on the global action of an organism so that a microenvironment dependent cellular PBM is in agreement with an action-dependent global PBM.

C.-P. Zhang et al. have studied effects of a low intensity He-Ne laser irradiation on the proliferative potential and cell-cycle progression of myoblasts. Primary myoblasts were

derived from hindlimb muscles of neonatal Wistar rats and cultured in Ham's F-10 nutrient mixture supplemented with 0%, 10%, and 20% fetal bovine serum (FBS), respectively. They found the promotion of the PBM on the proliferation, cyclin A, and cyclin D of the serum-free myoblasts. As they have observed, there was dysfunctional proliferation of myoblasts in Ham's F-10 nutrient mixture with 0% FBS. Therefore, the observed PBM just played a dPBM role.

S. Li et al. have studied PBM for cobalt chloride- ($CoCl_2$-) induced hypoxic dysfunction of rhesus monkey choroid-retinal (RF/6A) cells by 670 nm light-emitting diode (LED) irradiation. They observed the proliferation of RF/6A cells in Dulbecco's minimal essential medium (DMEM)/F12 with 10% FBS resisted the $CoCl_2$ at 100 μmol/L so that it was in its normoxia proliferation-specific homeostasis (nPlSH), and they found no dPBM on its cytochrome C oxidase (COX) activity and ATP concentration. They further observed $CoCl_2$ at 200 μmol/L disrupted the nPlSH and induced the dysfunctional proliferation, and they found a dPBM may completely recover the normal proliferation, but the COX activity and ATP concentration were only partially recovered. In other words, the established proliferation-specific homeostasis (PlSH) was different from the nPlSH and may be called hypoxic PlSH (hPlSH). The nPlSH and hPlSH maintain the same normal proliferation, but their mechanisms are different from each other.

X. Chen et al. have studied the effects of 808 nm LED light pretreatment of hypoxic primary mouse cortical neurons. They observed the LED light did not affect the COX activity and ATP concentration of the neurons in DMEM/F12 with 10% FBS and 10% horse serum so that the proliferation may be the normal proliferation in its nPlSH. The proliferation in its nPlSH could not resist $CoCl_2$ at 200 μmol/L but the LED light pretreated neurons could. It suggested LED light pretreatment enhanced the nPlSH so that the enhanced nPlSH (ePlSH) could resist $CoCl_2$ at 200 μmol/L. The LED light pretreatment just played an iPBM role. The iPBM did not affect the COX activity and ATP concentration. The normal proliferation in its ePlSH could resist $CoCl_2$ at 200 μmol/L but its COX activity and ATP concentration could not.

Acknowledgment

We are thankful to the contributing authors who have provided compelling work that will serve a springboard for thoughtful discussions and fuel for future studies.

Timon Cheng-Yi Liu
Quan-Guang Zhang
Lutz Wilden

Hindawi Publishing Corporation
International Journal of Photoenergy
Volume 2014, Article ID 297129, 11 pages
http://dx.doi.org/10.1155/2014/297129

Research Article

Significant Inhibition of Tumor Growth following Single Dose Nanoparticle-Enhanced Photodynamic Therapy

Shih-Hsun Cheng,[1,2] Chia-Hui Chu,[1] Nai-Tzu Chen,[1,2] Jeffrey S. Souris,[2] Chin-Tu Chen,[2] and Leu-Wei Lo[1]

[1] *Institute of Biomedical Engineering and Nanomedicine, National Health Research Institutes, Zhunan, Miaoli County 35053, Taiwan*
[2] *Department of Radiology, The University of Chicago, Chicago, IL 60637, USA*

Correspondence should be addressed to Leu-Wei Lo; lwlo@nhri.org.tw

Received 25 February 2014; Accepted 1 June 2014; Published 7 August 2014

Academic Editor: Quan-Guang Zhang

Photodynamic therapy (PDT) for cancer treatment involves the pathology's uptake of photosensitizers, which produce cytotoxic reactive oxygen species by photoirradiation. The use of nanoparticles as carriers of photosensitizers is one promising approach to this endeavor, owing to their small size, unique physicochemical properties, and easy/diverse functionalization. In the current work, we report on the *in vivo* assessment of PDT efficacy of these nanoconstructs in a murine model of human breast cancer, following a single (one-shot) nanoparticle dose and photoirradiation. Palladium-porphyrin (PdTPP) was administered intratumorally via injection of aqueous suspensions of either free PdTPP or MSN-conjugated PdTPP (MSN-PdTPP) at a dose of 50 μg. Mice were then exposed to a single photoirradiation session with total energy of 80 J. One month after one-shot PDT treatment, significantly greater reductions in tumor growth were observed in MSN-Pd treated animals than in PdTPP cohorts. Electron microscopy of tumor specimens harvested at various timepoints revealed excellent MSN-PdTPP uptake by cancer cells while immunohistologic analysis demonstrated marked increases in apoptotic response of MSN-PdTPP treated animals relative to PdTPP controls. Taken together, these findings suggest that considerable improvements in PDT efficacy can readily be achieved via the use of nanoparticle-based photosensitizers.

1. Introduction

Photodynamic therapy (PDT) has evolved considerably in recent years to treat a number of medical conditions that include wet macular degeneration, dermatologic disorders (e.g., acne, rosacea, and psoriasis), and several types of cancer including lung and esophageal cancer [1–6]. It is intrinsically a focal therapy far less invasive than surgical approaches and with fewer adverse effects than systemic chemotherapy. The most prevalent forms of PDT in use today are based on the photogeneration of cytotoxic, reactive oxygen species within tumor tissue via the optical stimulation of exogenous photosensitizing agents (PSs). The photosensitizer, in its ground (singlet) state, absorbs a photon that promotes the PS to a short-lived excited singlet state. Because the excited singlet state is so short-lived, the PS has little opportunity to transfer either energy or electrons to other molecules nearby and instead undergoes intersystem crossing to leave it in an excited, much longer-lived, triplet state. As the PS subsequently decays back to its initial ground (singlet) state, it transfers energy to nearby ground (triplet) state molecular oxygen, raising the latter to its first excited singlet state [7, 8]. Most photosensitizers in clinical use have been optimized/selected for their high, excited singlet state quantum efficiency and recursively generate substantial amounts of singlet oxygen from molecular oxygen rather than undergoing thermal decay (via internal conversion) or fluorescent emission [9, 10].

The most widely employed PSs at present are porphyrins. Photoirradiation of porphyrins at selective wavelengths of visible light (450–700 nm) leads to the photochemical conversion of molecular oxygen ($^3O_2$) into singlet oxygen ($^1O_2$),

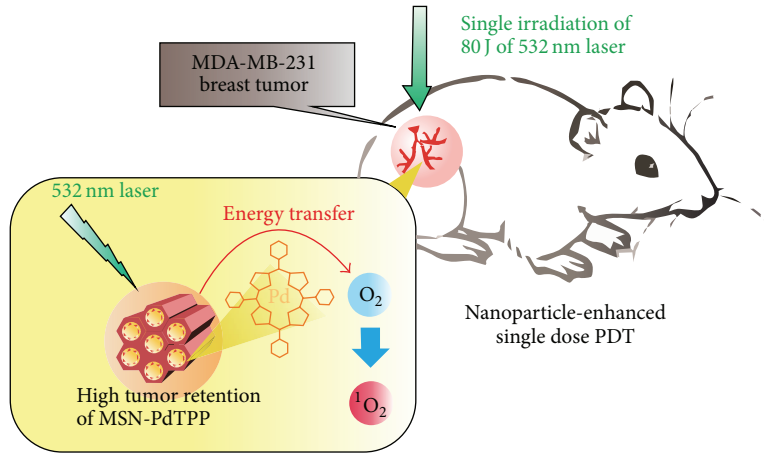

Scheme 1: The illustration of *in vivo* PDT studies using MSN-PdTPP with single photoirradiation on a murine model bearing human breast cancer cells.

an especially efficacious cytotoxic agent that leads to apoptosis or necrosis [11]. In the conventional PDT of cancer, a photosensitizer drug is administered to the patient, which then passively accumulates in the tumor tissue, though a few PSs have intrinsic proclivities for targeting the endothelial cells of vasculature. The involved tissue is then selectively illuminated with light which activates the photosensitizer inducing cell death. Photosensitizers have evolved over the years to maximize their potency and simultaneously minimize their systemic toxicity. Unfortunately, to date, the overwhelming majority of photosensitizers still possess multiple limitations that include high hydrophobicity, significant self-aggregation, and poor tumor selectivity, each limiting PDT efficiency and clinical benefit [12, 13]. As such, considerable effort has gone into developing compounds with improved "deliverability."

One approach to enhancing PS delivery is that of nanoparticle- (NP-) mediated transport. When compared to conventional unshielded delivery, NP-assisted conveyance of PSs has the added advantage of providing an exoplatform for the conjugation of polymers to prolong PS circulation half-lives and thereby increase PS accumulation in the leaky vasculature of tumors via the enhanced permeability and retention effect (EPR) [14–19]. Encapsulation of PSs within NPs also circumvents PS self-aggregation and enables high density PS delivery. NP conveyance of PSs also permits the incorporation of efficient, light-absorbing chromophores in close proximity to PSs, so as to greatly promote the energy transfer to PSs and thereby significantly enhance overall photodynamic efficiency [20–26]. One form of nanoparticles in particular has recently gained considerable interest for use both in cancer chemotherapy and in PDT: mesoporous silica nanoparticles (MSNs) [27–32].

MSNs are biocompatible, readily endocytosed, and easily modified after synthesis for the conjugation of targeting moieties on their outer surfaces [33–39]. The unique topology of MSNs also provides them with three distinct domains that can be independently functionalized: the silica framework, the hexagonal nanochannels/pores, and the nanoparticle's outermost surface. As such, MSNs are especially well suited to the task of incorporating the essential capabilities of a combined diagnostic/therapeutic (i.e., theranostic) platform in a single particle, with (1) separate domains for contrast agents that enable traceable imaging of PS targeting, (2) PS payloads for therapeutic intervention, and (3) biomolecular ligands for highly targeted PS delivery.

Previously, we reported the development and *in vitro* characterization of MSNs that were sequentially functionalized with the fluorescent contrast agent ATTO647N embedded within the MSN's silica framework for tracking, the cRGDyK peptide conjugated onto the MSN's exterior for targeting the $\alpha_v\beta_3$ integrin expression, and the photosensitizer Pd-porphyrin (PdTPP) covalently linked within the MSN's protective nanochannels for photodynamic therapy [40–42]. Herein we report the results of our *in vivo* PDT studies of MSNs-PdTPP using a murine model of human breast cancer and one-shot photoexcitation (Scheme 1).

2. Methods

2.1. Materials. Tetraethoxysilane (TEOS), cetyltrimethylammonium bromide (CTAB), ethanol, ammonium hydroxide (30%), N,N-dimethylformamide (DMF), and 3-Aminopropyltrimethoxysilane (APTMS) were purchased directly from Acros. Di(N-succinimidyl) carbonate (DSC) and N,N-diisopropylethylamine were obtained from Sigma Chemical Co.

2.2. Preparation of MSNs. The sol-gel co-condensation of TEOS to synthesize MSNs was as follows. First, CTAB (0.58 g) was dissolved in NH_4OH (0.51 M, 300 mL) at 40°C. After stirring for 1 h, diluted TEOS (0.2 M in 5 mL ethanol) was added and the solution was stirred for an additional 4 h. Then, high concentration of TEOS (1.0 M in 5.0 mL of ethanol) was added under vigorous stirring for an additional hour. The solution was aged in darkness at 40°C for 20 h. Samples were subsequently collected by centrifuging at 12,000 rpm for

20 min, washing, and redispersing the solids with deionized water and ethanol repeatedly. Surfactant templates were removed by extraction in 0.3 g of NH_4NO_3 and 50 mL of ethanol solution under reflux at 65°C for 12 h.

2.3. Preparation of MSN-PdTPP. As the surfactant templates were being removed to yield MSNs, 50 mg PdTPP and 150 mg di(N-succinimidyl) carbonate (DSC) were mixed with 100 μL N,N-diisopropylethylamine (99.5%) in N,N-dimethylformamide (DMF) (20 mL) solution for 2 h. The activated PdTPP was then reacted with 200 μL APTS for 1 h and purified by a PD-10 column (Amersham Biosciences). The amount of PdTPP loading in MSNs was determined by measuring the absorbance at 400 nm, the Soret band of PdTPP. The amounts of PdTPP in MSNs were thereby determined to be 5.5% w.t.

2.4. Characterization. The morphology of MSN samples was characterized via TEM (Hitachi, H-7650), operating at an acceleration voltage of 80 kV. Surface areas and pore sizes were determined by N_2 adsorption-desorption isotherm measurements at 77 K on a Micrometric ASAP 2010. Samples were outgassed at 10^{-3} Torr and 120°C for approximately 6 h prior to conducting adsorption experiments. Pore size distribution curves were obtained from analysis of the desorption portion of the isotherms using the BJH (Barrett-Joyner-Halenda) method. Steady-state absorption spectra were acquired with a DU800 UV spectrometer (Beckman). A Malvern Zetasizer Nano was used to measure the zeta potential of MSN samples in solution at pH 7.4.

2.5. Singlet Oxygen Measurement. We used a DPBF (8 mM) acetonitrile solution to measure single oxygen generation. 2 mL DPBF solution was added to the PdTPP and MSN-PdTPP samples and mixed thoroughly. The mixture was then irradiated at 532 nm via a laser operating at 250 ± 5 mW cm^{-2}. The absorption spectra of DPBF were detected at 400 nm every 20 seconds.

2.6. Cell Culture. MDA-MB-231 human breast carcinoma cells were maintained in RPMI-1640 medium (Gibco-BRL, NY, USA) with 10% heat-inactivated fetal bovine serum (FBS) (Hyclone, Utah, USA) and supplemented with 100 units/mL penicillin and 100 μg/mL streptomycin at 37°C with 5% CO_2.

2.7. In Vitro PDT. A total of 5000 MDA-MB-231 breast cancer cells were seeded on a 96-well and incubated for 24 h. Cells were then treated with 10, 25, and 50 μg/mL of either PdTPP or MSN-PdTPP in a serum-free medium for 1 h at 37°C in darkness, respectively. Cell viability was estimated by WST-1 assay. In the WST-1 assay, tetrazolium salt WST-1 {4-[3-(4-Iodophenyl)-2-(4-nitrophenyl)-2H-5-tetrazolio]-1, 3-benzene disulfonate} in live cells was cleaved by mitochondrial dehydrogenase to yield formazan. After treatment for 1 h, the supernatant was removed and added to 100 μL/well serum-free medium and 10 μL/well Cell Proliferation Reagent WST-1 (Roche). After incubation with WST-1 for 4 h, plates were shaken for 1 min and measured for optical absorbance at 450 nm using an ELISA reader (Infinite M200, TECAN). Six specimens were run for each concentration, with each experiment being repeated three times. For the PDT, cells were irradiated using a 532 nm laser operating at 250 ± 5 mW cm^{-2} at energies of 1.2, 2.5, or 5 J after treatment of either PdTPP or MSN-PdTPP in a serum-free medium for 1 h at 37°C.

2.8. Tumor Xenograft Animal Model. MDA-MB-231 human breast carcinoma cells (1×10^6 cells/200 μL sterile saline) were subcutaneously injected into the dorsal region of both thighs of male nude mice (*nu/nu*; 20–25 g; 6–8 weeks of age; BioLasco Taiwan Co., Ltd). Tumor growth curves were obtained using daily digital caliper measurement of tumor diameter once the bulge caused by the tumor cells at the injection site became visible (tumor size ~ 200 ± 50 mm^3). Tumor volume (mm^3) was calculated using the formla: 0.523 × (length × width × thickness) and assessed twice per week for one month. All experiments involving animals were performed in accordance with the guidelines of institutional animal care and use committee.

2.9. In Vivo Two-Photon Excited PDT. *In vivo* PDT experiments were performed when the tumor volume reached approximately 200 ± 50 mm^3. Mice were divided into groups of twelve animals to minimize variations in group weight and tumor size. Tumor-bearing nude mice were anaesthetized and treated by intratumoral injection of PdTPP or MSN-PdTPP at a concentration of 50 μg. One hour after injection, mice were subjected to 80 J of 532 nm laser irradiation such that the average power of light delivered to the skin was 235 mW. Control group mice received intratumoral injections of saline with or without irradiation, respectively. Mice were monitored for a maximum of 28 days. The length, width, and thickness of tumors were measured by digital calipers and assessed twice weekly for one month. All mice were euthanized at the end of the 28th day and tumors were removed for further study.

2.10. Tissue Preparation for Histopathology and Immunohistochemistry. At the end of experiments, a thorough necropsy of mice was carried out immediately after euthanasia. Samples of the tumor mass were embedded in OCT (Tissue-Tek) and stored in −20°C freezer. Samples were sectioned at 10 μm thickness and then stained with hematoxylin and eosin (H&E), caspase-3 (abcam), and TUNEL stain (Roche, *in situ* cell death detection kit) for examination by light microscopy.

For H&E staining, sections from cryopreserved tissues were fixed in 4% paraformaldehyde and stained with hematoxylin and eosin. Following staining, sections were dehydrated, mounted, and observed.

For caspase-3 staining, sections from cryopreserved tissues were incubated with 3% (v/v) hydrogen peroxide in methanol for 15 min and in 3% BSA for 1 h to block endogenous peroxidases and nonspecific binding. Sections were then incubated with polyclonal antibodies to active caspase-3 (1 : 500) in diluting buffer (1% bovine serum albumin,

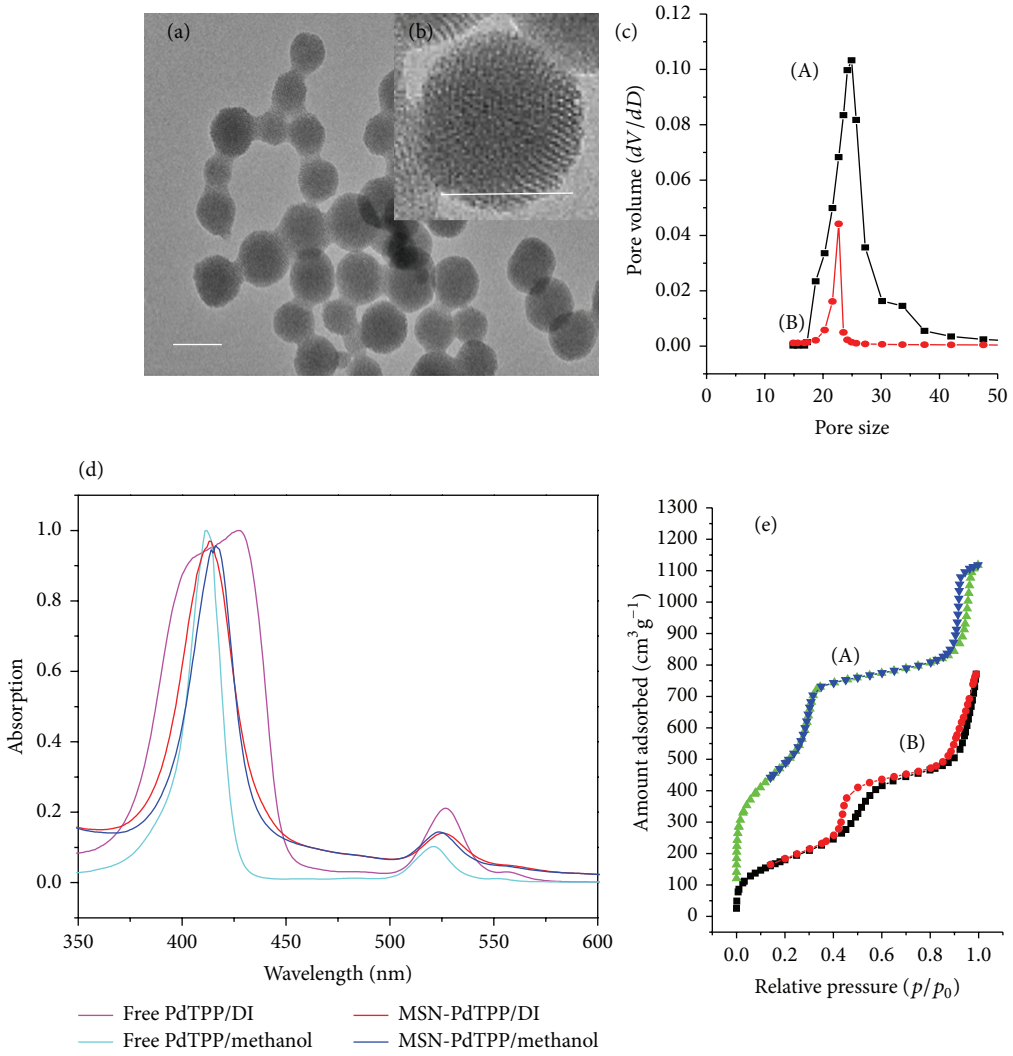

Figure 1: Nanoparticle characterization. (a) TEM images of MSN-PdTPP nanoparticles (scale bar: 100 nm). (b) Well-ordered porous structure of MSN-PdTPP (scale bar: 100 nm). (c) Pore size distribution of (A) MSN and (B) MSN-PdTPP derived from desorption isotherm measurements and BJH method. (d) UV-visible absorption spectra of PdTPP and MSN-PdTPP in DI water and methanol. (e) Nitrogen adsorption-desorption isotherms of (A) MSN and (B) MSN-PdTPP.

0.1% Tween-20 in PBS) overnight at 4°C. Sections were next incubated with goat anti-rabbit HRP secondary antibodies (Jackson, 1:10000) in PBS for 1 h. Detection of caspase-3 positive cells was undertaken via Diaminobenzidine (DAB) immunohistochemistry, followed by counterstaining with Gills Haematoxylin.

For TUNEL staining, sections were fixed in 4% paraformaldehyde and blocked in 3% hydrogen peroxide in methanol for 15 min. Next specimens were incubated in permeabilization solution (0.1% triton X-100 and 0.1% sodium citrate in PBS) for 2 min on ice. TUNEL reaction mixture was added and incubated for 1 h at 37°C in the dark. After PBS rinsing, samples were incubated with converter-POD for 30 min at 37°C. Detection of apoptosed cells was achieved using DAB immunohistochemistry, followed by counterstaining with Gills Haematoxylin.

2.11. Transmission Electron Microscopy Imaging of Tumor Tissue. For electron microscopy, tumor tissue specimens were fixed overnight in glutaraldehyde, buffered (2.5%) with PBS. Tissues were then washed with 3 changes of PBS and postfixed for 1 h in a solution containing OsO_4 buffered (2%) with PBS. Samples were next washed in 3 changes of dH_2O and dehydrated stepwise in ethanol. Tissues were polymerized using Spurr resin at 68°C for 15 hours. The embedded specimens were then thin-sectioned at 70 nm and viewed on a Hitachi H-7650 transmission electron microscope operating at 80 kV.

3. Results and Discussion

The intrinsic flexibility of MSN surface chemistry readily affords postsynthesis, application-specific modification, for

example, tailoring for optimal drug release, dispersion stability, cellular uptake, and attachment of imaging agents and targeting ligands. For the current application, the porphyrin-based photosensitizer PdTPP was attached via the addition of amino groups to the MSN's outer surfaces and nanochannel walls. Amino modification of MSN surfaces also served to increase the overall surface charge of the nanoplatform (zeta potential of MSN-PdTPP: +28.5 mV), thereby enhancing cell uptake and minimizing self-aggregation (and thus self-quenching). Di(N-succinimidyl) carbonate (DSC) coupling was used to encapsulate PdTPP to the MSNs. MSN-PdTPP morphology was characterized by combined transmission electron microscopy (TEM), N_2 adsorption-desorption isotherm measurement, and UV-Vis spectroscopy. TEM studies demonstrated well-ordered, hexagonal porous structures characteristic of mesoporous silica, with average particle diameters of 80 nm (Figures 1(a) and 1(b)). Surface area and pore size of MSNs and MSN-PdTPPs were determined by N_2 adsorption-desorption isotherm measurements (Figures 1(c) and 1(e)). Following PdTPP incorporation, nanoparticle surface areas decreased from 985 $m^2\ g^{-1}$ (MSN) to 632.06 $m^2\ g^{-1}$ (MSN-PdTPP). Measured UV absorption spectra of MSN-PdTPP and PdTPP showed MSN conjugation greatly increasing PdTPP solubility in water via possessing only slight differences in methanol solutions but significant differences in DI water (Figure 1(d))—a consequence of the solubility of PdTPP in water being poor, and its aggregation broadening the Soret band spectra. Quantization of the PdTPP content of MSN conjugates was achieved by measuring each sample's absorbance at 400 nm (PdTPP Soret band) while dissolved in HF-NaF, averaging 5.5% PdTPP by weight.

We assessed the generation of singlet oxygen ($^1O_2$) by photoirradiation of MSN-PdTPP in water using an indirect chemical method: one that employed 1,3-diphenylisobenzofuran (DPBF), whose optical absorption at 400 nm decreases in the presence of singlet oxygen. We also measured the singlet oxygen production of photoirradiated free PdTPP in water for comparison (10.4 μg of PdTPP, in both free form and MSN-conjugated form). Singlet oxygen generation in aqueous suspensions of MSN-PdTPP and free PdTPP, wth 532 nm laser diode irradiation and 20 sec interval spectra sampling, is shown in Figure 2 as a function of illumination time. Singlet oxygen generation of DPBF-only solutions and DPBF solutions bearing MSNs (data not shown) served as controls. Much steeper reductions were found in the optical absorption of DPBF solutions containing MSN-PdTPP than of nanoparticle-free samples, reflecting the former's significantly higher efficiency in generating $^1O_2$.

For the *in vitro* cytotoxicity analysis of our nanoplatforms, WST-1 assays of MDA-MB-231 cell viability were used following 1 h incubations with either 10, 25, or 50 $\mu g\ mL^{-1}$ of MSN-PdTPP or free PdTPP—both before and after photoirradiation. To assess optimal illumination, we photoirradiated these groups at one of three different total energies (1.5, 2.5, and 5 J) using a 532 nm diode-laser (250 ± 5 mW/cm^2). As shown in Figure 3(b), little photo-induced cytotoxicity was found for 25 μg and 50 μg free PdTPP treatments, with viabilities of 81% for 25 $\mu g\ mL^{-1}$ and 80% for 50 $\mu g\ mL^{-1}$ at 5 J

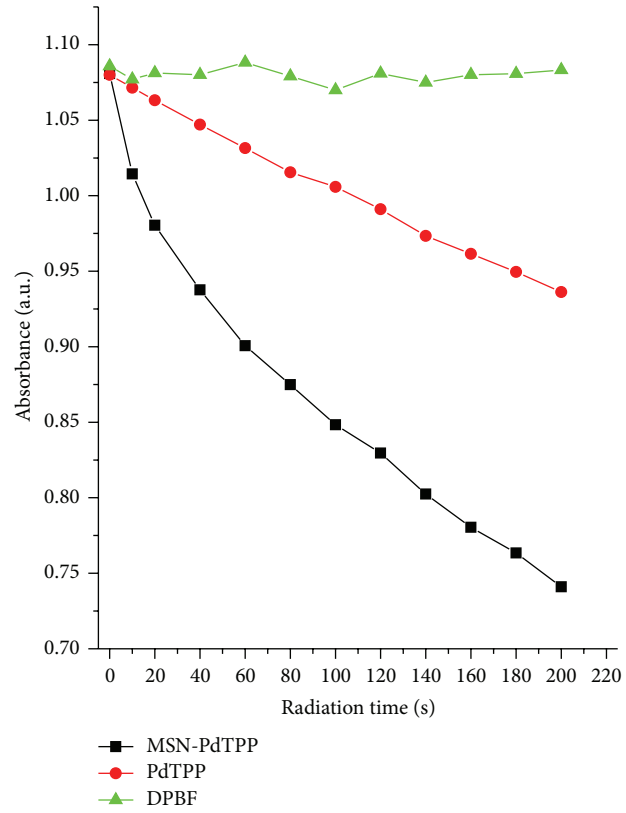

FIGURE 2: Decay curve of DPBF absorbance of $^1O_2$ generated from PdTPP and MSN-PdTPP upon photoirradiation. Green line denotes DPBF with photoirradiation (control).

irradiation, respectively. However, significant cytotoxicities were observed for 50 $\mu g\ mL^{-1}$ MSN-PdTPP at 2.5 J and 5 J irradiation (Figure 3(d)). As shown in Figures 3(a) and 3(c), no cytotoxic effects were observed for either free PdTPP or MSN-PdTPP prior to photoirradiation.

With these promising *in vitro* findings in hand, we then sought to characterize the *in vivo* utility of our nanoconstructs for PDT by using male *nu/nu* nude mice bearing MDA-MB-231 xenografts. MDA-MB-231 and MDA-MB-231-GFP tumor cells (1×10^6 cells/200 μL sterile saline) were injected subcutaneously into the dorsal region of the right and left thigh, respectively (Figure 4). The fluorescent MDA-MB-231-GFP tumor cells were inoculated for validation of tumor location and better visualization of growth. After tumors had grown to a volume of approximately 200 ± 50 mm^3, we conducted comparative PDT efficacy studies by first dividing animals into four groups ($n = 12$), so as to minimize intergroup weight and tumor size variation. Next two control groups (with/without photoirradiation) were intratumorally injected with 120 μL sterile saline solution (0.9% NaCl) while the remaining two groups were intratumorally injected with either 50 μg of MSN-PdTPP or the same PdTPP-concentration of free PdTPP. One hour after administration, one control group and both free PdTPP and MSN-PdTPP experimental groups were anesthetized and their tumors irradiated at 532 nm for total energy deposition

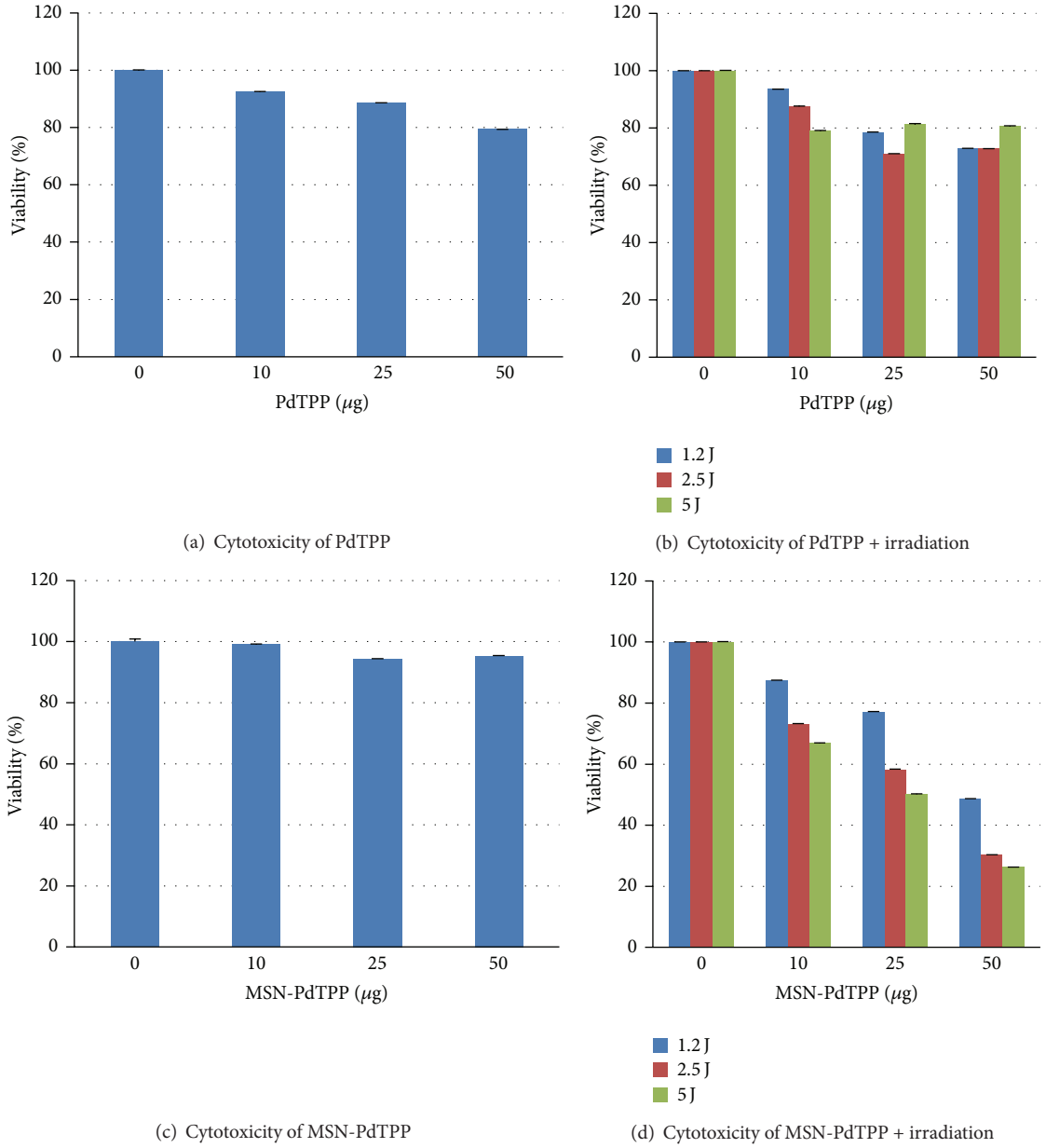

(a) Cytotoxicity of PdTPP

(b) Cytotoxicity of PdTPP + irradiation

(c) Cytotoxicity of MSN-PdTPP

(d) Cytotoxicity of MSN-PdTPP + irradiation

Figure 3: Dark (nonilluminated) cytotoxicity of MDA-MB-231 cells treated with various concentrations of (a) PdTPP and (c) MSN-PdTPP. Illumination cytotoxicity of MDA-MB-231 cells treated with various concentrations of (b) PdTPP and (d) MSN-PdTPP following 1.2 J, 2.5 J, and 5 J of photoirradiation.

of 80 J. Tumor size and body weight were subsequently monitored on a daily basis, for the next 28 days. As illustrated in Figure 5(a), a single intratumoral administration of MSN-PdTPP and exposure to a single-shot photoirradiation were significantly more efficacious in tumor volume reduction than either single-shot photoirradiated free PdTPP or saline/control (Figure 5(a)). We postulate that the observed marked increase in PDT efficacy afforded by MSN protected delivery of the PS arose primarily from nanoparticle-enhanced endocytosis and consequent retention of the PS-combining to delay PS clearance from the tumor site as well as to avoid environmental degradation.

Twenty-eight days after PDT treatment, mice were sacrificed and the tumors were removed for measurement (Figure 5(b)). No differences in the long-term PDT benefit were found between the 2 saline control groups (with/without photoirradiation) and the free PdTPP experimental groups (Figure 5(a)), with mean tumor volumes, at the study's end, measuring $10280 \pm 1648\,mm^3$ (saline, no irradiation, $n = 12$), $9850 \pm 525\,mm^3$ (saline, with irradiation, $n = 12$), and $10160 \pm 656\,mm^3$ (free PdTPP, with irradiation, $n = 12$). After intratumoral injection, free PdTPP molecules had the propensity to drain away from the tumor and thus imposed nonobservable PDT effect on tumor following localized

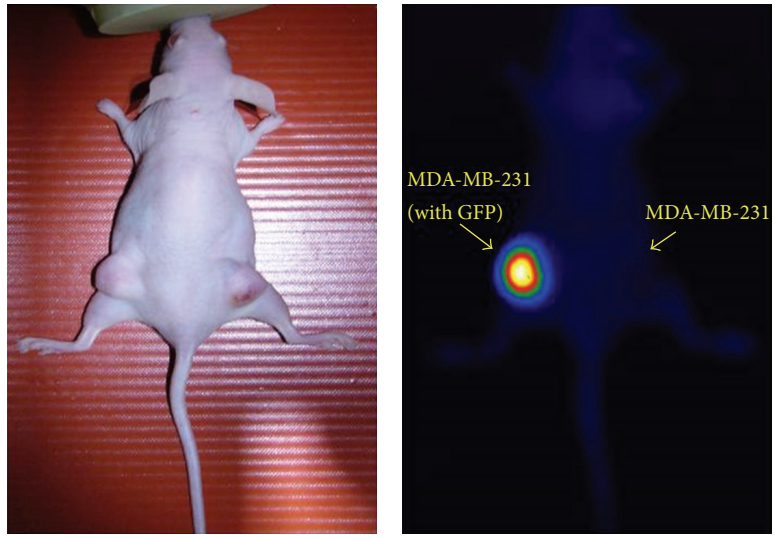

Figure 4: White light (a) and fluorescence (b) images of nude mouse bearing xenografts comprised of GFP-expressing MDA-MB-231 cells on animal's left thigh and nonfluorescent MDA-MB-231 cells on animal's right thigh.

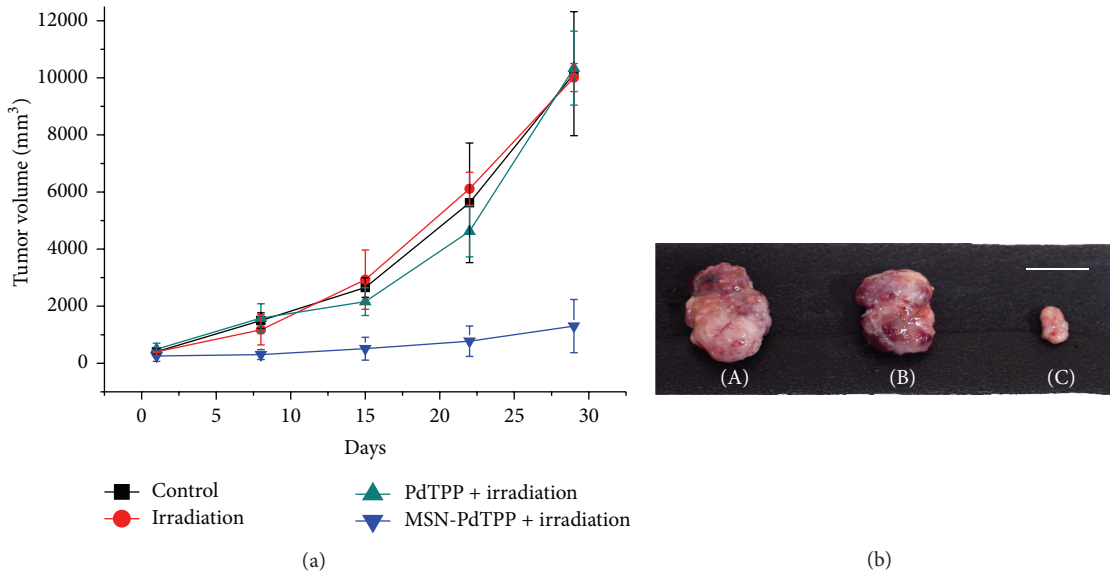

Figure 5: (a) 29-day comparative PDT efficacy studies of MDA-MB-231 s.c. xenograft nude mouse model subjected to a single intratumoral injection of (i) saline without photoirradiation (black squares), (ii) saline with photoirradiation (red circles), (iii) PdTPP with photoirradiation (green upward-pointing triangles), and (iv) MSN-PdTPP with photoirradiation (blue downward-pointing triangles)—showing MSN-PdTPP to be highly efficacious in tumor reduction. Datapoints denote mean of twelve mice per group. (b) Photographs of tumors harvested from mice 28 days after treatment with (A) saline (control), (B) PdTPP, and (C) MSN-PdTPP, all subjected to photoirradiation (scale bar: 1 cm).

irradiation. The MSN-PdTPP group, however, demonstrated dramatic PDT benefit at 28 days after irradiation, with a mean tumor volume of $780 \pm 567\,\text{mm}^3$ ($n = 12$) as can also be seen from a representative specimen in Figure 5. By contrast, the MSN-PdTPP group without irradiation demonstrated no significant PDT effect, whose tumor volume averagely increased 6-fold 15 days after injection and 13.5-fold 28 days after injection, respectively ($n = 5$). It illustrated a similar tumor growth curve to that of the saline control group.

We then performed hematoxylin and eosin (H&E) histological staining of excised tumor and injection site tissue sections, confirming the existence of extravasated blood that is characteristic of PDT (Figure 6(a)). To more precisely assess antitumor response to our nanoparticle PDT treatments, we compared terminal deoxynucleotidyl transferase dUTP nick end labeling (TUNEL) and caspase-3 immunohistochemical staining for apoptosis of tumors harvested from mice that had been treated with MSN-PdTPP nanoparticles for 0 h and 1 h

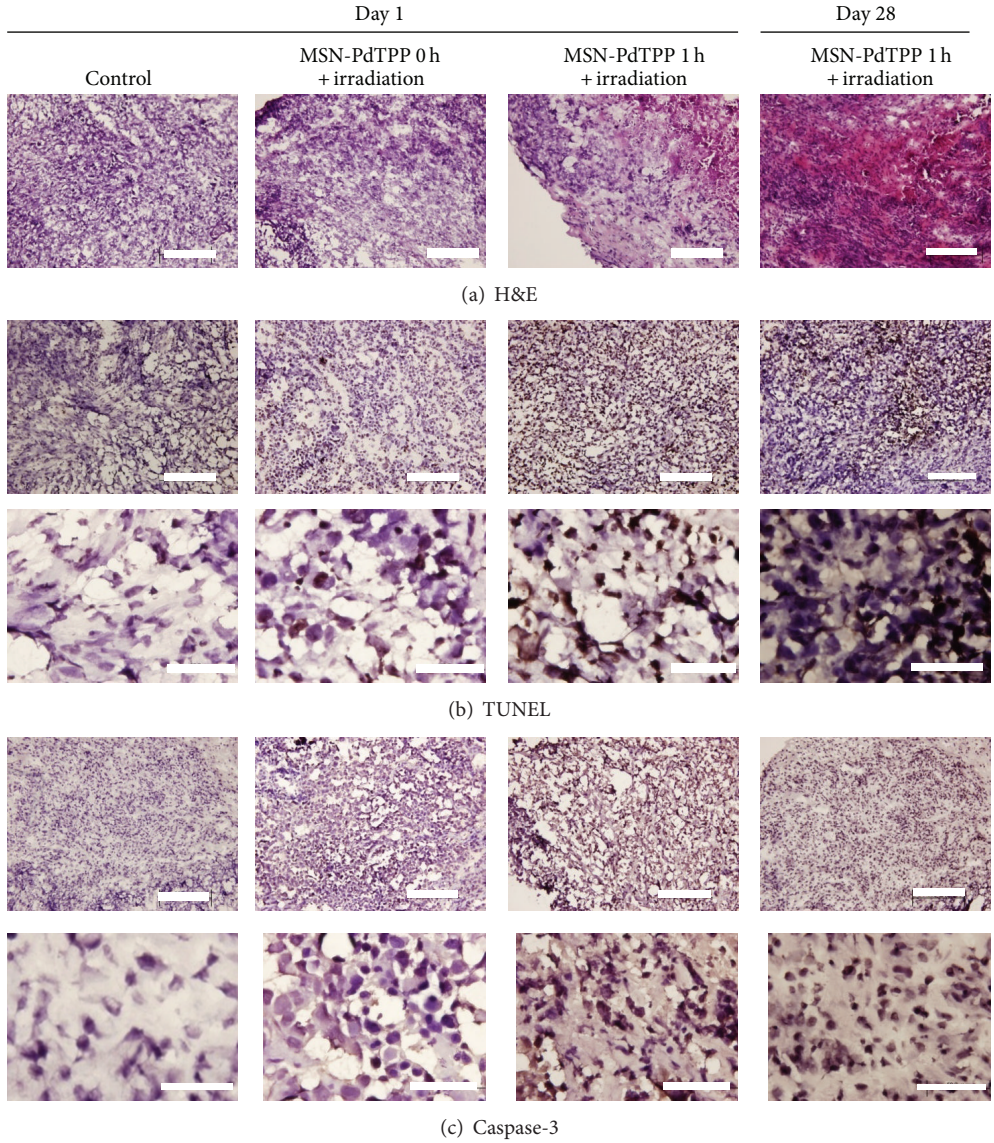

Figure 6: (a) Histological staining of the excised tumor sections on treatment day 1 of (i) saline with no photoirradiation (control), (ii) MSN-PdTPP with photoirradiation at 0 h after injection, (iii) MSN-PdTPP with photoirradiation at 1 h after injection, and on treatment day 28 of (iv) MSN-PdTPP with photoirradiation at 1 h after injection. H&E staining; scale bars: 200 μm. (b) TUNEL staining of consecutive sections for each group at 200x magnification (upper, scale bars: 200 μm) and 1000x magnification (upper, scale bars: 50 μm). (c) Caspase-3 staining of consecutive sections for each group at 200x magnification (upper, scale bars: 200 μm) and 1000x magnification (upper, scale bars: 50 μm).

with irradiation, as well as from negative controls (Figures 6(b) and 6(c)). Tumors treated with MSN-PdTPP for 1 h demonstrated considerable apoptosis one day following their photoirradiation. Stained sections of MSN-PdTPP-treated tumors harvested 28 days after irradiation revealed much greater apoptosis still. By contrast, TUNEL and caspase-3 staining of samples that had been immediately photoirradiated following MSN-PdTPP administration revealed little apoptosis. These findings suggested that, even with MSN-PdTPP's appreciable generation of $^1O_2$, PDT therapeutic benefit strongly depended upon efficient nanoplatform endocytosis.

To further characterize our nanoparticle's uptake by cancer cells *in vivo*, we conducted TEM of MDA-MB-231 tumor sections harvested 0, 1, and 6 h after intratumoral injection (Figure 7). As shown in Figures 7(a) and 7(b), the TEM images of tumors treated 1 h prior with MSN-PdTPP demonstrated greater nanoparticle uptake than those harvested immediately following nanoparticle administration, with nanoparticles mostly confined to the periphery of cells at 0 h and not yet significantly endocytosed. TEM images of tumors treated 6 h prior, however, revealed few nanoparticles remaining within harvested tumors. Taken together we posit that optimal endocytosis and thus optimal photoirradiation

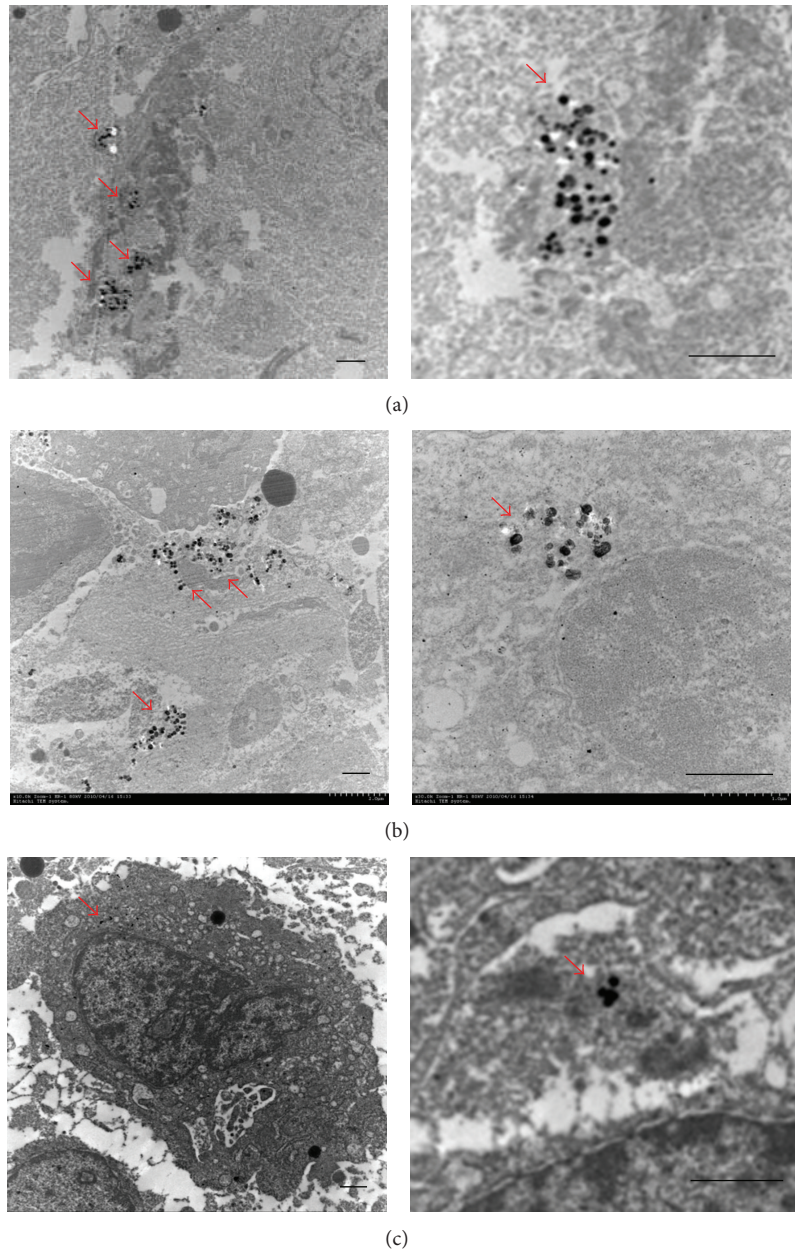

Figure 7: TEM images of tissue sections of tumors harvested at (a) 0 h, (b) 1 h, and (c) 6 h following intratumoral injection of MSN-PdTPP nanoparticles. Red arrows indicate MSN-PdTPP nanoparticle accumulations (scale bars: 1 μm).

are likely to be somewhere between 1 and 6 h following intratumoral injection of our nanoparticles.

4. Conclusions

In this work we describe significant enhancement of photodynamic therapy efficacy achieved via the use of nanoparticle-based photosensitizers, even when treatment is limited to a single photosensitizer dose and a single photoirradiation session. By covalently conjugating large numbers of the photosensitizer Pd-porphyrin onto the environmentally communicative nanochannel walls of mesoporous silica nanoparticles, we circumvent our hydrophobic photosensitizer's tendency to self-aggregate and self-quench. The benefits of this protected conveyance of substantial quantities of photosensitizer, our nanoplatform's proclivity for endocytosis, and thereby photosensitizer accumulation within tumor permit the use of much lower photosensitizer dose than free photosensitizer and with much greater antitumor response. Current efforts are aimed at the surface functionalization of

our nanoplatform for pathology-specific targeting and further optimization of pathology-dependent timing/frequency of nanoparticle dose and photoirradiation.

Conflict of Interests

The authors declare that there is no conflict of interests regarding the publication of this paper.

Acknowledgments

The authors acknowledge financial support from the National Health Research Institutes of Taiwan (BN-103-PP-04 and NM-103-PP-01) and the National Science Council of Taiwan (NSC-100-2911-I-400-502 and NSC102-2113-M-400-001-MY3).

References

[1] D. E. J. G. J. Dolmans, D. Fukumura, and R. K. Jain, "Photodynamic therapy for cancer," *Nature Reviews Cancer*, vol. 3, no. 5, pp. 380–387, 2003.

[2] T. J. Dougherty, C. J. Gomer, G. Jori et al., "Photodynamic therapy," *Journal of the National Cancer Institute*, vol. 90, no. 12, pp. 889–905, 1998.

[3] R. R. Allison, V. S. Bagnato, and C. H. Sibata, "Future of oncologic photodynamic therapy," *Future Oncology*, vol. 6, no. 6, pp. 929–940, 2010.

[4] C. M. Moore, D. Pendse, and M. Emberton, "Photodynamic therapy for prostate cancer—a review of current status and future promise," *Nature Clinical Practice Urology*, vol. 6, no. 1, pp. 18–30, 2009.

[5] A. E. O'Connor, W. M. Gallagher, and A. T. Byrne, "Porphyrin and nonporphyrin photosensitizers in oncology: preclinical and clinical advances in photodynamic therapy," *Photochemistry and Photobiology*, vol. 85, no. 5, pp. 1053–1074, 2009.

[6] J. Saczko, A. Chwiłkowska, J. Kulbacka et al., "Photooxidative action in cancer and normal cells induced by the use of photofrin in photodynamic therapy," *Folia Biologica*, vol. 54, no. 1, pp. 24–29, 2008.

[7] M. A. El-Sayed, "The triplet state: Its radiative and nonradiative properties," *Accounts of Chemical Research*, vol. 1, no. 1, pp. 8–16, 1968.

[8] S. P. McGlynn, T. Azumi, and M. Kinoshita, *Molecular Spectroscopy of the Triplet State*, Prentice Hall, Englewood Cliffs, NJ, USA, 1969.

[9] M. C. DeRosa and R. J. Crutchey, "Photosensitized singlet oxygen and its applications," *Coordination Chemistry Reviews*, vol. 223-234, pp. 351–371, 2002.

[10] Z. Luksiene, "Photodynamic therapy: mechanism of action and ways to improve the efficiency of treatment," *Medicina*, vol. 39, no. 12, pp. 1137–1150, 2003.

[11] I. J. MacDonald and T. J. Dougherty, "Basic principles of photodynamic therapy," *Journal of Porphyrins and Phthalocyanines*, vol. 5, no. 2, pp. 105–129, 2001.

[12] D. K. Chatterjee, L. S. Fong, and Y. Zhang, "Nanoparticles in photodynamic therapy: an emerging paradigm," *Advanced Drug Delivery Reviews*, vol. 60, no. 15, pp. 1627–1637, 2008.

[13] D. Bechet, P. Couleaud, C. Frochot, M. Viriot, F. Guillemin, and M. Barberi-Heyob, "Nanoparticles as vehicles for delivery of photodynamic therapy agents," *Trends in Biotechnology*, vol. 26, no. 11, pp. 612–621, 2008.

[14] W. C. Zamboni, V. Torchilin, A. K. Patri et al., "Best practices in cancer nanotechnology: perspective from NCI nanotechnology alliance," *Clinical Cancer Research*, vol. 18, no. 12, pp. 3229–3241, 2012.

[15] L. Zhang, F. X. Gu, J. M. Chan, A. Z. Wang, R. S. Langer, and O. C. Farokhzad, "Nanoparticles in medicine: therapeutic applications and developments," *Clinical Pharmacology and Therapeutics*, vol. 83, no. 5, pp. 761–769, 2008.

[16] R. Tong and D. S. Kohane, "Shedding light on nanomedicine," *WIREs Nanomed Nanobiotechnol*, vol. 4, no. 6, pp. 638–662, 2012.

[17] C. Lim, J. Heo, S. Shin et al., "Nanophotosensitizers toward advanced photodynamic therapy of cancer," *Cancer Letters*, vol. 334, no. 2, pp. 176–187, 2013.

[18] E. Paszko, C. Ehrhardt, M. O. Senge, D. P. Kelleher, and J. V. Reynolds, "Nanodrug applications in photodynamic therapy," *Photodiagnosis and Photodynamic Therapy*, vol. 8, no. 1, pp. 14–29, 2011.

[19] S. H. Cheng and L. W. Lo, "Inorganic nanoparticles for enhanced photodynamic cancer therapy," *Current Drug Discovery Technologies*, vol. 8, no. 3, pp. 250–268, 2011.

[20] J. M. Tsay, M. Trzoss, L. Shi et al., "Singlet oxygen production by peptide-coated quantum dot-photosensitizer conjugates," *Journal of the American Chemical Society*, vol. 129, no. 21, pp. 6865–6871, 2007.

[21] Y. Liu, W. Chen, S. Wang, and A. G. Joly, "Investigation of water-soluble x-ray luminescence nanoparticles for photodynamic activation," *Applied Physics Letters*, vol. 92, no. 4, Article ID 043901, 2008.

[22] D. K. Chatterjee and Z. Yong, "Upconverting nanoparticles as nanotransducers for photodynamic therapy in cancer cells," *Nanomedicine*, vol. 3, no. 1, pp. 73–82, 2008.

[23] J. P. Celli, B. Q. Spring, I. Rizvi et al., "Imaging and photodynamic therapy: mechanisms, monitoring, and optimization," *Chemical Reviews*, vol. 110, no. 5, pp. 2795–2838, 2010.

[24] S. H. Cheng, C. C. Hsieh, N. T. Chen et al., "Well-defined mesoporous nanostructure modulates three-dimensional interface energy transfer for two-photon activated photodynamic therapy," *Nano Today*, vol. 6, no. 6, pp. 552–563, 2011.

[25] M. Gary-Bobo, Y. Mir, C. Rouxel et al., "Mannose-functionalized mesoporous silica nanoparticles for efficient two-photon photodynamic therapy of solid tumors," *Angewandte Chemie International Edition*, vol. 50, no. 48, pp. 11425–11429, 2011.

[26] C. Liu, S. Cheng, N. Chen, and L. Lo, "Intra/inter-particle energy transfer of luminescence nanocrystals for biomedical applications," *Journal of Nanomaterials*, vol. 2012, Article ID 706134, 9 pages, 2012.

[27] J. Lu, Z. Li, J. I. Zink, and F. Tamanoi, "In vivo tumor suppression efficacy of mesoporous silica nanoparticles-based drug-delivery system: enhanced efficacy by folate modification," *Nanomedicine*, vol. 8, no. 2, pp. 212–220, 2012.

[28] L. Li, F. Tang, H. Liu et al., "In vivo delivery of silica nanorattle encapsulated docetaxel for liver cancer therapy with low toxicity and high efficacy," *ACS Nano*, vol. 4, no. 11, pp. 6874–6882, 2010.

[29] Y. Cao, R. A. Depinho, M. Ernst, and K. Vousden, "Cancer research: past, present and future," *Nature Reviews Cancer*, vol. 11, no. 10, pp. 749–754, 2011.

[30] V. Mamaeva, J. M. Rosenholm, L. T. Bate-Eya et al., "*Mesoporous silica* nanoparticles as drug delivery systems for targeted inhibition of notch signaling in cancer," *Molecular Therapy*, vol. 19, no. 8, pp. 1538–1546, 2011.

[31] H. Meng, M. Xue, T. Xia et al., "Use of size and a copolymer design feature to improve the biodistribution and the enhanced permeability and retention effect of doxorubicin-loaded mesoporous silica nanoparticles in a murine xenograft tumor model," *ACS Nano*, vol. 5, no. 5, pp. 4131–4144, 2011.

[32] J. Lu, M. Liong, Z. Li, J. I. Zink, and F. Tamanoi, "Biocompatibility, biodistribution, and drug-delivery efficiency of mesoporous silica nanoparticles for cancer therapy in animals," *Small*, vol. 6, no. 16, pp. 1794–1805, 2010.

[33] J. E. Lee, N. Lee, T. Kim, J. Kim, and T. Hyeon, "Multifunctional mesoporous silica nanocomposite nanoparticles for theranostic applications," *Accounts of Chemical Research*, vol. 44, no. 10, pp. 893–902, 2011.

[34] Z. Li, J. C. Barnes, A. Bosoy, J. F. Stoddart, and J. I. Zink, "Mesoporous silica nanoparticles in biomedical applications," *Chemical Society Reviews*, vol. 41, no. 7, pp. 2590–2605, 2012.

[35] V. Mamaeva, C. Sahlgren, and M. Lindén, "Mesoporous silica nanoparticles in medicine—recent advances," *Advanced Drug Delivery Reviews*, vol. 65, no. 5, pp. 689–702, 2012.

[36] Y. W. Yang, "Towards biocompatible nanovalves based on mesoporous silica nanoparticles," *MedChemComm*, vol. 2, no. 11, pp. 1033–1049, 2011.

[37] S. Wu, Y. Hung, and C. Mou, "Mesoporous silica nanoparticles as nanocarriers," *Chemical Communications*, vol. 47, no. 36, pp. 9972–9985, 2011.

[38] F. Tang, L. Li, and D. Chen, "Mesoporous silica nanoparticles: synthesis, biocompatibility and drug delivery," *Advanced Materials*, vol. 24, no. 12, pp. 1504–1534, 2012.

[39] W. Huang and J. J. Davis, "Multimodality and nanoparticles in medical imaging," *Dalton Transactions*, vol. 40, no. 23, pp. 6087–6103, 2011.

[40] S. H. Cheng, C. H. Lee, M. C. Chen et al., "Tri-functionalization of mesoporous silica nanoparticles for comprehensive cancer theranostics: the trio of imaging, targeting and therapy," *Journal of Materials Chemistry*, vol. 20, no. 29, pp. 6149–6157, 2010.

[41] S. Cheng, C. Lee, C. Yang, F. Tseng, C. Mou, and L. Lo, "Mesoporous silica nanoparticles functionalized with an oxygen-sensing probe for cell photodynamic therapy: potential cancer theranostics," *Journal of Materials Chemistry*, vol. 19, no. 9, pp. 1252–1257, 2009.

[42] H.-L. Tu, Y.-S. Lin, H.-Y. Lin et al., "In vitro studies of functionalized mesoporous silica nanoparticles for photodynamic therapy," *Advanced Materials*, vol. 21, no. 2, pp. 172–177, 2009.

Hindawi Publishing Corporation
International Journal of Photoenergy
Volume 2014, Article ID 205839, 8 pages
http://dx.doi.org/10.1155/2014/205839

Research Article

Stimulative Effects of Low Intensity He-Ne Laser Irradiation on the Proliferative Potential and Cell-Cycle Progression of Myoblasts in Culture

Cui-Ping Zhang,[1] Shao-Dan Li,[2] Yan Chen,[3] Yan-Ming Jiang,[4] Peng Chen,[5] Chang-Zhen Wang,[5] Xiao-Bing Fu,[1] Hong-Xiang Kang,[5] Ben-Jian Shen,[5] and Jie Liang[5]

[1] *Department of Wound Healing and Cell Biology, Burns Institute, The First Affiliated Hospital, General Hospital of Chinese People's Liberation Army, Beijing 100048, China*
[2] *Institute of Traditional Chinese Medicine, General Hospital of Chinese People's Liberation Army, Beijing 100853, China*
[3] *Department of Pharmacy, General Hospital of Beijing Military Region, Beijing 100700, China*
[4] *Department of Ophthalmology, Second Artillery Gerenal Hospital of Chinese People's Liberation Army, Beijing 100088, China*
[5] *Department of Electromagnetic and Laser Biology, Institute of Radiation Medicine, Academy of Military Medical Sciences, Beijing 100850, China*

Correspondence should be addressed to Peng Chen; chenbj2002@sina.com

Received 17 April 2014; Accepted 10 June 2014; Published 21 July 2014

Academic Editor: Timon Cheng-Yi Liu

Low intensity laser irradiation (LILI) was found to promote the regeneration of skeletal muscle *in vivo* but the cellular mechanisms are not fully understood. Myoblasts, normally quiescent and inactivated in adult skeletal muscle, are a type of myogenic progenitor cells and considered as the major candidates responsible for muscle regeneration. The aim of the present study was to study the effect of LILI on the growth potential and cell-cycle progression of the cultured myoblasts. Primary myoblasts isolated from rat hind legs were cultured in nutrient-deficient medium for 36 hours and then irradiated by helium-neon laser at a certain energy density. Immunohistochemical and flow cytometric analysis revealed that laser irradiation could increase the expression of cellular proliferation marker and the amount of cell subpopulations in the proliferative phase as compared with the nonirradiated control group. Meanwhile, the expressions of cell-cycle regulatory proteins in the laser-treated myoblasts were markedly upregulated as compared to the unirradiated cells, indicating that LILI could promote the reentry of quiescent myoblasts into the cell division cycle. These results suggest that LILI at certain fluences could promote their proliferation, thus contributing to the skeletal muscle regeneration following trauma and myopathic diseases.

1. Introduction

Lasers have been widely used in biological and medical fields for many years [1, 2]. Low intensity laser irradiation (LILI) is usually a laser with milliwatt-grade output power which could produce special biomodulation effects for disease treatment yet without irreversible damage to tissues [3–5]. LILI has achieved positive effects in clinical treatment of wound healing, chronic pain relief, fracture rehabilitation, and so on [6–8]. Studies have demonstrated that LILI could significantly enhance the regeneration process of skeletal muscle in mammals and amphibians [9, 10]. However, the possible cellular and molecular mechanisms still remain unclear as yet.

In the sight of traditional histopathology, mature skeletal muscle contains postmitotic muscle fibers where they themselves have very limited remodeling capability [9]. Under normal circumstances, adult mammalian skeletal muscle is a stable tissue with very little turnover of nuclei. However, upon injury and with external stimulus, skeletal muscle has the remarkable ability to initiate a repair process involving the activation of various cellular responses. This remodeling process is largely accomplished by myogenic precursors, also

termed myoblasts, which lie beneath the basement membrane of the muscle fiber and could replicate themselves in growing postnatal muscle where they add myonuclei to enlarge muscle fibers [11, 12]. Yet, in adult skeletal muscle, the number of myoblasts was few and most of them were in quiescent and inactive state, which made tissue regeneration and function repair very difficult following muscle injury. Researchers have found that, under the action of certain growth factors, myoblasts in wounded adult skeletal muscle could be activated to enter the mitotic cycle and proliferate and then differentiate to form new myofibers, thus contributing to the maintenance and restoration of muscle integrity and mass [13].

Previously, it was shown that, relative to nonirradiated control, LILI of the injured site markedly accelerated tissue repair and regeneration of skeletal muscle [9, 10]. Although the LILI-promoted muscle regeneration has been amply studied *in vivo*, questions remain, especially regarding the direct effect of this treatment on myoblasts *in vitro* and the biomodulatory mechanisms by which dormant myoblasts following LILI are activated to participate in muscle regeneration. Therefore, in this experiment, we used myoblasts cultured *in vitro* to explore the effect of LILI on the proliferative potential and cell-cycle progression of myoblasts and further find out the involved cell-cycle regulatory proteins in this process, with an attempt to provide evidence for the applications of LILI in clinical practice.

2. Materials and Methods

2.1. Cell Cultures and Identification. Primary myoblasts were derived from hindlimb muscles of neonatal Wistar rats and cultured in Ham's F-10 nutrient mixture supplemented with 20% fetal bovine serum (FBS) and incubated in a CO_2-enriched (5%) humid atmosphere at 37°C. During the first several passages of the primary cultures, myoblasts were enriched by preplating method. Immunocytochemical identification of myoblasts was performed by using a monoclonal antibody to desmin, the muscle-specific intermediate filament protein, and screened under the laser scanning confocal microscope (LSCM).

2.2. Laser Irradiation Protocol. In this experiment, a He-Ne laser with a wavelength of 632.8 nm was used. Prior to laser irradiation, myoblasts were initially seeded on the cell-culture plates at a density of 4×10^4 cells/mL. At the desired time points, irradiation was performed in the dark at room temperature. Laser irradiation was delivered to the culture plate from above via combination of optical lens. The distance between cells sample and lens was adjusted to make the laser beam diameter the same as the width of culture plates. The power density of irradiation on the cells was measured to be 6 mW/cm^2 and the irradiation time was set to 3 min based on our preexperiment. The nonirradiated control cells were subjected to the same experimental conditions as the irradiated cells, except for the irradiation.

2.3. Cell Preconditioning and Grouping. To simulate the initial physiological state of myoblasts *in vivo* and rule out the possible effects of unknown factors in serum, myoblasts were pretreated with serum starvation, so that we can analyze the effect of laser irradiation on myoblasts more accurately. In brief, myoblasts after passage were firstly cultured overnight in growth medium containing 20% FBS and then switched into serum-free culture medium for 36 hours. The cells which were rendered quiescent and synchronized in G0/G1 phase by serum starvation were then either refed with 10% FBS (hereafter called "10% FBS group," the same as below) or irradiated as described above (laser group). The cells neither serum-refed nor irradiated were set as negative control (control group). After serum starvation, myoblasts in laser and control group continued to be kept in the serum-free medium. Meanwhile the cells cultured throughout in serum with 20% FBS without any treatment (neither starvation nor irradiation) were used as a positive control (20% FBS group) in this study.

2.4. Flow Cytometric Assay. Myoblasts were harvested 24 h after laser irradiation or serum refeeding. Following fixation with 75% ethanol, the cells were digested with DNase-free RNase in phosphate-buffered saline (PBS) containing 5 μg/mL propidium iodide for DNA staining. The propidium iodide fluorescence and forward light scattering were detected by a flow cytometer equipped with CELLQuest software. The percentage of cells in G0/G1 and S/G2/M phases of the cell cycle was calculated, respectively.

2.5. Immunohistochemistry. Myoblasts were fixed with 4% paraformaldehyde and then incubated with mouse mAb to proliferate cell nuclear antigen (PCNA) at 4°C for 20 hours. After thorough rinsing with PBS, cells were incubated with biotinylated goat anti-mouse IgG and HRP-conjugated streptavidin successively. The peroxidase reaction was performed using AEC as chromogen and examined under a microscope. Three independent experiments in each condition were performed and a total of at least 100 cells were counted for each specimen.

2.6. Western Blotting. After irradiation/refeeding, cells were harvested quickly at desired time points, and the total protein was extracted with lysis buffer. Extracts were quantified with a protein assay kit, fractionated by 6% SDS/PAGE, and then transferred to a poly membrane. After blocking, membranes were incubated with mouse mAb to cyclin A and cyclin D, respectively, and then treated with goat anti-mouse IgG conjugated with horseradish peroxidase. Immune complexes on the membrane were visualized by using diaminobenzidine system. The relative gray values of corresponding bands and β-actin were compared and semiquantified by image analysis software.

2.7. Statistical Analysis. All of the experimental data were from experiments that were repeated at least three times, unless otherwise indicated. Statistical analysis was performed

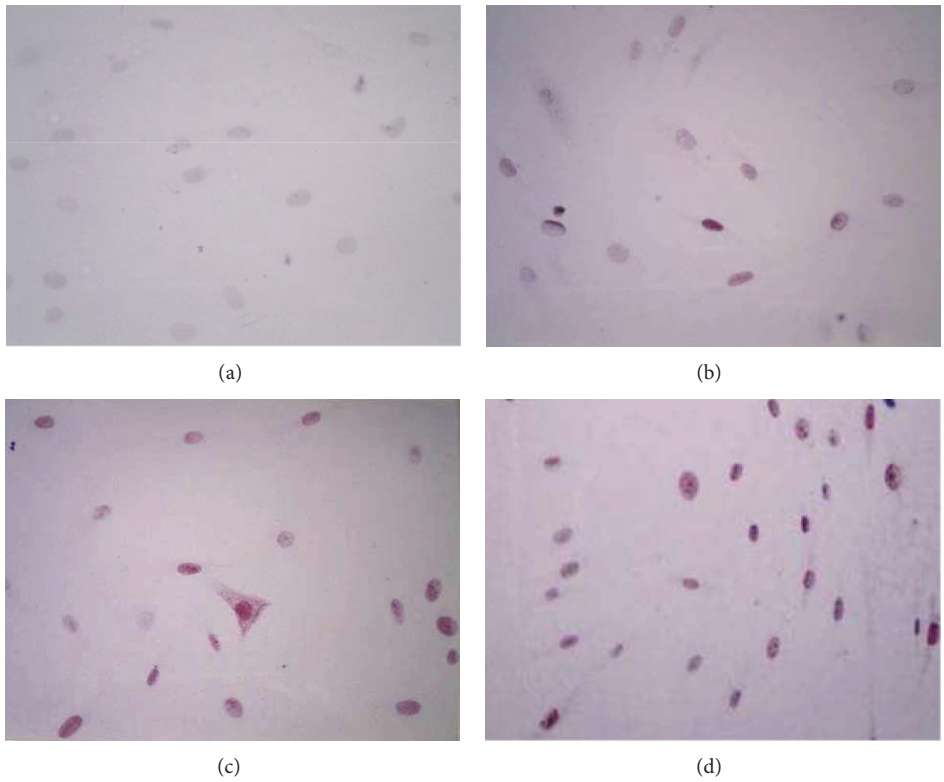

(a) (b) (c) (d)

Figure 1: Immunohistochemical detection of PCNA expression in myoblasts after preconditioning with serum starvation (IHC × 400). (a), (b), (c), and (d) were from control, laser, 10% FBS, and 20% FBS group, respectively, the grouping as described above. There was obvious difference in the levels of PCNA expression between each group.

by t-test. A statistical probability of $P < 0.05$ was considered to be significant.

3. Results

3.1. Growth Characteristics of Myoblasts. The enriched primary myoblasts displayed remarkable proliferation potential. Pure myoblast cultures have been expanded beyond 30 population doublings. There were no detectable changes of growth rate or cell morphology even after extensive proliferation *in vitro*. Because of the extraordinary growth potential of primary myoblasts under these culture conditions, the serum-starved pretreatment described above was made possible and was not limited by the number of available cells. The cells used for laser irradiation were passaged 3–6 times unless otherwise indicated.

3.2. Effect of LILI on PCNA Expression of Myoblasts. PCNA, proliferating cell nuclear antigen, is the necessary component for DNA duplication of cell chromatosome. Its synthesis and expression were related to cell proliferative cycle. Quantification of PCNA expression is one kind of simple and feasible method for evaluating cell proliferative activity. In this study, the expression of PCNA was detected by immunohistochemical method (IHC) and assessed using semiquantitative analysis. Ours results showed that, 24 hours after laser irradiation, PCNA expression in the laser group was significantly higher than in the control group and the same in the 10% FBS group but less than that of 20% FBS group (Figure 1).

3.3. Effect of LILI on Proliferation Index of Myoblasts. Proliferation index (PI) is defined as the total number of cells in all the phases of the cell cycle (G0, G1, S, G2, and M phase) divided by the number of cells that went into division (S, G2, and M phase); that is, PI = (S + G2/M)/(G0/G1 + S + G2/M). The proliferation index reflects the percentage of proliferative cells in the S phase and G2/M phase of the cell cycle and can be used with the PCNA expression assay to give a more complete understanding of growth characteristics of myoblasts. As shown in Figures 2 and 3, twenty-four hours after laser irradiation or serum-refeeding, more myoblasts (about 42%) were in S phase and G2/M phase of the cell cycle as compared with myoblasts in the control group (less than 12%), whereas the values were slightly lower than that of myoblasts in 20% FBS group (approximately 65%). The results here suggested that more myoblasts entered the proliferative phase after LILI, which was consistent with the above data.

3.4. Effect of LILI on Expression of Cell-Cycle Regulatory Proteins of Myoblasts. The division cycle of eukaryotic cells is regulated by a family of cell-cycle regulatory proteins (also known as cyclin) and the cyclin-dependent kinases (CDK) complex, of which cyclin D and cyclin A are the key molecules that can trigger cell-cycle entry, thus driving the cells from

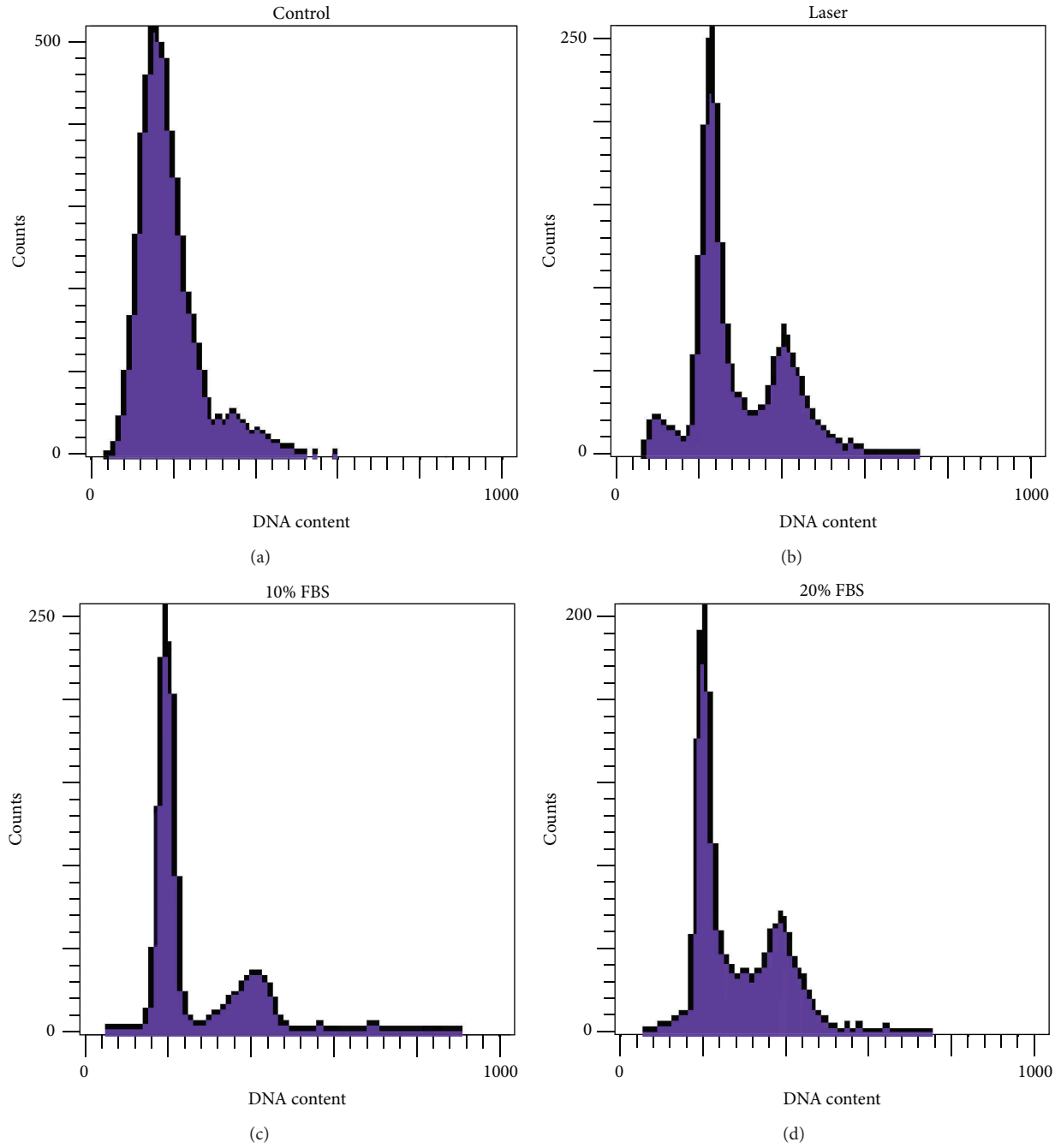

Figure 2: Effects of LLLI on the proliferation index of myoblasts 24 h after irradiation/refeeding. Typical flow cytometric DNA histograms of the myoblasts from control (a), laser irradiation (b), 10% FBS (c), and 20% FBS (d) groups, respectively.

quiescence to the mitotic cycle. The periodic change of their expression is synchronized to cell-cycle progression. As presented in Figure 4, only a slight expression of cyclin D was detected in control cells, whereas the cyclin D protein levels showed an approximately fivefold or sevenfold increase just 30 min after irradiation/refeeding in irradiated or serum-refed cells, respectively. The expression of Cyclin A was also induced 2 h after irradiation in the irradiated cells and the expression level was compatible with its induction in the serum-refed cells, whereas its expression was almost undetectable in nonirradiated control cells. These results suggested that LILI could modulate early cell-cycle regulatory genes and promote cell-cycle entrance from the G0/G1 phase in myoblasts, thereby facilitating the cell-cycle progression and increasing their proliferative potential after serum-starved pretreatment.

4. Discussion

It is well known that skeletal muscle repair is a highly synchronized process involving the activation of various cellular responses [11, 14]. Among these, myogenic stem cells,

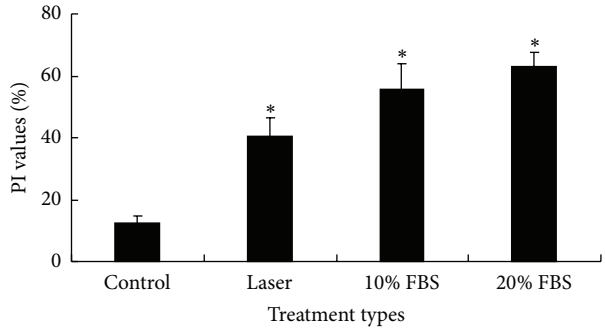

Figure 3: Cartogram of flow cytometric analysis about the proliferation index of myoblasts from each group as described above. Data are means ± SEM. $^{*}P < 0.05$, as compared with control.

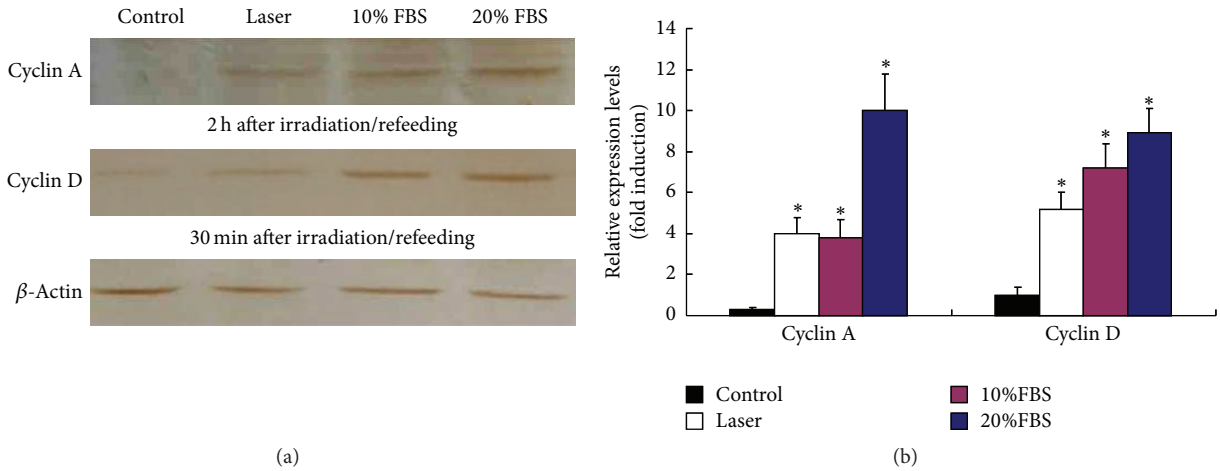

Figure 4: Western blot analysis of cyclin D and cyclin A protein expression after irradiation/refeeding (a). The expression levels of cyclin D and cyclin A were subsequently measured by densitometric analysis (b). The relative protein expression values were normalized to that of β-actin. $^{*}P < 0.05$ compared with nontreated controls.

also known as myoblasts, play a crucial role in this process. In adult skeletal muscle, the number of myoblasts was few and most of them were normally dormant, which made tissue regeneration and function repair difficult following muscle injury [15]. Yet, under the action of exogenous stimulus such as growth factors, these cells could be activated to enter the mitotic cycle and proliferate and further fuse each other to form new muscle fibers, which eventually led to the replacement of injured ones and rapid muscle regeneration [16]. Previous results have demonstrated that following LILI the irradiated site of the injured skeletal muscle featured more newborn myofiber formation, suggesting that the major candidates for muscle regeneration responding to laser irradiation may also be myoblasts [9, 17].

So far, however, many laboratory results remain controversial regarding the laser-induced photobiomodulatory effects, and differences of the irradiation parameters and growth conditions used in various studies complicate the issue of making meaningful comparisons [18–20]. In this study, the low-energy helium-neon laser (632.8 nm) with a power density of approximately 6 mW/cm^2 was used for myoblasts irradiation *in vitro*. This treatment dosage (power density and irradiation time) was found to be optimal for biostimulation of myoblasts proliferation, based on a series of preliminary experiments with the cell cultures. In our pre-experiment, three different energy densities (6 mW/cm^2 with 1 min, 3 min or 10 min comprising 0.36, 1.08, or 3.6 J/cm^2, resp.) were used. We initially investigated the effect of He-Ne laser with different irradiation times on the cell number and myotube formation to determine the optimal energy density for LILI-induced biological effect. We found that irradiation for 3 min could produce maximal biomodulation on myoblasts. Thus, the energy density which gave the best preliminary results (3 min) was used in the present study where cells were serum starved, given that the cellular response to LILI mainly depended on the initial physiological state of the target cells [3, 4, 21, 22]. So in the next experiment, previous to laser irradiation, myoblasts were initially pretreated for 36 h with serum-deficient medium when grown to nearly confluent and then either refed with 10% FBS or subjected to laser irradiation. The cells had been previously reported to enter quiescence upon serum starvation which can only maintain survival of young postmitotic cells, so that the physiological state of myoblasts *in vivo* was simulated

and the cellular response to LILI could be screened out independently.

However, in this paper, an interesting aspect of the nonirradiated control myoblasts was that these cells, which were maintained throughout in serum-free cultures conditions, also display a little of cell proliferation as shown in Figure 3. In general, the cell cultured in the absence of serum could neither proliferate as usual [23] nor be activated by other stimuli such as LILI [24]. Nevertheless, the growth mediums (Ham's F-10) used in this experiment for myoblasts *in vitro* culture somehow contained the component of serum according to literature [25], which thus contributed to the low degree of proliferation index of myoblasts in the control group, despite the fact that this kind of cell proliferation in serum-free medium was actually a type of dysfunctional proliferation. Yet, as indicated in our results, this type of dysfunctional proliferation or proliferation imbalance in myoblasts under serum-deficient conditions could be improved notably by LILI. As previously mentioned, in adult skeletal muscle, myoblasts were normally dormant, but once injured they could be activated to initiate the proliferation cycle. If the activated myoblasts could proliferate in a normal way, the injured muscle could automatically renew themselves and LILI can just accelerate this regeneration process by indirect photobiomodulation (PBM) [4, 21]. Whereas, if these cells were in a state of dysfunctional proliferation (just like under serum-starved conditions *in vitro*), LILI would directly promote the proliferation of myoblasts *in vivo* and thus substantially facilitate the recovery of muscle injuries.

Researches have shown that the expression of PCNA, an early cell-cycle protein, which is upregulated in the late G1 phase, could be markedly affected by low intensity laser irradiation [26]. In the present experiment, after 36 h of serum starvation followed by LILI, PCNA protein levels as well as PI value were also evaluated in primary myoblasts. It has been demonstrated that a growing cell population is composed of cells in all the phases of cell cycle (G1, S, G2, and M phase), and the estimation of cell subpopulations in S phase and G2/M phase of the cell cycle can be used for cell proliferation evaluation [27]. Normally, there was no obvious PCNA expression in cells of G0/G1 phase, whereas its expression in late G1 phase was substantially increased. The expression reached a peak in S phase and decreased significantly in G2/M phase. The periodical variations in PCNA expression, as well as PI value, were consistent with the phases of cellular DNA synthesis and thus can reflect proliferation activity of the cultured myoblasts [28]. Our results showed that PCNA expression and the proportion of myoblasts in the S/G2/M phase of cell cycle greatly increased 24 hours after laser irradiation, suggesting that LILI could drive more myoblasts from the quiescent G0/G1 phase entering into mitotic phase and thus enhance their proliferation capacity, which was further confirmed by the upregulated expressions of cyclin D and cyclin A.

As is well known, cyclin D and cyclin A are the initiating factors for G0/G1 conversion and their inducible expression contributed to cell-cycle progression of the LILI-activated myoblasts. Previous studies [26, 29] of mouse myogenic cells under low growth conditions have established that LILI could stimulate cells into the cell cycle up to 24 h after irradiation and the induction of cyclin D1 expression was detected in the irradiated cells as early as 6 min after irradiation. Thus, it is more likely that the increased proliferation ability following LILI involves the translation of cyclins that are required for entrance and progression through the G1 phase of the cell cycle. Quantitative results of western blot analysis in this experiment showed that 36 h after serum withdrawal, cyclin D and cyclin A had only trace expression in control cells, suggesting that myoblasts had been synchronized to the G0/G1 phase after serum starvation; while in a very short time after irradiation, the expressions of cyclin D and cyclin A increased obviously. Thus, these findings along with previous results imply that LILI mediates its stimulative effect on myoblasts proliferation by affecting very early events in the cell cycle, such as the inducible expressions of early cell-cycle regulatory genes.

Further, in a preliminary experiment we also found that LILI with different energy densities had dissimilar influences on myoblasts growth *in vitro* (data not shown). In this study, LILI for 1 min had weak promotion on cell number and cell-cycle progression; however, laser irradiation for 10 min could somehow inhibit myoblasts proliferation, indicating that the biomodulatory effect of LILI on primary myoblasts is dose-dependent, which is also consistent with the biological characteristics of LILI.

In our experiment, the ability of irradiated myoblasts to survive and proliferate in the absence of serum sustenance is remarkable as compared with the nonirradiated cells. Laser irradiation appears to be analogous to the components of serum responsible for myoblasts survival and growth whether myoblasts being dormant *in vivo* or arrested in G0/G1 phase *in vitro* and in some ways, it can substitute for the myoblasts serum requirement to reenter the cell cycle from quiescence. It also stands to reason that the cellular response to LILI would be weaken or absent if the myoblasts were initially maintained under serum-sufficient growth conditions instead of the serum-deficient culture medium, particularly considering the fact that, for the laser-induced photobiomodulation, the initial physiological state of the target cells is critical for the treatment response [21, 22, 30, 31].

5. Conclusion

Taken together, our studies suggest that myoblasts in culture can be promoted from quiescence into cell proliferation cycle in response to laser irradiation at a certain fluence. These results also indicate that LILI affects early cell-cycle regulatory genes and enhances proliferative potential of myoblasts, thereby increasing cell proliferation and contributing to muscle regeneration *in vivo*.

Conflict of Interests

The authors declare that there is no conflict of interests regarding the publication of this paper.

Authors' Contribution

Cui-Ping Zhang, Shao-Dan Li, Yan Chen, and Yan-Ming Jiang contributed equally to this work.

Acknowledgments

This work was supported by the National Natural Science Foundation of China (81171798, 81121004, and 81230041), Beijing Municipal Natural Science Foundation (7142124), and the National Basic Science and Development Program (973 Program, 2012CB518105).

References

[1] C. Y. Liu and P. Zhu, *Intranasal Low Intensity Laser Therapy*, People's Military Medical Press, Beijing, China, 2009.

[2] X. Liu, J. Zhang, J. Lu, and T. C. Liu, "Laser acupuncture reduces body fat in obese female undergraduate students," *International Journal of Photoenergy*, vol. 2012, Article ID 730351, 4 pages, 2012.

[3] T. Karu, *The Science of Low-Power Laser Therapy*, Gordon and Breach, Amsterdam, The Netherlands, 1998.

[4] T. C. Liu, Y. Y. Liu, E. X. Wei, and F. H. Li, "Photobiomodulation on stress," *International Journal of Photoenergy*, vol. 2012, Article ID 628649, 11 pages, 2012.

[5] R. Lubart, M. Eichler, R. Lavi, H. Friedman, and A. Shainberg, "Low-energy laser irradiation promotes cellular redox activity," *Photomedicine and Laser Surgery*, vol. 23, no. 1, pp. 3–9, 2005.

[6] S. B. Rabelo, A. B. Villaverde, R. A. Nicolau, M. A. C. Salgado, M. D. S. Melo, and M. T. T. Pacheco, "Comparison between wound healing in induced diabetic and nondiabetic rats after low-level laser therapy," *Photomedicine and Laser Surgery*, vol. 24, no. 4, pp. 474–479, 2006.

[7] C. S. Enwemeka, "Intricacies of dose in laser phototherapy for tissue repair and pain relief," *Photomedicine and Laser Surgery*, vol. 27, no. 3, pp. 387–393, 2009.

[8] S. K. Kazem Shakouri, J. Soleimanpour, Y. Salekzamani, and M. R. Oskuie, "Effect of low-level laser therapy on the fracture healing process," *Lasers in Medical Science*, vol. 25, no. 1, pp. 73–77, 2010.

[9] J. Nakano, H. Kataoka, J. Sakamoto, T. Origuchi, M. Okita, and T. Yoshimura, "Low-level laser irradiation promotes the recovery of atrophied gastrocnemius skeletal muscle in rats," *Experimental Physiology*, vol. 94, no. 9, pp. 1005–1015, 2009.

[10] P. C. L. Silveira, L. A. da Silva, C. A. Pinho et al., "Effects of low-level laser therapy (GaAs) in an animal model of muscular damage induced by trauma," *Lasers in Medical Science*, vol. 28, no. 2, pp. 431–436, 2013.

[11] S. B. P. Chargé and M. A. Rudnicki, "Cellular and molecular regulation of muscle regeneration," *Physiological Reviews*, vol. 84, no. 1, pp. 209–238, 2004.

[12] A. J. Wagers and I. M. Conboy, "Cellular and molecular signatures of muscle regeneration: current concepts and controversies in adult myogenesis," *Cell*, vol. 122, no. 5, pp. 659–667, 2005.

[13] X. Shi and D. J. Garry, "Muscle stem cells in development, regeneration, and disease," *Genes and Development*, vol. 20, no. 13, pp. 1692–1708, 2006.

[14] A. Asakura, P. Seale, A. Girgis-Gabardo, and M. A. Rudnicki, "Myogenic specification of side population cells in skeletal muscle," *The Journal of Cell Biology*, vol. 159, no. 1, pp. 123–134, 2002.

[15] M. Buckingham, "Skeletal muscle formation in vertebrates," *Current Opinion in Genetics and Development*, vol. 11, no. 4, pp. 440–448, 2001.

[16] M. Buckingham, "Myogenic progenitor cells and skeletal myogenesis in vertebrates," *Current Opinion in Genetics and Development*, vol. 16, no. 5, pp. 525–532, 2006.

[17] K. Rochlin, S. Yu, S. Roy, and M. K. Baylies, "Myoblast fusion: when it takes more to make one," *Developmental Biology*, vol. 341, no. 1, pp. 66–83, 2010.

[18] X. G. Liu, Y. J. Zhou, T. C. Liu, and J. Q. Yuan, "Effects of low-level laser irradiation on rat skeletal muscle injury after eccentric exercise," *Photomedicine and Laser Surgery*, vol. 27, no. 6, pp. 863–869, 2009.

[19] A. C. Amaral, N. A. Parizotto, and T. F. Salvini, "Dose-dependency of low-energy HeNe laser effect in regeneration of skeletal muscle in mice," *Lasers in Medical Science*, vol. 16, no. 1, pp. 44–51, 2001.

[20] H. Ma, Y. X. Li, H. L. Chen, Y. X. Cui, and T. C. Y. Liu, "Effects of low-intensity laser irradiation on wound healing in diabetic rats," *International Journal of Photoenergy*, vol. 2012, Article ID 838496, 7 pages, 2012.

[21] T. C. Y. Liu, D. F. Wu, L. Zhu, P. Peng, L. Liu, and X. B. Yang, "Microenvironment dependent photobiomodulation on function-specific signal transduction pathways," *International Journal of Photoenergy*, vol. 2014, Article ID 904304, 8 pages, 2014.

[22] T. Karu, "Photobiology of low-power laser effects," *Health Physics*, vol. 56, no. 5, pp. 691–704, 1989.

[23] M. Wu and T. C. Liu, "Single-cell analysis of protein kinase C activation during anti-apoptosis and apoptosis induced by laser irradiation," *Photomedicine and Laser Surgery*, vol. 25, no. 2, pp. 129–130, 2007.

[24] M. A. Pogrel, J. W. Chen, and K. Zhang, "Effects of low-ener-gy gallium-aluminum-arsenide laser irradiation on cultured fibroblasts and keratinocytes," *Lasers in Surgery and Medicine*, vol. 20, no. 4, pp. 426–432, 1997.

[25] D. Loutradis, P. Drakakis, K. Kallianidis et al., "Biological factors in culture media affecting in vitro fertilization, preimplantation embryo development, and implantation," *Annals of the New York Academy of Sciences*, vol. 900, pp. 325–335, 2000.

[26] N. Ben-Dov, G. Shefer, A. Irinitchev, A. Wernig, U. Oron, and O. Halevy, "Low-energy laser irradiation affects satellite cell proliferation and differentiation in vitro," *Biochimica et Biophysica Acta*, vol. 1448, no. 3, pp. 372–380, 1999.

[27] L. H. Hartwell and M. B. Kastan, "Cell cycle control and cancer," *Science*, vol. 266, no. 5192, pp. 1821–1828, 1994.

[28] P. Kurki, M. Vanderlaan, F. Dolbeare, J. Gray, and E. M. Tan, "Expression of proliferating cell nuclear antigen (PCNA)/cyclin during the cell cycle," *Experimental Cell Research*, vol. 166, no. 1, pp. 209–219, 1986.

[29] G. Shefer, I. Barash, U. Oron, and O. Halevy, "Low-energy laser irradiation enhances de novo protein synthesis via its effects on translation-regulatory proteins in skeletal muscle myoblasts," *Biochimica et Biophysica Acta*, vol. 1593, no. 2-3, pp. 131–139, 2003.

[30] Y. Y. Xu, T. C. Y. Liu, and L. Cheng, "Photobiomodulation process," *International Journal of Photoenergy*, vol. 2012, Article ID 374861, 7 pages, 2012.

[31] T. Karu, L. Pyatibrat, and G. Kalendo, "Irradiation with He-Ne laser increases ATP level in cells cultivated in vitro," *Journal of Photochemistry and Photobiology B: Biology*, vol. 27, no. 3, pp. 219–223, 1995.

Hindawi Publishing Corporation
International Journal of Photoenergy
Volume 2014, Article ID 785386, 6 pages
http://dx.doi.org/10.1155/2014/785386

Research Article

Effects of Low-Level Laser Therapy and Eccentric Exercises in the Treatment of Patellar Tendinopathy

Xiao-Guang Liu,[1] Lin Cheng,[1,2] and Ji-Mei Song[1]

[1] *Laboratory of Laser Sports Medicine, South China Normal University, Guangzhou 510006, China*
[2] *Sichuan University for Nationalities, Sichuan 626001, China*

Correspondence should be addressed to Xiao-Guang Liu; tygx@jnu.edu.cn

Received 18 April 2014; Revised 4 July 2014; Accepted 7 July 2014; Published 16 July 2014

Academic Editor: Timon Cheng-Yi Liu

The study aims to investigate if low-level laser therapy (LLLT) combined with eccentric exercises could more effectively treat patellar tendinopathy than LLLT alone and eccentric exercises alone. Twenty-one patients with patellar tendinopathy were randomized to three groups: laser alone, exercise alone, or laser plus exercise, with seven in each group. Laser irradiations were administered at the inferior pole of the patella and the two acupoints of Extra 36 (Xiyan) with the intensity of 1592 mW/cm^2. Eccentric training program consisted of three sets of 15 repetitions of unilateral squat on level ground. All patients received six treatments per week for four weeks. Knee pain and function and quadriceps muscle strength and endurance were evaluated at baseline and the end of treatment. After the 4-week intervention, all groups showed significant improvements in all the outcomes ($P < 0.01$). The laser + exercise group had significantly greater improvements in all the outcomes than the other two groups ($P < 0.05$), except nonsignificant difference in pain relief between the laser + exercise group and the laser group. In conclusion, LLLT combined with eccentric exercises is superior to LLLT alone and eccentric exercises alone to reduce pain and improve function in patients with patellar tendinopathy.

1. Introduction

Patellar tendinopathy is an overuse injury of the patellar tendon and most prevalent in sports involving some form of jumping, such as volleyball, basketball, soccer, and athletics. Patients with patellar tendinopathy clinically manifested activity-related, anterior knee pain associated with focal patellar-tendon tenderness [1, 2]. Histopathological and biochemical evidences indicate that patellar tendinopathy is mainly due to collagen fiber degeneration and inflammation plays a minor role in its pathophysiology [3]. There are many treatment methods for patellar tendinopathy, including anti-inflammatory drugs, massage, eccentric training, low-level laser, ultrasound, surgery, and other modalities [3, 4]. However, no ideal treatment has emerged for the management of patellar tendinopathy.

Eccentric training has proven to be a useful treatment for patellar tendinopathy in a number of randomized controlled trials [5, 6]. Researchers have recommended eccentric training as an important conservative treatment for patellar tendinopathy [4, 7]. However, eccentric training intervention needs a fairly long period and often induces some transient discomfort and pain. To increase efficacy and reduce exercise-induced pain, some adjunctive interventions have been added to eccentric training for treating patellar tendinopathy. Dimitrios et al. [8] have shown that eccentric training and static stretching exercises produced a larger effect than eccentric training alone in the treatment of patellar tendinopathy. In a clinical trial to treat patellar tendinopathy by Cannell et al. [9], cryotherapy was used to reduce pain of the patellar tendon after eccentric drop squats.

Low-level laser therapy (LLLT) has been widely applied in the field of sports medicine. LLLT can exert effects of reducing inflammation and pain and promoting tissues regeneration in the treatment of soft tissue injuries [10–12]. Bjordal et al. [13] and Tumilty et al. [14] have reviewed LLLT for tendinopathy and have founded that LLLT can potentially be effective in treating tendinopathy when recommended dosages are used. Stergioulas et al. [15] have shown that LLLT can accelerate clinical recovery from Achilles tendinopathy when added to

an eccentric training regimen. However, it remains unclear whether LLLT can bring about additional benefits to eccentric training in the treatment of patellar tendinopathy.

In the current study, we conducted a randomized controlled trial to investigate if LLLT combined with eccentric exercises could more effectively treat patients with patellar tendinopathy than LLLT alone and eccentric exercises alone.

2. Materials and Methods

The study protocol was approved by the Ethics Committee of the Faculty of South China Normal University, Guangzhou, China. Written informed consent was obtained from each participant prior to the start of treatment.

2.1. Subjects and Groups. Twenty-one patients with patellar tendinopathy aged 18–23 years were enrolled in this study. All patients were male undergraduate students studying at School of Physical Education and Sports Science of South China Normal University. The study was conducted at the Laboratory of Laser Sports Medicine of South China Normal University in Guangzhou in April and May 2013.

The selection criteria for the study were the following [1–3]:

(i) unilateral painful activity-related symptoms from the patellar tendon region for at least three months;

(ii) tenderness with palpation over the inferior pole of the patella;

(iii) no history of trauma to the knee;

(iv) unsuccessful conservative treatment before entering the study, but not in the preceding one month;

(v) no other current knee or lower extremity problems including chondromalacia, muscle strains, and hip or ankle injuries;

(vi) positive decline squat test. This is a clinical diagnostic test.

All patients were randomly divided into three groups: (1) laser group receiving low-level laser treatment alone; (2) exercise group receiving eccentric exercise treatment alone; (3) laser + exercise group receiving low-level laser and eccentric exercise treatment, seven in each group.

2.2. Laser Irradiation Procedure. A GaAlAs laser (Model LD-1, Guangzhou, China) with a continuous output power of 0–500 mW and wavelength of 810 nm was used. The subjects in the laser group and the laser + exercise group received laser irradiations with the intensity of 1592 mW/cm^2 (power: 200 mW, beam diameter: 0.4 cm) at the inferior pole of the patella for 10 minutes and the two acupoints of Extra 36 (Xiyan) medial and lateral to the patellar tendon for 5 minutes each acupoint, once daily, six times per week, for four weeks. The laser irradiations were applied directly to the skin of the points with a perpendicular beam.

2.3. Eccentric Exercise Program. The eccentric training was the same for the exercise group and the laser + exercise group. As eccentric exercises, participants carried out three sets of 15 repetitions of unilateral squat on a flat floor. The squat was performed at a slow speed of 30 counts in 10 seconds at every treatment session [8], following an audio file. As they moved from the standing to the squat position, the quadriceps muscle and patellar tendon by inference were loaded eccentrically; no following concentric loading was done, as the noninjured leg was used to get back to the start position. At the beginning the load consisted of the body weight and participants were standing with all their body weight on the injured leg. The load was increased by 5 kg per week in a backpack. Between each set there was a one-minute rest. After the eccentric training, double lean-back quadriceps stretch was performed as described by Walker [16]. Each stretch lasted one minute. Each training session was to be completed once daily, six times per week, for four weeks. The subjects in the laser + exercise group received the laser treatment after each training session.

2.4. Outcome Measures. Perceived pain, functional capacity of knee, and strength and endurance of the quadriceps muscle were evaluated at baseline and the end of treatment.

Pain intensity was quantified on a 100 mm visual analogue scale (VAS). A modified Victorian Institute of Sport Assessment (VISA) questionnaire was used to evaluate the functional capacity of knee in patients with patellar tendinopathy, which consisted of ten items to cover walking, squatting, standing, running, jumping, weight-bearing movement, training, and sports performance [17]. The range of scores was from 0 to 100 and the highest score represented the maximum of functional capacity.

Maximal isometric strength of the quadriceps muscle was measured in a sitting position with both hip and knee at 90° with a leg extension ergometer (Model NH-3000W, Seoul, Korea). Relative muscle strength was calculated as maximal isometric strength divided by body weight. Quadriceps muscle endurance was evaluated using a single-leg wall squat test. The test was conducted as described by Beck and Norling [18]. During the test, subjects stood comfortably on both feet with their back against av smooth wall. They then slid their back down the wall until a 90° angle at the hip and knee was achieved. One foot was lifted off the ground, at which time the stop watch was started. The watch was stopped when subjects had to return the raised foot to the ground. Measures were taken in seconds.

2.5. Statistical Analysis. Data were expressed as mean ± standard deviation. Differences between before and after treatment in each group were analyzed by paired t-tests. Differences between group means were analyzed using one-way ANOVA with post hoc test. The statistical level of significance was set at $P < 0.05$. SPSS 17.0 statistical software was used for the statistical analysis.

Table 1: Changes in VAS score before and after treatment in all therapy groups.

Group	Before treatment	After treatment	Change over time
Laser	67.86 ± 13.18	15.00 ± 13.54**	52.86 ± 12.20
Exercise	65.71 ± 15.39	19.29 ± 12.93**	46.43 ± 10.69
Laser + exercise	67.86 ± 12.20	5.00 ± 4.08**	62.86 ± 10.35#

Asterisks indicate significant differences from pretreatment (** $P < 0.01$). Crosses indicate significant differences from the exercise group (# $P < 0.05$).

Table 2: Changes in modified-VISA score before and after treatment in all therapy groups.

Group	Before treatment	After treatment	Change over time
Laser	63.14 ± 9.75	88.14 ± 7.22**	25.00 ± 6.40
Exercise	67.00 ± 10.05	90.71 ± 7.85**	23.71 ± 5.83
Laser + exercise	58.86 ± 12.62	96.57 ± 2.07**	37.71 ± 11.77△#

Asterisks indicate significant differences from pretreatment (** $P < 0.01$). Triangles indicate significant differences from the laser group (△ $P < 0.05$). Crosses indicate significant differences from the exercise group (# $P < 0.05$).

3. Results

3.1. Pain. There were no significant differences for VAS score at baseline between any groups (Table 1). After 4 weeks of intervention, all the groups exhibited significant pain reductions ($P < 0.01$). The mean VAS scores in the laser group, the exercise group, and the laser + exercise group were reduced by 52.86, 46.43, and 62.86 points (percent reductions: 77.9%, 70.1%, and 92.6%), respectively. The proportion of patients who became pain free was 2/7 (28.6%) in the laser + exercise group and 1/7 (14.3%) in the laser group within four weeks. No patient became pain free in the exercise group. The drop of VAS score in the laser + exercise group was significantly greater than in the exercise group. There was no significant difference for VAS score after treatment between the laser group and the exercise group.

3.2. Functional Capacity. There was no difference for modified-VISA score of knee function at baseline between any groups (Table 2). After 4 weeks of intervention, all groups exhibited significant improvements in functional capacity of knee ($P < 0.01$). The mean modified-VISA scores in the laser group, the exercise group, and the laser + exercise group were increased by 25.00, 23.71, and 37.71 points (percentage increment: 39.6%, 35.4%, and 64.1%), respectively. The laser + exercise group showed a significantly greater improvement in functional capacity of knee than the other two groups ($P < 0.05$). There was no significant difference in functional capacity of knee after treatment between the laser group and the exercise group.

3.3. Quadriceps Muscle Strength. There was no difference for relative quadriceps muscle strength at baseline between any groups (Table 3). After 4 weeks of intervention, all groups exhibited significant improvements in quadriceps muscle strength ($P < 0.01$). The mean relative quadriceps muscle strengths in the laser group, the exercise group, and the laser + exercise group were increased by 0.16, 0.19, and 0.31 kg/kg body weight (percentage increment: 42.1%, 50.0%, and 70.5%), respectively. The laser + exercise group had a significantly greater increment in quadriceps muscle strength than the other two groups ($P < 0.05$). There was no significant difference in quadriceps muscle strength after treatment between the laser group and the exercise group.

3.4. Quadriceps Muscle Endurance. There was no difference in quadriceps muscle endurance represented by the wall squat test time at baseline between any groups (Table 4). After 4 weeks of intervention, all groups exhibited significant improvements in quadriceps muscle endurance ($P < 0.01$). The mean times of wall squat test in the laser group, the exercise group, and the laser + exercise group were increased by 22.54, 23.14, and 40.97 seconds (percentage increment: 85.0%, 84.7%, and 149.0%), respectively. The laser + exercise group had a significantly greater improvement in quadriceps muscle endurance than the other two groups ($P < 0.05$). There was no significant difference in quadriceps muscle endurance after treatment between the laser group and the exercise group.

4. Discussion

This randomized controlled study demonstrates that LLLT combined with eccentric training can produce greater improvements in knee pain and function and quadriceps muscle strength and endurance for patients with patellar tendinopathy than LLLT alone and eccentric training alone.

VAS score and VISA-P score have been widely used in orthopedic and sports injury investigations [17, 19, 20]. In this study, pain and function in patients with patellar tendinopathy were evaluated using VAS and modified VISA-P questionnaire, respectively. LLLT and eccentric exercises reduced pain by 77.9% and 70.1% and increased the questionnaire score by 39.6% and 35.4%, respectively, over the 4-week intervention. Although there was no significant difference, LLLT was more effective for pain relief than eccentric exercises in the treatment of patellar tendinopathy. The combination of LLLT and eccentric exercises provided a pain reduction by 92.6% and a function score increment by 64.1% over the treatment period. The results indicated that LLLT can increase effects of

Table 3: Changes in relative quadriceps muscle strength before and after treatment in all therapy groups.

Group	Before treatment	After treatment	Change over time
Laser	0.38 ± 0.04	0.54 ± 0.06**	0.16 ± 0.08
Exercise	0.38 ± 0.10	0.57 ± 0.12**	0.19 ± 0.09
Laser + exercise	0.44 ± 0.14	0.75 ± 0.10**	0.31 ± 0.10$^{\triangle\#}$

Values are expressed in kg/kg body weight. Asterisks indicate significant differences from pretreatment ($^{**}P < 0.01$). Triangles indicate significant differences from the laser group ($^{\triangle}P < 0.05$). Crosses indicate significant differences from the exercise group ($^{\#}P < 0.05$).

Table 4: Changes in wall squat test time before and after treatment in all therapy groups.

Group	Before treatment	After treatment	Change over time
Laser	26.53 ± 6.79	49.07 ± 13.19**	22.54 ± 14.74
Exercise	27.33 ± 7.06	50.47 ± 10.98**	23.14 ± 12.67
Laser + exercise	27.44 ± 12.65	68.41 ± 23.92**	40.97 ± 12.63$^{\triangle\#}$

Values are expressed in seconds. Asterisks indicate significant differences from pretreatment ($^{**}P < 0.01$). Triangles indicate significant differences from the laser group ($^{\triangle}P < 0.05$). Crosses indicate significant differences from the exercise group ($^{\#}P < 0.05$).

eccentric exercises on pain relief and functional improvement of knee in the treatment of patellar tendinopathy.

Single-leg wall squat test is a simple isometric strength test to assess quadriceps muscle endurance and has been shown to be reliable and valid in physical fitness assessment [18, 21]. In this study, quadriceps muscle endurance in patients with patellar tendinopathy was measured using the functional test, while quadriceps muscle strength was measured using the leg extension ergometer. With respect to quadriceps muscle endurance, LLLT and eccentric exercises increased the squat test time after treatment by 85.0% and 84.7%, respectively. With respect to quadriceps muscle strength, LLLT and eccentric exercises increased the relative strength after treatment by 42.1% and 50.0%, respectively. Therefore, eccentric exercises seem more effective for strength improvement than LLLT in the treatment of patellar tendinopathy. After the four weeks of treatment, LLLT combined with eccentric exercises increased the squat test time by 149.0% and the relative quadriceps muscle strength by 70.5%, with greater efficacies than LLLT alone and exercise alone. The results indicated that LLLT can increase effects of eccentric exercises on strength and endurance of the quadriceps muscle in the treatment of patellar tendinopathy.

There are some factors influencing efficacy of eccentric exercise for tendinopathy, including eccentric exercise protocol, sports training during the treatment period, and subject's compliance. Some authors advocated that eccentric exercises be performed at a slow speed with mild pain [8, 22, 23]. In contrast, other authors have found exercising without induced pain to be beneficial to healing [24, 25]. This study has adopted the eccentric exercise program at a slow speed without pain and has obtained good results. To avoid painful sports activities is crucial for tendinopathy treatment, because it has been reported that eccentric training is not effective for patellar tendinopathy in volleyball players during the competitive season [26].

In accordance with our results, previous studies have shown that LLLT could exert effects on pain relief and function improvement in the treatment of tendinopathies [15, 27–29]. Bjordal et al. [27] have demonstrated that LLLT can reduce peritendinous prostaglandin E2 (PGE2) concentrations in activated Achilles tendinitis. Therefore, LLLT may reduce pain in patients with tendinopathy through modulating inflammation. On the other hand, the biostimulatory effects of LLLT on collagen fibers synthesis may be responsible for the muscle strength improvement of patients with tendinopathy, because Reddy et al. [30] have shown that LLLT can increase collagen production in healing rabbit Achilles tendon. It is well known that the therapeutic effect of LLLT is dose-dependent [13, 31]. Bjordal et al. [13] have recommended that power densities of LLLT for Achilles, patellar, and elbow tendinopathies be between 2 and 100 mW/cm^2. The results of LLLT trials for tendinopathies with the recommended power densities seem to be consistently positive [15, 27, 32]. Nonsignificant effects of LLLT have been observed in clinical trials for treating elbow tendinopathy with power densities between 100 and 500 mW/cm^2 [33, 34]. However, LLLT with power densities above 1 W/cm^2 has shown positive effects on reducing exercise-induced muscle damage and fatigue in some randomized controlled studies [35–37]. Our results showed that LLLT with an 810 nm GaAlAs laser at 1592 mW/cm^2 was significantly effective in patients with patellar tendinopathy. Of course, further researches are needed to identify the optimal intensity and dose of LLLT in the treatment of patellar tendinopathy.

5. Conclusion

Low-level laser therapy combined with eccentric exercises is superior to low-level laser therapy alone and eccentric exercises alone to reduce pain and improve function in patients with patellar tendinopathy. It is suggested that low-level laser therapy can be used as an important adjunct to eccentric exercises in the treatment of tendinopathies.

Conflict of Interests

The authors declare that there is no conflict of interests regarding the publication of this paper.

References

[1] S. J. Warden and P. Brukner, "Patellar tendinopathy," *Clinics in Sports Medicine*, vol. 22, no. 4, pp. 743–759, 2003.

[2] A. Kountouris and J. Cook, "Rehabilitation of Achilles and patellar tendinopathies," *Best Practice and Research: Clinical Rheumatology*, vol. 21, no. 2, pp. 295–316, 2007.

[3] K. M. Khan, N. Maffulli, B. D. Coleman, J. L. Cook, and J. E. Taunton, "Patellar tendinopathy: some aspects of basic science and clinical management," *British Journal of Sports Medicine*, vol. 32, no. 4, pp. 346–355, 1998.

[4] E. C. Rodriguez-Merchan, "The treatment of patellar tendinopathy," *Journal of Orthopaedics and Traumatology*, vol. 14, no. 2, pp. 77–81, 2013.

[5] C. R. Purdam, P. Johnsson, H. Alfredson, R. Lorentzon, J. L. Cook, and K. M. Khan, "A pilot study of the eccentric decline squat in the management of painful chronic patellar tendinopathy," *British Journal of Sports Medicine*, vol. 38, no. 4, pp. 395–397, 2004.

[6] P. Jonsson and H. Alfredson, "Superior results with eccentric compared to concentric quadriceps training in patients with jumper's knee: a prospective randomised study," *British Journal of Sports Medicine*, vol. 39, no. 11, pp. 847–850, 2005.

[7] H. Visnes and R. Bahr, "The evolution of eccentric training as treatment for patellar tendinopathy (jumper's knee): a critical review of exercise programmes," *British Journal of Sports Medicine*, vol. 41, no. 4, pp. 217–223, 2007.

[8] S. Dimitrios, M. Pantelis, and S. Kalliopi, "Comparing the effects of eccentric training with eccentric training and static stretching exercises in the treatment of patellar tendinopathy. A controlled clinical trial," *Clinical Rehabilitation*, vol. 26, no. 5, pp. 423–430, 2012.

[9] L. J. Cannell, J. E. Taunton, D. B. Clement, C. Smith, and K. M. Khan, "A randomised clinical trial of the efficacy of drop squats or leg extension/leg curl exercises to treat clinically diagnosed jumper's knee in athletes: pilot study," *British Journal of Sports Medicine*, vol. 35, no. 1, pp. 60–64, 2001.

[10] P. Douris, V. Southard, R. Ferrigi et al., "Effect of phototherapy on delayed onset muscle soreness," *Photomedicine and Laser Surgery*, vol. 24, no. 3, pp. 377–382, 2006.

[11] X. G. Liu, Y. J. Zhou, T. C. Y. Liu, and J. Q. Yuan, "Effects of low-level laser irradiation on rat skeletal muscle injury after eccentric exercise," *Photomedicine and Laser Surgery*, vol. 27, no. 6, pp. 863–869, 2009.

[12] A. Bibikova and U. Oron, "Promotion of muscle regeneration in the toad (Bufo viridis) gastrocnemius muscle by low-energy laser irradiation," *Anatomical Record*, vol. 235, no. 3, pp. 374–380, 1993.

[13] J. M. Bjordal, C. Couppe, and A. E. Ljunggren, "Low level laser therapy for tendinopathy. Evidence of a dose-response pattern," *Physical Therapy Reviews*, vol. 6, no. 2, pp. 91–99, 2001.

[14] S. Tumilty, J. Munn, S. McDonough, D. A. Hurley, J. R. Basford, and G. D. Baxter, "Low level laser treatment of tendinopathy: a systematic review with meta-analysis.," *Photomedicine and laser surgery*, vol. 28, no. 1, pp. 3–16, 2010.

[15] A. Stergioulas, M. Stergioula, R. Aarskog, R. A. B. Lopes-Martins, and J. M. Bjordal, "Effects of low-level laser therapy and eccentric exercises in the treatment of recreational athletes with chronic achilles tendinopathy," *The American Journal of Sports Medicine*, vol. 36, no. 5, pp. 881–887, 2008.

[16] B. Walker, *The Anatomy of Stretching*, North Atlantic Books, Berkeley, Calif, USA, 2007.

[17] P. J. Visentini, K. Khan, and J. Cook, "The VISA score: an index of severity of symptoms in patients with jumper's knee (patellar tendinosis). Victorian Institute of Sport Tendon Study Group," *Journal of Science and Medicine in Sport*, vol. 1, no. 1, pp. 22–28, 1998.

[18] B. R. Beck and T. L. Norling, "The effect of 8 mos of twice-weekly low- or higher intensity whole body vibration on risk factors for postmenopausal hip fracture," *American Journal of Physical Medicine & Rehabilitation*, vol. 89, no. 12, pp. 997–1009, 2010.

[19] E. Kremer, J. A. Hampton Atkinson, and R. J. Ignelzi, "Measurement of pain: patient preference does not confound pain measurement," *Pain*, vol. 10, no. 2, pp. 241–248, 1981.

[20] K. M. Khan, P. J. Visentini, Z. S. Kiss et al., "Correlation of ultrasound and magnetic resonance imaging with clinical outcome after patellar tenotomy: prospective and retrospective studies," *Clinical Journal of Sport Medicine*, vol. 9, no. 3, pp. 129–137, 1999.

[21] P. N. Whitehead, B. K. Schilling, D. D. Peterson, and L. W. Weiss, "Possible new modalities for the Navy physical readiness test," *Military Medicine*, vol. 177, no. 11, pp. 1417–1425, 2012.

[22] H. Alfredson, T. Pietilä, P. Jonsson, and R. Lorentzon, "Heavy-load eccentric calf muscle training for the treatment of chronic achilles tendinosis," *The American Journal of Sports Medicine*, vol. 26, no. 3, pp. 360–366, 1998.

[23] K. G. Silbernagel, R. Thomeé, P. Thomeé, and J. Karlsson, "Eccentric overload training for patients with chronic Achilles tendon pain—a randomised controlled study with reliability testing of the evaluation methods," *Scandinavian Journal of Medicine and Science in Sports*, vol. 11, no. 4, pp. 197–206, 2001.

[24] W. D. Stanish, R. T. Rubinovich, and S. Curwin, "Eccentric exercise in chronic tendinitis," *Clinical Orthopaedics and Related Research*, vol. 208, pp. 65–68, 1986.

[25] T. A. Ammar, "Microcurrent electrical nerve stimulation in tennis elbow," *Bulletin of Faculty of Physical Therapy Cairo University*, vol. 16, no. 2, 2011.

[26] H. Visnes, A. Hoksrud, J. Cook, and R. Bahr, "No effect of eccentric training on jumper's knee in volleyball players during the competitive season: a randomized clinical trial," *Clinical Journal of Sport Medicine*, vol. 15, no. 4, pp. 227–234, 2005.

[27] J. M. Bjordal, R. A. B. Lopes-Martins, and V. V. Iversen, "A randomised, placebo controlled trial of low level laser therapy for activated Achilles tendinitis with microdialysis measurement of peritendinous prostaglandin E2 concentrations," *British Journal of Sports Medicine*, vol. 40, no. 1, pp. 76–80, 2006.

[28] O. Vasseljen Jr., N. Hoeg, B. Kjeldstad, A. Johnsson, and S. Larsen, "Low level laser versus placebo in the treatment of tennis elbow," *Scandinavian Journal of Rehabilitation Medicine*, vol. 24, no. 1, pp. 37–42, 1992.

[29] Ö. Öken, Y. Kahraman, F. Ayhan, S. Canpolat, Z. R. Yorgancioglu, and Ö. F. Öken, "The short-term efficacy of laser, brace, and ultrasound treatment in lateral epicondylitis: a prospective, randomized, controlled trial," *Journal of Hand Therapy*, vol. 21, no. 1, pp. 63–68, 2008.

[30] G. K. Reddy, L. Stehno-Bittel, and C. S. Enwemeka, "Laser photostimulation of collagen production in healing rabbit Achilles tendons," *Lasers in Surgery and Medicine*, vol. 22, no. 5, pp. 281–287, 1998.

[31] R. Á. B. Lopes-Martins, S. C. Penna, J. Joensen, V. Vereid Iversen, and J. Magnus Bjordal, "Low level laser therapy [LLLT] in inflammatory and rheumatic diseases: a review of therapeutic mechanisms," *Current Rheumatology Reviews*, vol. 3, no. 2, pp. 147–154, 2007.

[32] A. Stergioulas, "Effects of low-level laser and plyometric exercises in the treatment of lateral epicondylitis," *Photomedicine and Laser Surgery*, vol. 25, no. 3, pp. 205–213, 2007.

[33] M. Krasheninnikoff, N. Ellitsgaard, B. Rogvi-Hansen et al., "No effect of low power laser in lateral epicondylitis," *Scandinavian Journal of Rheumatology*, vol. 23, no. 5, pp. 260–263, 1994.

[34] E. S. Papadopoulos, R. W. Smith, M. I. D. Cawley, and R. Mani, "Low-level laser therapy does not aid the management of tennis elbow," *Clinical Rehabilitation*, vol. 10, no. 1, pp. 9–11, 1996.

[35] D. A. Sussai, P. D. T. C. D. Carvalho, D. M. Dourado, A. C. G. Belchior, F. A. Dos Reis, and D. M. Pereira, "Low-level laser therapy attenuates creatine kinase levels and apoptosis during forced swimming in rats," *Lasers in Medical Science*, vol. 25, no. 1, pp. 115–120, 2010.

[36] E. C. P. Leal Junior, R. Á. B. Lopes-Martins, A. A. Vanin et al., "Effect of 830 nm low-level laser therapy in exercise-induced skeletal muscle fatigue in humans," *Lasers in Medical Science*, vol. 24, no. 3, pp. 425–431, 2009.

[37] E. C. P. Leal, R. Á. B. Lopes-Martins, F. Dalan et al., "Effect of 655-nm low-level laser therapy on exercise-induced skeletal muscle fatigue in humans," *Photomedicine and Laser Surgery*, vol. 26, no. 5, pp. 419–424, 2008.

Hindawi Publishing Corporation
International Journal of Photoenergy
Volume 2014, Article ID 637601, 7 pages
http://dx.doi.org/10.1155/2014/637601

Research Article

Photodynamic Action of LED-Activated Curcumin against *Staphylococcus aureus* Involving Intracellular ROS Increase and Membrane Damage

Yuan Jiang,[1] Albert Wingnang Leung,[2] Heyu Hua,[2] Xiancai Rao,[3] and Chuanshan Xu[2,4]

[1] *Department of Rehabilitation Medicine, Second Affiliated Hospital, Chongqing Medical College, Chongqing 400010, China*
[2] *School of Chinese Medicine, Faculty of Medicine, The Chinese University of Hong Kong, Shatin, Hong Kong*
[3] *Department of Microbiology, College of Basic Medical Science, Third Military Medical University, Chongqing 400038, China*
[4] *Shenzhen Research Institute, The Chinese University of Hong Kong, Shenzhen 518057, China*

Correspondence should be addressed to Albert Wingnang Leung; awnleung@cuhk.edu.hk and Chuanshan Xu; xcshan@163.com

Received 27 January 2014; Accepted 28 April 2014; Published 14 May 2014

Academic Editor: Timon Cheng-Yi Liu

Aim. To investigate the effect of photodynamic action of LED-activated curcumin on cell viability, membrane permeability, and intracellular reactive oxygen species of *Staphylococcus aureus*. *Methods*. *Staphylococcus aureus* was incubated with the different concentrations of curcumin for 60 min and then irradiated by blue light with the wavelength of 470 nm and with light dose of 3 J/cm^2. The colony forming unit assay was used to investigate photocytotoxicity of curcumin on *Staphylococcus aureus*, confocal laser scanning microscopy (CLSM) and flow cytometry (FCM) for assaying membrane permeability, FCM analysis with DCFH-DA staining for measuring the intracellular ROS level, and transmission electron microscopy (TEM) for observing morphology and structure. *Results*. Blue light-activated curcumin significantly killed *Staphylococcus aureus* in a curcumin dose-dependent manner. TEM observed remarkable structural damages in *S. aureus* after light-activated curcumin. More red fluorescence of PI dye was found in *S. aureus* treated by blue light-activated curcumin than in those of the controlled bacterial cells. Intracellular ROS increase was observed after light-activated curcumin. *Conclusion*. Blue light-activated curcumin markedly damaged membrane permeability, resulting in cell death of *Staphylococcus aureus* and highlighted that intracellular ROS increase might be an important event in photodynamic killing of *Staphylococcus aureus* in the presence of curcumin.

1. Introduction

Staphylococcus aureus is one of the commonest opportunistic pathogens in veterinary medicine, which usually causes skin and soft tissue infections as well as respiratory infection diseases and bacteremia [1–4]. Antibiotics are the commonest drugs currently used in the clinical settings. However, prolonged antibiotic treatment easily resulted in the emergency of antibiotic-resistant bacterial strains, which affect and lower the therapeutic efficacy of antibiotics. Therefore, there is an urgent need in exploring novel and more efficient strategies for eradicating *S. aureus*.

Photodynamic therapy (PDT) is an alternative way to eradicate fast growing cells and tissues. In PDT, nontoxic dyes, also called photosensitizers, are activated by a harmless visible light to produce cytotoxic reactive oxygen species (ROS), which induce fatal damages on target cells and tissues [5–8]. PDT as an alternative regime has been approved by many countries to treat the patients with malignant tumors as well as age-related macular degeneration (AMD). Recently, growing data showed that photodynamic action could effectively kill pathogenic microorganisms, termed photodynamic inactivation (PDI) and photodynamic antimicrobial chemotherapy (PACT) [5–7, 9–11]. In comparison to conventional antibiotic treatment, PDI has unique advantages of dual specificity in targeting eradication of pathogenic microorganisms: preferential absorption of pathogenic microorganisms and target lesion irradiated from laser or visible light. Furthermore, the resistance of bacteria

to PDI is very unlikely because of the nonspecific damage of PDI on bacteria [12]. So, PDI has shown potential promise in eradicating pathogenic microorganisms and treating infectious diseases.

Curcumin (CUR), isolated from the rhizomes of *Curcuma longa*, is a naturally occurring polyphenolic compound. Many investigations have found various biological activities of curcumin including antiproliferative, antimicrobial, and antioxidant activity [13] and the activities of curcumin could be enhanced in the presence of visible light irradiation at the wavelength of around 400–500 nm [14]. These data also demonstrate that curcumin is a kind of effectively natural photosensitizer. Therefore, in the present study our aim is to investigate the effect of photodynamic action of LED-activated curcumin on cell viability, membrane permeability, and intracellular reactive oxygen species (ROS) of *Staphylococcus aureus*.

2. Materials and Methods

2.1. Photosensitizer. Curcumin was used as a photosensitizer in the present study from Sigma (America). A stock solution was made in dimethyl sulfoxide (DMSO) at a concentration of 100 mM and kept in the dark at −20°C.

2.2. Bacterial Strain. *S. aureus* strain was gifted by Mr. Liangku Wong from the Second Affiliated Hospital, Chon- gqing Medical University, China. The strain was originally isolated from a patient with *S. aureus* pneumonia and identified by CHROM agar technique. The bacterial cells were grown overnight at 37°C in Luria-Bertani (LB) medium with shaking. And Bacterial suspension was then spread over LB-Agar plates and cultured aerobically as described by our previous report [15].

2.3. Photocytoxicity Assay of Curcumin on Bacteria. The bacterial cells of *S. aureus* grown in exponential phase in LB medium were harvested by centrifugation at 4 000 rpm for 5 min. Bacterial suspension (10^8 cfu/mL) was prepared and incubated with different concentrations of curcumin (0, 0.5, 1, 1.5, 2, and 2.5 μM) in a 6-well plate at room temperature for 60 min in the dark and then irradiated by blue light emitted from a LED light source with the wavelength of 470 nm and the power density of 60 mW/cm^2 described by Jiang et al. [16].

All experiments were randomly divided into four groups as follows.

(1) Group 1 (sham control): the bacterial cells in the sham control were treated by neither curcumin nor blue light.

(2) Group 2 (curcumin treatment alone): the cells in the curcumin treatment alone group were treated by curcumin without light irradiation.

(3) Group 3 (blue light irradiation alone): the cells in the light irradiation alone group were irradiated by blue light with the dose of 3 J/cm^2 without curcumin treatment.

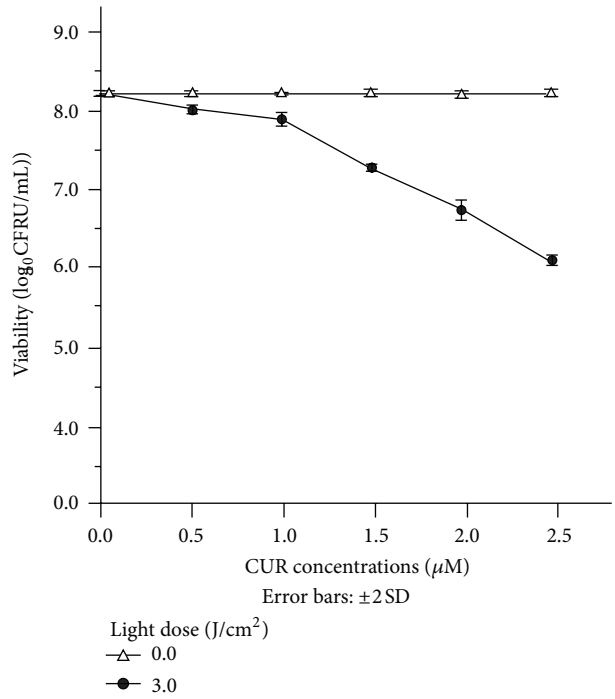

Figure 1: Viability of *S. aureus* after light-activated curcumin. Bacteria were incubated with different concentrations of curcumin (0, 0.5, 1.0, 1.5, 2.0, and 2.5 μM) and then irradiated by blue light from LED light source with wavelength of 470 nm and light dose of 3 J/cm^2.

(4) Group 4 (blue light-activated curcumin): the cells in blue light-activated curcumin group were preincubated by various concentrations of curcumin in combination with blue light with the dose of 3 J/cm^2.

After light-activated curcumin, bacteria were serially diluted 10-fold in phosphate buffered saline (PBS) to obtain dilutions of 10^{-1} ~ 10^{-6} times of the original concentration. 50 μL of each dilution was then spread on LB-Agar plates and cultured aerobically in the dark for 16 h at 37°C. The viability of bacteria was investigated through counting the colony forming units.

2.4. Membrane Permeability Assay. Membrane permeability of bacterial cells was investigated using confocal laser scanning microscopy (CLSM) and flow cytometry (FCM). In brief, bacteria were firstly incubated with curcumin (2.5 μM) for 60 min in the dark at 37°C and then irradiated by blue light with the dose of 3 J/cm^2. After photodynamic treatment, bacteria were harvested (at 4 000 rpm, 5 min) and propidium iodide (PI) (10 μg/mL) was then added into each well. After the incubation for 20 min in the dark, membrane permeability of the stained cells was observed immediately using a CLSM and the images were recorded using a colorful charge-coupled device camera. In addition, membrane permeability of the cells stained by PI was also analyzed using a FCM (SE, Becton Dickinson, USA) with the excitation of the light at the wavelength of 488 nm.

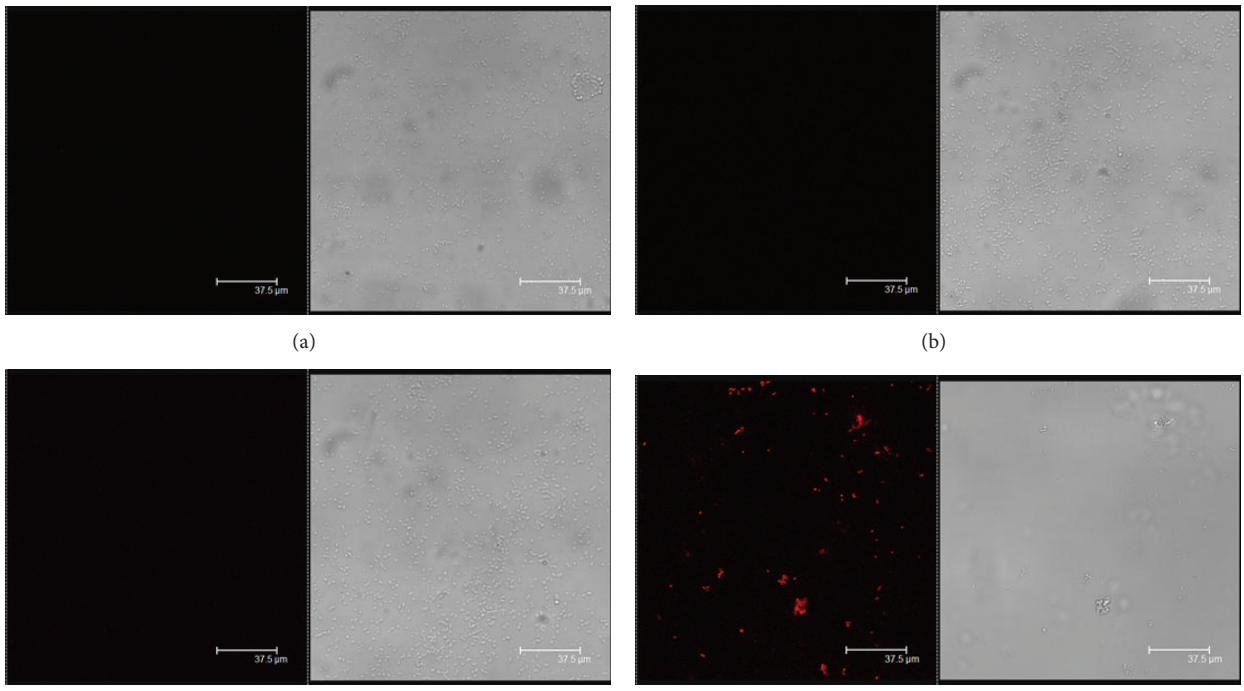

FIGURE 2: Membrane permeability of *S. aureus* was observed under CLSM with PI staining after LED light-activated curcumin (2.5 μM, 3 J/cm^2). (a) Sham control; (b) curcumin treatment alone; (c) blue light irradiation alone; (d) blue light-activated curcumin.

2.5. ROS Measurement. After bacterial cells were photosensitized in curcumin (2.5 μM, 3 J/cm^2), bacterial cells were incubated with 1 μL 2,7-dichlorodihydrofluorescein diacetate (DCFH-DA, 10 mM, Beyotime, Jiangsu, China) for 20 min in the dark at 37°C. ROS were analyzed using flow cytometry (FCM) (SE, Becton Dickinson, USA) with the excitation of the light at the wavelength of 488 nm and the signals were finally acquired at the FL-2 channel.

2.6. Ultrastructural Observation. After light-activated curcumin (2.5 μM, 3 J/cm^2), bacterial cells were fixed for 1 day in 2% glutaraldehyde and postfixed with 2% OsO_4, dehydrated with graded alcohol and embedded with Epon 812 (Electron Microscopy Sciences, Fort Washington, PA, USA). Ultrathin sections (100 nm) of bacteria cells were stained in uranyl acetate and lead citrate and observed under a transmission electron microscopy (TEM) (H-600; Hitachi, Japan).

2.7. Statistical Analysis. All data were expressed as mean ± SD and statistically analyzed using SPSS 18.0 for Windows. One-way ANOVA (analysis of variance) was used to compare the differences between groups. A P value less than 0.05 was considered significant difference.

3. Results

3.1. Photocytoxicity Assay. Photocytoxicity of curcumin on *S. aureus* was measured using colony forming unit assay. Figure 1 showed that blue light-activated curcumin significantly inactivated *S. aureus* in a curcumin concentration-dependent manner. No significant inactivation activity was found in the controlled cells treated by curcumin alone or blue light irradiation alone ($P > 0.05$).

3.2. Membrane Permeability Assay. The membrane permeability of bacterial cells was measured using a CLSM after PI staining. More red fluorescence was found in *S. aureus* treated by blue light-activated curcumin than those of cells from sham control, curcumin treatment alone, and blue light irradiation alone. There was no remarkable difference between sham control, curcumin treatment alone, and blue light irradiation alone (Figure 2). Flow cytometry showed that the positive rate of bacteria stained by PI in sham treatment was 1.27%, 1.46% in curcumin treatment alone, and 1.50% in blue light irradiation alone, however, the positive rate of PI stained cells remarkably increased up to 28.31% after the combined treatment of curcumin and blue light irradiation (Figure 3).

3.3. ROS Production. After DCFH-DA staining, FCM investigation showed the spectral shift of the fluorescence curves to the right, indicating that the ROS level in *S. aureus* after light-activated curcumin was markedly higher than the controlled bacteria from sham control group, curcumin treatment alone group, and blue light irradiation alone group (Figure 4).

3.4. Ultrastructural Changes. TEM observed that the *S. aureus* cells from curcumin treatment alone group (2.5 μM)

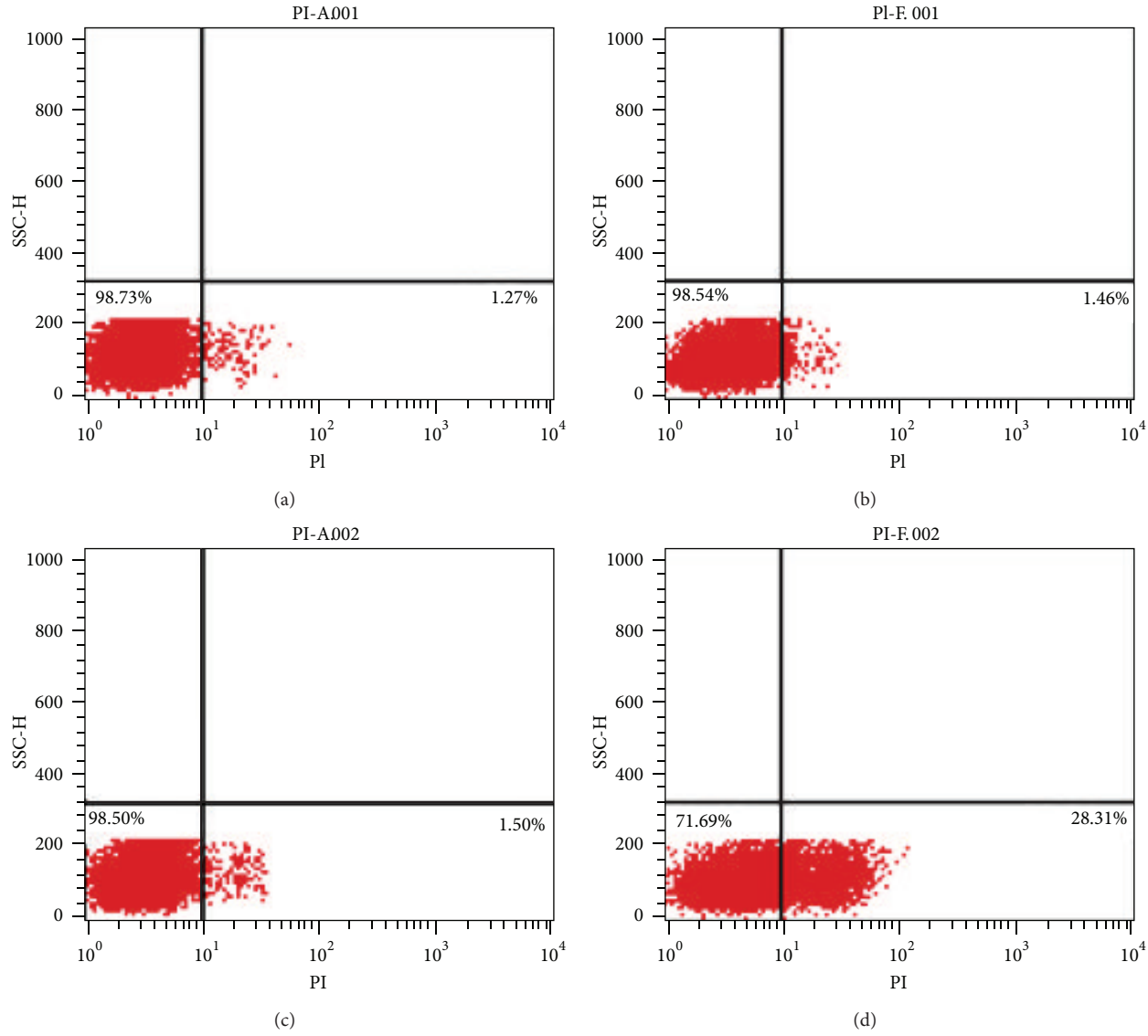

Figure 3: Membrane permeability of *S. aureus* was measured using flow cytometry with PI staining after LED light-activated curcumin (2.5 μM, 3 J/cm^2). (a) Sham control; (b) curcumin treatment alone; (c) blue light irradiation alone; (d) blue light-activated curcumin.

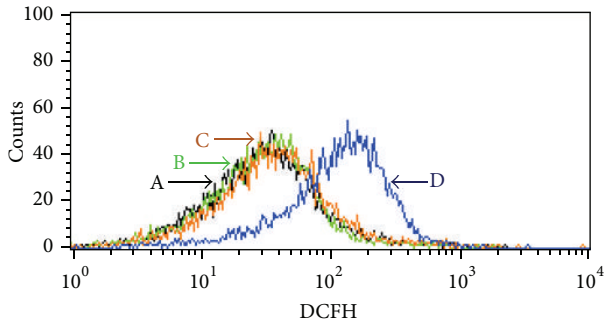

Figure 4: The ROS level in *S. aureus* was analyzed using FCM with DCFH-DA staining after curcumin (2.5 μM) treatment and blue light irradiation (3 J/cm^2). (A) Sham control; (B) curcumin treatment alone; (C) blue light irradiation alone; (D) blue light-activated curcumin.

and blue light irradiation alone group (3 J/cm^2) are intact and smooth (Figures 5(b) and 5(c)), similar to those of the sham control group (Figure 5(a)), whereas the electron density of the bacterial cells treated by blue light-activated curcumin was lower than those of the control groups (Figure 5(d)) and the vacuoles were observed in most *S. aureus* cells after LED-activated curcumin treatment. The results indicated that partial cytoplasm leakage occurred after the combined treatment of curcumin (2.5 μM) and blue light irradiation (3 J/cm^2).

4. Discussion

Medical plants are found to contain numerous active components killing pathogenic microorganisms [17]. Chinese herbs

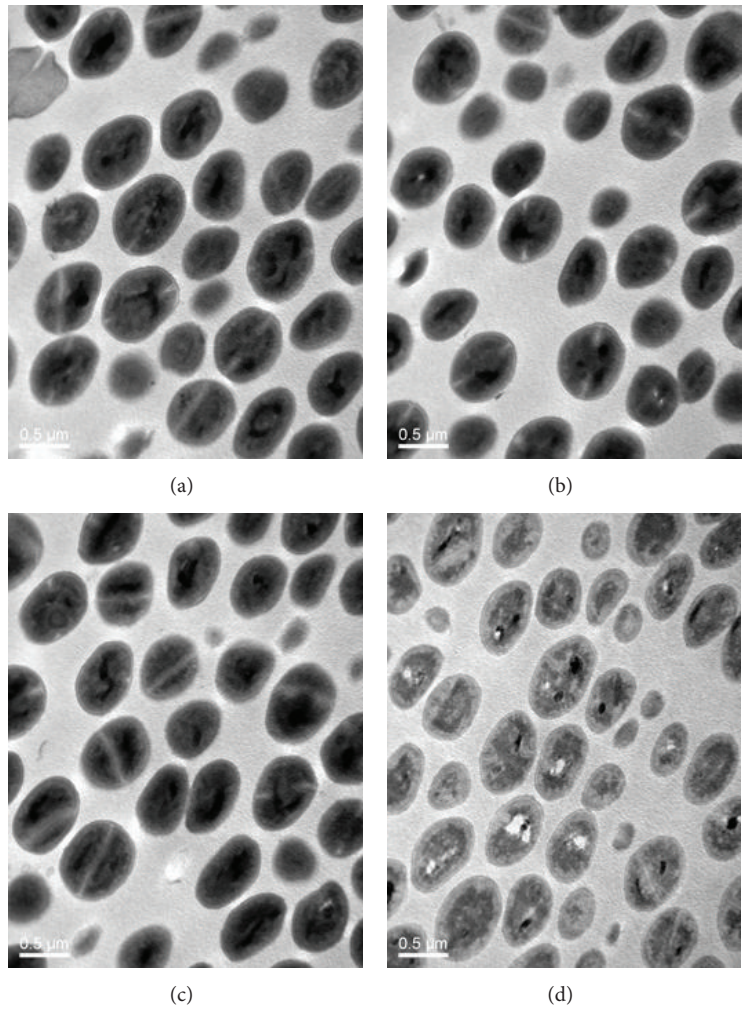

Figure 5: The ultrastructural changes of *S. aureus* were observed under a TEM after the treatment of light-activated curcumin (2.5 μM, 3 J/cm^2). (a) Sham control; (b) curcumin treatment alone; (c) blue light irradiation alone; (d) blue light-activated curcumin.

are some specific medical plants, which are widely used in traditional medicine to combat a variety of clinical diseases [18]. Of which many traditional Chinese herbs such as cleaning hot and detoxification herbs have been widely used to treat infectious diseases. Curcumin is a naturally occurring pigment isolated from a traditional Chinese herb *Curcuma longa*. Numerous studies and clinical evidences have shown that curcumin has many medical activities including antioxidant, antitumor, antibacterial, and immunomodulation [13, 19–23]. Curcumin was found to induce bacterial FtsZ assembly and inhibit bacterial cytokinesis and even interrupt quorum sensing (QS) to reduce pathogenicity [13, 24]. Recent studies showed that curcumin inhibited Sortase A and *S. aureus* cell adhesion to fibronectin [25]. However, higher drug dose is often needed to achieve bactericidal efficacy of curcumin [26]. Interestingly, growing evidences showed that visible light irradiation could activate curcumin and enhance its antibacterial and antitumoral activity [8, 14]. In order to effectively activate curcumin we have successfully set up a blue light source using LED. In the present study, photodynamic action of blue light-activated curcumin against *S. aureus* was investigated using the CFU assay. We observed a significant reduction in viability of *S. aureus* after the combined treatment of curcumin and blue light irradiation and curcumin at lower doses significantly killed *S. aureus* upon blue light irradiation. Our TEM results also observed markedly ultrastructural damage in bacterial cells after the combined treatment of curcumin and blue light irradiation. The fact of PDI that it can kill pathogenic bacteria has been confirmed by us and other scientists [5–7, 9–11]. Curcumin, an active compound with multitarget activity from food and traditional Chinese herb, is a safe and effective antimicrobial agent and is also a naturally occurring photosensitizer [8, 13–16, 24, 25]. The combination of curcumin and light irradiation would have dual antibacterial effect, including direct antibacterial activity of curcumin itself and ROS-mediated antibacterial effect of curcumin upon blue light irradiation. Thus, blue light-activated curcumin might be a potential way to kill *S. aureus*.

Membrane integrity is a prerequirement of bacterial survival. PI is fluorescent nucleic acid binding dyes which is excluded by the intact cell membranes of both bacteria

and eukaryotes and is generally used as indicator of cell membrane permeability [27]. In the present study CLSM with PI staining observed more bacteria with red fluorescence after curcumin treatment in combination with blue light irradiation than that of the controls, including sham irradiation, curcumin treatment alone, and blue light irradiation alone. Flow cytometry also reinforced the observation of CLSM, demonstrating that blue light-activated curcumin markedly damaged the membrane of *S. aureus*. TEM found vacuoles in many bacterial cells, showing partial cytoplasm leakage after the combined treatment of curcumin and blue light irradiation. The observations indicated the damages of membrane integrity might directly lead to the loss of cytoplasm contents, subsequently resulting in bacterial death.

Excessive accumulation of intracellular ROS is a direct or indirect cause of cell death [15]. Excessive ROS can destruct cell membrane, cytoplasmic membrane, and nuclear membrane to directly cause cell death. Furthermore, ROS can indirectly cause fatal cell damage through oxidizing intracellular biomolecules such as nucleus acid and protein [6, 15, 28–31]. Our flow cytometry with DCFH-DA staining also observed that intracellular ROS level significantly increased after the combined treatment of curcumin and blue light irradiation, indicating that blue light-activated curcumin damaged membrane permeability probably through excessive accumulation of intracellular ROS to cause cell death of *S. aureus*. However, photodynamic action of curcumin is a complex cellular and molecular event; the exact mechanism will further be explored in our future investigations.

5. Conclusion

The rise of antibiotic-resistant bacteria and relatively slow development of new antibiotics are driving the researchers to seek novel antibacterial strategies. Our present data showed that blue light-activated curcumin damaged membrane permeability, causing cell death of *S. aureus* and highlighted that intracellular ROS increase might be an important cause to photodynamically kill *S. aureus* in the presence of curcumin.

Conflict of Interests

The authors declare that there is no conflict of interests regarding the publication of this paper.

Acknowledgments

This work was supported by the general research fund (GRF) Grant from Hong Kong RGC (476912), the Direct Grant from the Chinese University of Hong Kong (4053026), and Innovation and Technology Fund of Shenzhen (CXZZ20120619150627260). The authors express their sincere thanks to Dr. Wu Jufeng, Mr. Liangku Wong, and Mr. Liumiao for their helpful assistance.

References

[1] H. Humphrys, "*Staphylococcus aureus*: the enduring pathogen in surgery," *Surgeon*, vol. 10, no. 6, pp. 357–360, 2012.

[2] N. C. W. Tan, A. Foreman, C. Jardeleza, R. Douglas, H. Tran, and P. J. Wormaald, "The multiplicity of *Staphylococcus aureus* in chroniic rhinoosinusitis: correlating surface biofilm and intracellular residence," *Laryngoscope*, vol. 122, no. 8, pp. 1655–1660, 2012.

[3] K. Leszczynska, D. Namiot, F. J. Byfield et al., "Antibacterial activity of the human host denfence peptide LL-37 and selected synthetic cationic lipids against bacteria associated oral and upper respiratory tract infections," *Journal of Antimicrobial Chemotherapy*, vol. 68, no. 3, pp. 610–618, 2013.

[4] S. Wiriyachaiporn, P. H. Howarth, K. D. Bruce, and L. A. Dailey, "Evaluation of a rapid lateral flow immunoassay for *Staphylococcus aureus* detection in respiratory samples," *Diagnostic Microbiology and Infectious Disease*, vol. 75, no. 1, pp. 28–36, 2013.

[5] P. S. Zolfaghari, S. Packer, M. Singer et al., "In vivo killing of *Staphylococcus aureus* using a light-activated antimicrobial agent," *BMC Microbiology*, vol. 9, article 27, 2009.

[6] T. Maisch, J. Baier, B. Franz et al., "The role of singlet oxygen and oxygen concentration in photodynamic inactivation of bacteria," *Proceedings of the National Academy of Sciences of the United States of America*, vol. 104, no. 17, pp. 7223–7228, 2007.

[7] J. Wu, H. Xu, W. Tang, R. Kopelman, M. A. Philbert, and C. Xi, "Eradication of bacteria in suspension and biofilms using methylene blue-loaded dynamic nanoplatforms," *Antimicrobial Agents and Chemotherapy*, vol. 53, no. 7, pp. 3042–3048, 2009.

[8] H. K. Koon, A. W. N. Leung, K. K. M. Yue, and N. K. Mak, "Photodynamic effect of curcumin on NPC/CNE2 cells," *Journal of Environmental Pathology, Toxicology and Oncology*, vol. 25, no. 1-2, pp. 205–215, 2006.

[9] H. M. Tang, M. R. Hamblin, and C. M. N. Yow, "A comparative in vitro photoinactivation study of clinical isolates of multidrug-resistant pathogens," *Journal of Infection and Chemotherapy*, vol. 13, no. 2, pp. 87–91, 2007.

[10] J. Walther, M. J. Bröcker, D. Wätzlich et al., "Protochlorophyllide: a new photosensitizer for the photodynamic inactivation of Gram-positive and Gram-negative bacteria," *FEMS Microbiology Letters*, vol. 290, no. 2, pp. 156–163, 2009.

[11] M. Wainwright, "Photodynamic antimicrobial chemotherapy (PACT)," *Journal of Antimicrobial Chemotherapy*, vol. 42, no. 1, pp. 13–28, 1998.

[12] K. Sahu, M. Sharma, H. Bansal, A. Dube, and P. K. Gupta, "Topical photodynamic treatment with poly-l-lysine-chlorin p6 conjugate improves wound healing by reducing hyperinflammatory response in *Pseudomonas aeruginosa*-infected wounds of mice," *Lasers in Medical Science*, vol. 28, no. 2, pp. 465–471, 2013.

[13] D. Rai, J. K. Singh, N. Roy, and D. Panda, "Curcumin inhibits FtsZ assembly: an attractive mechanism for its antibacterial activity," *Biochemical Journal*, vol. 410, no. 1, pp. 147–155, 2008.

[14] L. N. Dovigo, A. C. Pavarina, J. C. Carmello, A. L. MacHado, I. L. Brunetti, and V. S. Bagnato, "Susceptibility of clinical isolates of Candida to photodynamic effects of curcumin," *Lasers in Surgery and Medicine*, vol. 43, no. 9, pp. 927–934, 2011.

[15] Y. Jiang, A. W. Leung, X. Wang, H. Zhang, and C. Xu, "Inactivation of *Staphylococcus aureus* by photodynamic action of hypocrellin B," *Photodiagnosis and Photodynamic Therapy*, vol. 10, no. 4, pp. 600–606, 2013.

[16] Y. Jiang, A. W. Leung, X. Wang, H. Zhang, and C. Xu, "Effect of photodynamic therapy with hypocrellin B on apoptosis, adhesion, and migration of cancer cells," *International Journal of Radiation Biology*, 2014.

[17] D. Wojnicz, A. Z. Kucharska, A. Sokol-Letowska, M. Kicia, and D. Tichaczek-Goska, "Medicinal plants extracts affect virulence factors expression and biofilm formation by the uropathogenic *Escherichia coli*," *Urological Research*, vol. 40, no. 6, pp. 683–697, 2012.

[18] S. Chusri, K. Sompetch, S. Mukdee et al., "Inhibition of *Staphylococcus epidermidis* biofilm formation by traditional Thai herbal recipes used for wound treatment," *Evidence-Based Complementary and Alternative Medicine*, vol. 2012, Article ID 159797, 8 pages, 2012.

[19] C. Alarcón de la Lastra, "Curcumin: a promising spice for therapeutics," *Molecular Nutrition & Food Research*, vol. 52, no. 9, p. 985, 2008.

[20] P. Anand, S. G. Thomas, A. B. Kunnumakkara et al., "Biological activities of curcumin and its analogues (Congeners) made by man and Mother Nature," *Biochemical Pharmacology*, vol. 76, no. 11, pp. 1590–1611, 2008.

[21] C. Chen, T. D. Johnston, H. Jeon et al., "An in vitro study of liposomal curcumin: stability, toxicity and biological activity in human lymphocytes and Epstein-Barr virus-transformed human B-cells," *International Journal of Pharmaceutics*, vol. 366, no. 1-2, pp. 133–139, 2009.

[22] M. Montopoli, E. Ragazzi, G. Froldi, and L. Caparrotta, "Cell-cycle inhibition and apoptosis induced by curcumin and cis-platin or oxaliplatin in human ovarian carcinoma cells," *Cell Proliferation*, vol. 42, no. 2, pp. 195–206, 2009.

[23] M.-H. Teiten, S. Reuter, S. Schmucker, M. Dicato, and M. Diederich, "Induction of heat shock response by curcumin in human leukemia cells," *Cancer Letters*, vol. 279, no. 2, pp. 145–154, 2009.

[24] T. Rudrappa and H. P. Bais, "Curcumin, a known phenolic from *Curcuma longa*, attenuates the virulence of *Pseudomonas aeruginosa* PAO1 in whole plant and animal pathogenicity models," *Journal of Agricultural and Food Chemistry*, vol. 56, no. 6, pp. 1955–1962, 2008.

[25] B.-S. Park, J.-G. Kim, M.-R. Kim et al., "*Curcuma longa* L. constituents inhibit sortase A and *Staphylococcus aureus* cell adhesion to fibronectin," *Journal of Agricultural and Food Chemistry*, vol. 53, no. 23, pp. 9005–9009, 2005.

[26] S. Mishra, U. Narain, R. Mishra, and K. Misra, "Design, development and synthesis of mixed bioconjugates of piperic acid-glycine, curcumin-glycine/alanine and curcumin-glycine-piperic acid and their antibacterial and antifungal properties," *Bioorganic and Medicinal Chemistry*, vol. 13, no. 5, pp. 1477–1486, 2005.

[27] D. J. Novo, N. G. Perlmutter, R. H. Hunt, and H. M. Shapiro, "Multiparameter flow cytometric analysis of antibiotic effects on membrane potential, membrane permeability, and bacterial counts of *Staphylococcus aureus* and *Micrococcus luteus*," *Antimicrobial Agents and Chemotherapy*, vol. 44, no. 4, pp. 827–834, 2000.

[28] C. S. Lunde, S. R. Hartouni, J. W. Janc, M. Mammen, P. P. Humphrey, and B. M. Benton, "Telavancin disrupts the functional integrity of the bacterial membrane through targeted interaction with the cell wall precursor lipid II," *Antimicrobial Agents and Chemotherapy*, vol. 53, no. 8, pp. 3375–3383, 2009.

[29] P. S. Thakuri, R. Joshi, S. Basnet, S. Pandey, S. D. Taujale, and N. Mishra, "Antibacterial photodynamic therapy on *Staphylococcus aureus* and *Pseudomonas aeruginosa* in-vitro," *Nepal Medical College Journal*, vol. 13, no. 3, pp. 281–284, 2011.

[30] J. C. Ahn, J. W. Kang, J. I. Shin, and P. S. Chung, "Combination treatment with photodynamic therapy and curcumin induces mitochondria-dependent apoptosis in AMC-HN3 cells," *International Journal of Oncology*, vol. 41, no. 6, pp. 2184–2190, 2012.

[31] L. Huang, Y. Xuan, Y. Koide, T. Zhiyentayev, M. Tanaka, and M. R. Hamblin, "Type I and type II mechanisms of antimicrobial photodynamic therapy: an in vitro study on gram-negative and gram-positive bacteria," *Lasers in Surgery and Medicine*, vol. 44, no. 6, pp. 490–499, 2012.

Hindawi Publishing Corporation
International Journal of Photoenergy
Volume 2014, Article ID 521209, 6 pages
http://dx.doi.org/10.1155/2014/521209

Research Article

Effect of Light-Activated Hypocrellin B on the Growth and Membrane Permeability of Gram-Negative *Escherichia coli* Cells

Yuan Jiang,[1] Wingnang Leung,[2] Qingjuan Tang,[3] Hongwei Zhang,[2] and Chuanshan Xu[2,4]

[1] *Department of Rehabilitation Medicine, Second Affiliated Hospital, Chongqing Medical University, Chongqing 400010, China*
[2] *School of Chinese Medicine, Faculty of Medicine, The Chinese University of Hong Kong, Shatin, Hong Kong*
[3] *College of Food Science and Engineering, Ocean University of China, Qingdao 266003, China*
[4] *Shenzhen Research Institute, The Chinese University of Hong Kong, Shenzhen 518057, China*

Correspondence should be addressed to Wingnang Leung; awnleung@cuhk.edu.hk and Chuanshan Xu; xcshan@163.com

Received 25 February 2014; Revised 25 April 2014; Accepted 28 April 2014; Published 14 May 2014

Academic Editor: Timon Cheng-Yi Liu

Aim. To investigate the effect of light-activated hypocrellin B on the growth and membrane permeability of Gram-negative bacteria. *Methods*. *Escherichia coli* (*E. coli*) as a model bacterium of Gram-negative bacteria was incubated with various concentrations of hypocrellin B for 60 min and was subsequently irradiated by blue light with wavelength of 470 nm at the dose of 12 J/cm^2. Colony forming units were counted and the growth inhibition rate of *E. coli* cells was calculated after light-activated hypocrellin B. Membrane permeability was measured using flow cytometry and confocal laser scanning microscopy (CLSM) with propidium iodide (PI) staining. Bacterial morphology was observed using transmission electron microscopy (TEM). Reactive oxygen species in bacterial cells were measured using flow cytometry with DCFH-DA staining. *Results*. Significant growth inhibition rate of *E. coli* cells was observed after photodynamic action of hypocrellin B. Remarkable damage to the ultrastructure of *E. coli* was also observed by TEM. Flow cytometry and CLSM observation showed that light-activated hypocrellin B markedly increased membrane permeability of *E. coli*. Flow cytometry showed the intracellular ROS increase in *E. coli* treated by photodynamic action of hypocrellin B. *Conclusion*. Light-activated hypocrellin B caused intracellular ROS increase and structural damages and inhibited the growth of Gram-negative *E. coli* cells.

1. Introduction

Bacterial infection is a threat to human beings and the problem can be exacerbated by the emergence of resistant strains through the use of antibiotics. Thus, there is an urgent need to explore alternative strategies for combating pathogenic bacteria.

Photodynamic inactivation (PDI) is a promising method to eradicate pathogenic bacteria because PDI kills pathogenic bacteria via cytotoxic reactive oxygen species (ROS) produced by the photosensitive drug after light irradiation. The nonspecific damages of ROS on bacteria are unlikely to cause the resistance of bacteria to PDI [1–4]. Therefore, PDI draws our interest to explore its role in combating bacterial infections.

In our previous study we investigated photodynamic activity of some naturally occurring photosensitive compounds from traditional Chinese herbs [5–7]. Hypocrellin B is one of the most frequently explored photosensitive drugs from traditional Chinese herb *Hypocrella bambuase* [8, 9]. Our studies observed that light-activated hypocrellin B could produce intracellular ROS level, which can cause significant cell death and damage to Gram-positive bacteria *Staphylococcus aureus* [5, 6, 10]. However, growing evidence shows that Gram-negative bacteria are more resistant to PDI than Gram-positive bacteria [11]. To kill Gram-negative bacteria many photosensitizers were investigated, including methylene blue, toluidine blue, phthalocyanines, chlorins, porphyrins, chlorophyll, bacteriochlorophyll, fullerenes, and their nanoparticles [12]. In the present study, we chose

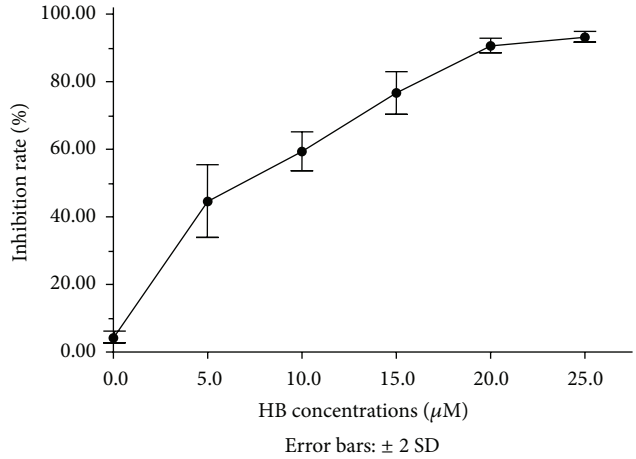

Figure 1: Inhibition of *E. coli* induced by photodynamic treatment of hypocrellin B. *E. coli* cells were incubated with different concentrations of hypocrellin B (0, 5, 10, 15, 20, and 25 μM) and irradiated by blue light with wavelength of 470 nm and energy density of 12 J/cm^2.

E. coli as a Gram-negative model bacterium and focused on observing the effect of light-activated hypocrellin B on the growth and membrane permeability of Gram-negative bacteria.

2. Materials and Methods

2.1. Bacterial Strain. *E. coli* strain DH5α was a generous gift from Dr. Wu Junfeng, P2 Lab of Children's Hospital of Chongqing Medical University, China. After *E. coli* cells were cultured overnight at 37°C in Luria-Bertani (LB) medium at 200 rpm, *E. coli* suspension (10^{-5} cfu/mL, 100 μL) was spread over LB-Agar plates and then incubated for 16 h at 37°C in a humidified atmosphere containing 5% CO_2.

2.2. Colony Forming Unit Assay. *E. coli* cells growing in exponential phase were harvested by centrifugation (at 4000 rpm, 5 min). Bacterial suspension (10^8 cfu/mL) was prepared and incubated with different concentrations of hypocrellin B (0, 5, 10, 15, 20, and 25 μM) in 6-well plate. After incubation for 60 min in the dark at room temperature, bacterial suspension was irradiated by blue light from a novel LED light source with the wavelength of 470 nm and the power density of 60 mW/cm^2. After light irradiation, bacteria cells were serially diluted 10-fold in PBS. Each sample (50 μL) was spread on LB-Agar plates and incubated for 16 h at 37°C in the dark. The colony forming units (CFU) were counted and the inhibition rate of bacterial growth was calculated by the following formula: the growth inhibition rate (%) = (CFU of the control group − CFU of the treatment group)/CFU of the control group × 100%.

All experiments were randomly divided into 4 groups.

Group A: Sham Control. The bacteria in the control were treated by neither hypocrellin B nor light irradiation.

Group B: Hypocrellin B Treatment Alone. The bacteria in the group were treated by hypocrellin B without light irradiation.

Group C: Light Irradiation Alone. The bacteria in the group were irradiated by LED light without hypocrellin B treatment.

Group D: Light-Activated Hypocrellin B. The bacterial cells in this group were incubated by various concentrations of hypocrellin B and irradiated by LED light with the energy density of 12 J/cm^2.

2.3. Membrane Permeability Measurement. Bacterial cells were incubated with hypocrellin B (25 μM) for 60 min in the dark at 37°C and were then exposed to blue light with light dose of 12 J/cm^2. After light irradiation, bacterial cells were immediately harvested and incubated with propidium iodide (PI, 10 μg/mL) for 20 min in the dark. Membrane permeability of the stained cells was observed immediately using a confocal laser scanning microscopy (CLSM) and the images were recorded using a colorful charge-coupled device camera. At the meantime, bacterial cells were also analyzed using flow cytometry (SE, Becton Dickinson) with the excitation setting at 488 nm.

2.4. Bacterial Morphology. After light activation of hypocrellin B, the bacterial cells were immediately fixed, post-fixed, dehydrated, and embedded in Epon 812 (Electron Microscopy Sciences, Fort Washington, PA) and were cut into ultrathin sections (100 nm) to be stained in uranyl acetate and lead citrate. Ultrastructural changes were observed using an electron microscopy (H-600; Hitachi, Japan).

2.5. ROS Measurement. After light-activation of hypocrellin B, bacterial cells were immediately harvested and incubated with 2,7-dichlorodihydrofluorescein diacetate (DCFH-DA, 10 μM, Beyotime, Jiangshu, China) for 20 min at 37°C in the dark and were then analyzed using a flow cytometry (SE, Becton Dickinson) with the excitation setting at 488 nm.

2.6. Statistical Analysis. All data expressed as mean ± SD were statistically analyzed using SPSS 18.0 for Windows.

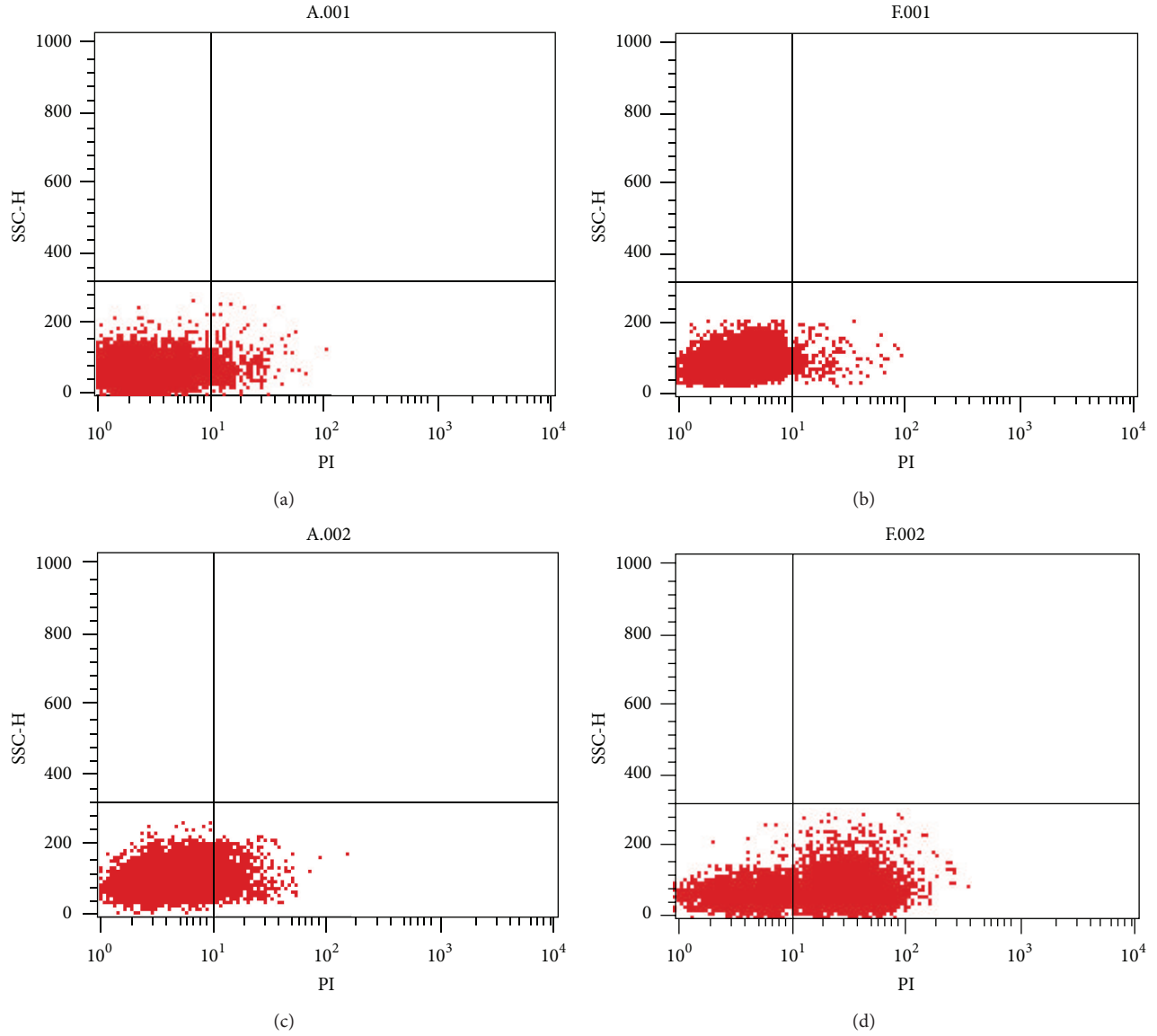

Figure 2: Membrane permeability of *E. coli* cells was measured using flow cytometry with PI staining after photodynamic treatment of hypocrellin B (25 μM), in which the energy density of blue light was 12 J/cm^2. (a) Sham control; (b) hypocrellin B treatment alone; (c) blue light irradiation alone; and (d) photodynamic treatment of hypocrellin B.

The differences between groups were analyzed using one-way ANOVA (analysis of variance). A P value < 0.05 was considered as significant difference.

3. Results

3.1. Colony Forming Unit Assay. Colony forming units of *E. coli* were investigated after treatment of light-activated hypocrellin B and the growth inhibition rate of *E. coli* cells was calculated. Figure 1 showed a significant growth inhibition rate of *E. coli* cells treated by light-activated hypocrellin B in hypocrellin concentration-dependent manner ($P < 0.05$). No significant difference was shown in the cells treated by hypocrellin alone or light irradiation alone ($P > 0.05$).

3.2. Membrane Permeability. The membrane permeability of *E. coli* cells was observed using a CLSM and flow cytometry with PI staining. Flow cytometry showed the positive rate of cells stained by PI was 3.71% in the sham group, 2.24% in the hypocrellin B treatment alone group, and 8.04% in the light irradiation group. The positive rate of cells remarkably increased up to 69.24% in the light-activated hypocrellin treatment group (Figure 2). CLSM also observed that more red fluorescence was found in *E. coli* cells treated by light-activated hypocrellin B than those of the control cells including sham control, hypocrellin treatment alone, and light irradiation alone. No marked difference was found between sham control, hypocrellin treatment alone, and light irradiation alone (Figure 3).

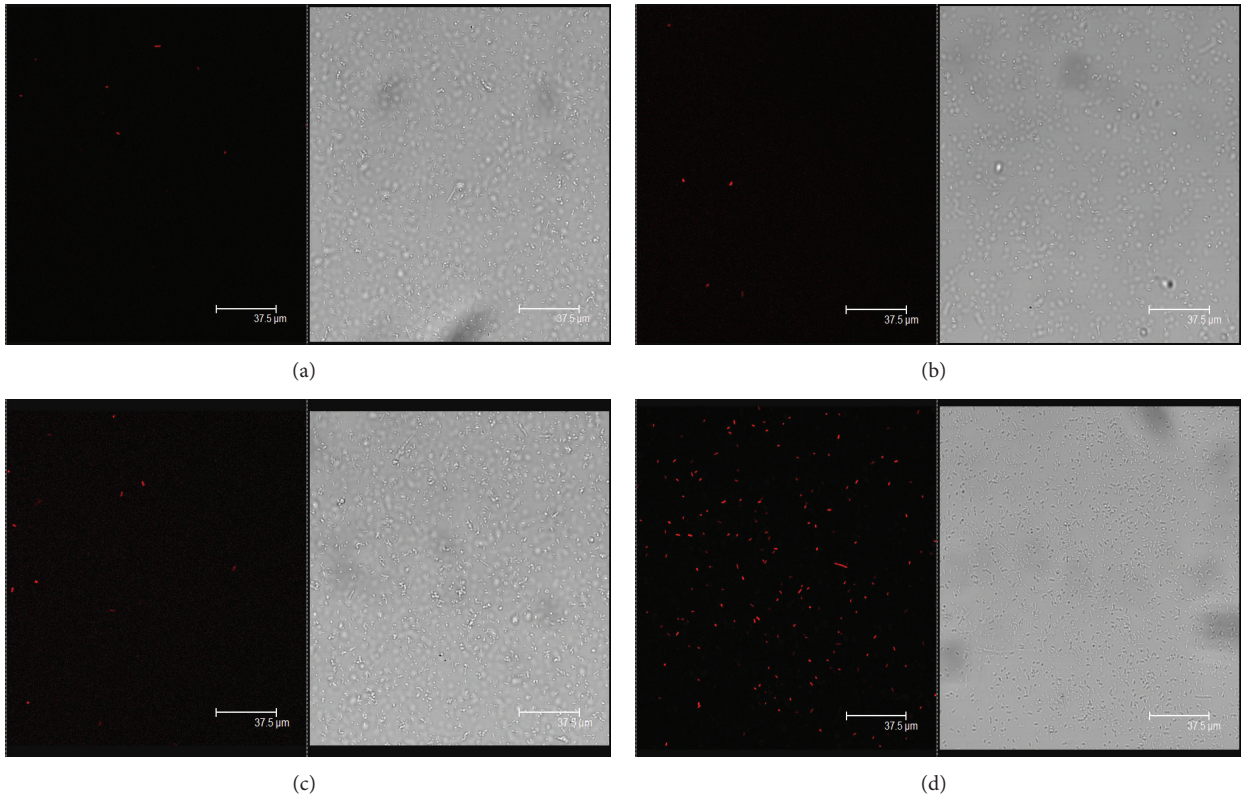

Figure 3: Membrane permeability of *E. coli* cells was measured using confocal laser scanning microscopy with PI staining after photodynamic treatment of hypocrellin B (25 μM), in which the energy density of blue light was 12 J/cm^2. (a) Sham control; (b) hypocrellin B treatment alone; (c) blue light irradiation alone; and (d) photodynamic treatment of hypocrellin B.

3.3. Bacterial Morphology. The ultrastructural changes of bacteria were observed using TEM. Intact and smooth cells were observed in sham control, hypocrellin B treatment alone, and light irradiation alone (Figures 4(a), 4(b), and 4(c)), whereas partial cytoplasm leakage was found in cells treated by light-activated hypocrellin B (Figure 4(d)).

3.4. Reactive Oxygen Species. The level of reactive oxygen species (ROS) in *E. coli* cells was analyzed using flow cytometry with DCFH-DA staining. Flow cytometry showed the spectral shift of the fluorescence curves to the right after light activation of hypocrellin B, indicating significant increase of the intracellular ROS level in *E. coli* (Figure 5).

4. Discussion

Traditional Chinese herbs have a long history as folk medicine for treating infectious diseases. Growing evidences have shown that many active compounds isolated from traditional Chinese herbs are capable of producing anti-infection and anti-inflammation effect [13, 14]. Hypocrellin B as an active component of a traditional Chinese herb *Hypocrella bambuase* has been confirmed to have significant activities against pathogenic microbes and malignant tumors [5, 6, 10, 11, 15–17]. Our recent study showed that hypocrellin B as a naturally occurring photosensitizer could cause significant damage to Gram-positive bacteria *S. aureus* cells as well as cancer cells while it was activated by blue light [5, 6, 10]. Our preliminary study also observed that *E. coli* cells were more resistant to photodynamic action of hypocrellin B than *S. aureus*. Thus, in the present study, we chose higher concentrations of hypocrellin B (0, 5, 10, 15, 20, and 25 μM) and higher energy density of blue light (12 J/cm^2) to investigate the effect of light-activated hypocrellin B on *E. coli* cells. Colony forming unit assay showed hypocrellin B had significantly photodynamic inhibition on *E. coli* cells.

Our previous studies reported that blue light could activate hypocrellin B to increase the intracellular ROS level in tumor cells and Gram-positive bacteria strain *S. aureus* [5, 6, 10]. In the present study flow cytometry with DCFH-DA staining also showed the ROS increase in Gram-negative bacteria strain *E. coli* cells. Our TEM observed notable cytoplasm leakage in *E. coli* cells after the treatment of light-activated hypocrellin B. Flow cytometry with PI staining showed that the positive rate of cells stained by PI increased remarkably up to 69.24% in the light-activated hypocrellin treatment group and confocal laser scanning microscopy also found more red fluorescence of PI in cells after light-activated hypocrellin B, demonstrating that light-activated hypocrellin B increased membrane permeability of the treated *E. coli* cells. The results were consistent with our past report on *S. aureus* treated by photodynamic action of hypocrellin B [10]. These findings demonstrated that nonspecific damage of ROS

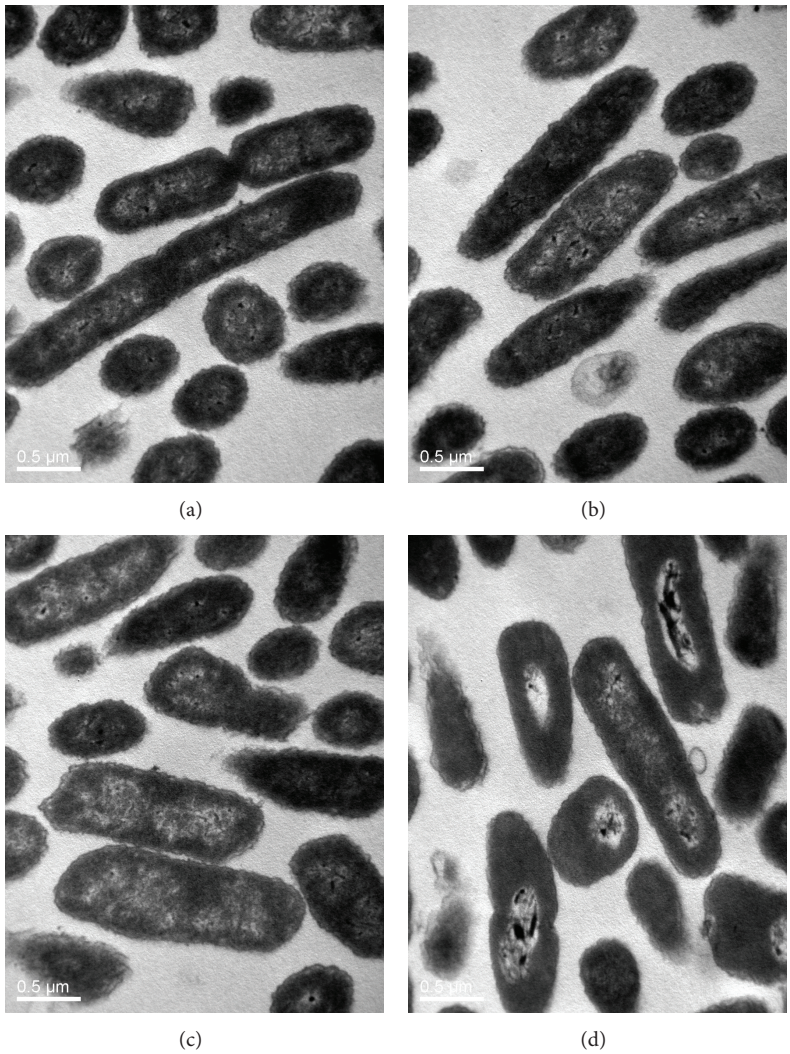

Figure 4: The ultrastructural morphology of *E. coli* cells was observed under a transmission electron microscopy (TEM) after photodynamic action of hypocrellin B (25 μM), in which the energy density of blue light was 12 J/cm^2. (a) Sham control; (b) hypocrellin B treatment alone; (c) blue light irradiation alone; and (d) photodynamic treatment of hypocrellin B (×30000).

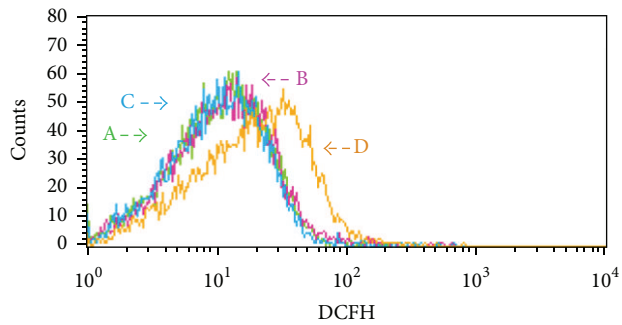

Figure 5: Reactive oxygen species (ROS) in *E. coli* cells were analyzed using flow cytometry with DCFH-DA staining after treatment of hypocrellin B (25 μM) and blue light irradiation (12 J/cm^2). A: sham control; B: hypocrellin B treatment alone; C: blue light irradiation alone; and D: photodynamic treatment of hypocrellin B.

generated by photosensitization of hypocrellin B to bacterial cells was an important cause of damage in the morphological structure of bacteria and in their general inhibition.

In summary, our study found that Gram-negative bacterial strain *E. coli* cells were more resistant to photodynamic treatment of hypocrellin B than Gram-positive bacteria, but light-activated hypocrellin B could also increase the ROS level in *E. coli* cells to cause damage of bacterial structure and inhibit growth of Gram-negative bacteria while higher concentrations of hypocrellin B and higher energy density of light irradiation were used in photodynamic treatment.

Conflict of Interests

The authors declare that there is no conflict of interests regarding the publication of this paper.

Acknowledgments

This work was supported by the GRF Grant from Hong Kong RGC (476912), the Direct Grant from the Chinese University of Hong Kong (4053026), and Innovation and Technology Fund of Shenzhen (CXZZ20120619150627260). The authors express their sincere thanks to Mr. Eric Pun, Dr. Wu Jufeng, Mr. Liangku Wong, and Mr. Liumiao for their helpful assistance.

References

[1] T. Maisch, J. Baier, B. Franz et al., "The role of singlet oxygen and oxygen concentration in photodynamic inactivation of bacteria," *Proceedings of the National Academy of Sciences of the United States of America*, vol. 104, no. 17, pp. 7223–7228, 2007.

[2] H. M. Tang, M. R. Hamblin, and C. M. N. Yow, "A comparative in vitro photoinactivation study of clinical isolates of multidrug-resistant pathogens," *Journal of Infection and Chemotherapy*, vol. 13, no. 2, pp. 87–91, 2007.

[3] M. Wainwright, "Photodynamic antimicrobial chemotherapy (PACT)," *Journal of Antimicrobial Chemotherapy*, vol. 42, no. 1, pp. 13–28, 1998.

[4] K. Sahu, M. Sharma, H. Bansal, A. Dube, and P. K. Gupta, "Topical photodynamic treatment with poly-l-lysine-chlorin p6 conjugate improves wound healing by reducing hyperinflammatory response in Pseudomonas aeruginosa-infected wounds of mice," *Lasers in Medical Science*, vol. 28, no. 2, pp. 465–471, 2013.

[5] Y. Jiang, A. W. N. Leung, J. Y. Xiang, and C. S. Xu, "Blue light-activated hypocrellin B damages ovarian cancer cells," *Laser Physics*, vol. 22, no. 1, pp. 300–305, 2012.

[6] Y. Jiang, X. S. Xia, A. W. N. Leung, J. Y. Xiang, and C. S. Xu, "Apoptosis of breast cancer cells induced by hypocrellin B under light-emitting diode irradiation," *Photodiagnosis and Photodynamic Therapy*, vol. 9, no. 4, pp. 337–343, 2012.

[7] X. B. Zeng, A. W. N. Leung, X. S. Xiac et al., "Effect of blue light radiation on curcumin-induced cell death of breast cancer cells," *Laser Physics*, vol. 20, no. 6, pp. 1500–1503, 2010.

[8] W. Nenghui and Z. Zhiyi, "Relationship between photosensitizing activities and chemical structure of hypocrellin A and B," *Journal of Photochemistry and Photobiology B: Biology*, vol. 14, no. 3, pp. 207–217, 1992.

[9] G. Ma, S. I. Khan, M. R. Jacob et al., "Antimicrobial and antileishmanial activities of hypocrellins A and B," *Antimicrobial Agents and Chemotherapy*, vol. 48, no. 11, pp. 4450–4452, 2004.

[10] Y. Jiang, A. W. Leung, X. Wang, H. Zhang, and C. Xu, "Inactivation of Staphylococcus aureus by photodynamic action of hypocrellin B," *Photodiagnosis and Photodynamic Therapy*, vol. 10, no. 4, pp. 600–606, 2013.

[11] J. Walther, M. J. Bröcker, D. Wätzlich et al., "Protochlorophyllide: a new photosensitizer for the photodynamic inactivation of Gram-positive and Gram-negative bacteria," *FEMS Microbiology Letters*, vol. 290, no. 2, pp. 156–163, 2009.

[12] F. F. Sperandio, Y. Y. Huang, and M. R. Hamblin, "Antimicrobial photodynamic therapy to kill gram-negative bacteria," *Recent Patents on Anti-Infective Drug Discovery*, vol. 8, no. 2, pp. 108–120, 2013.

[13] F. Ma, Y. Chen, J. Li et al., "Screening test for anti-Helicobacter pylori activity of traditional Chinese herbal medicines," *World Journal of Gastroenterology*, vol. 16, no. 44, pp. 5629–5634, 2010.

[14] J. Shao, H. Cheng, C. Wang, and Y. Wang, "A phytoanticipin derivativie, sodium houttuyfonate, induces in vitro synergistic effects with levofloxacin against biofilm formation by Pseudomonas aeruginosa," *Molecules*, vol. 17, no. 9, pp. 11242–11254, 2012.

[15] S. M. Ali, S. K. Chee, G. Y. Yuen, and M. Olivo, "Hypericin and hypocrellin induced apoptosis in human mucosal carcinoma cells," *Journal of Photochemistry and Photobiology B: Biology*, vol. 65, no. 1, pp. 59–73, 2002.

[16] C. Yu, S. Xu, S. Chen, M. Zhang, and T. Shen, "Investigation of photobleaching of hypocrellin B in non-polar organic solvent and in liposome suspension," *Journal of Photochemistry and Photobiology B: Biology*, vol. 68, no. 2-3, pp. 73–78, 2002.

[17] S. Xu, S. Chen, M. Zhang, and T. Shen, "Hypocrellin derivative with improvements of red absorption and active oxygen species generation," *Bioorganic and Medicinal Chemistry Letters*, vol. 14, no. 6, pp. 1499–1501, 2004.

Hindawi Publishing Corporation
International Journal of Photoenergy
Volume 2014, Article ID 895761, 5 pages
http://dx.doi.org/10.1155/2014/895761

Research Article

Study on the Relationship between Sports Skills and Visual Image Operation

Peng Zeng,[1] Long Liu,[2] Timon Cheng-Yi Liu,[1] and Xiang-Bo Yang[1,3]

[1] *College of Physical Education and Sports Science, South China Normal University, University Town, Guangzhou 510006, China*
[2] *Department of Chemistry and Biology, College of Science, National University of Defense Technology, Changsha 410073, China*
[3] *MOE Key Laboratory of Laser Life Science and Institute of Laser Life Science, College of Biophotonics, South China Normal University, Guangzhou 510631, China*

Correspondence should be addressed to Timon Cheng-Yi Liu; liutcy@scnu.edu.cn

Received 27 February 2014; Revised 22 April 2014; Accepted 22 April 2014; Published 6 May 2014

Academic Editor: Quan-Guang Zhang

120 college athletes including 30 gymnasts, 30 ball players, 30 athletes in track and field, and 30 swimmers with different levels of sports skills were measured on the operation speed and accuracy of visual images in the present study. The results showed that there was a close relationship between sport skill level and the operation level of visual images. The higher the sport skill level was, the higher the operation level was. The gymnasts were faster in the operation of visual images than the other athletes, but there was no significant difference among athletes of other sports games in visual image operation. The athletes achieved great improvement in their ability of visual image, but there was no significant difference between different genders.

1. Introduction

Visual image refers to the general image formed from the visual perception in the brain. There is a correlation between visuospatial working-memory capacity and motor sequence chunk length [1, 2]. It has been found that the operation of visual image, especially motor image, has been generalized to tasks beyond video-game playing. For example, training in action video games can increase the speed of perceptual processing [3] and cognitive flexibility [4]. On the other hand, some studies have investigated the influence of motor activities, such as baseball playing and tennis playing [5], volleyball playing and rowing [6], archery [7], kung fu [8], and Suryanamaskar [9], on the visual image operation. For example, Kida et al. [5] have studied the visual image operation Go or No go of 82 university students (22 baseball players, 22 tennis players, and 38 nonathletes) and 17 professional baseball players and found that intensive practice improved the reaction time. The present study investigated the reaction time and error of 120 college athletes including 30 gymnasts, 30 ball players, 30 athletes in track and field, and 30 swimmers on the visual image operation.

2. Methodology

2.1. Subjects. Altogether 120 college athletes including 30 gymnasts, 30 ball players, 30 athletes in track and field, and 30 swimmers with different sports levels were selected from colleges and universities in Guangdong, China. Three groups with high, medium, and low sports levels were formed with 40 students in each group. And the male and female subjects were balanced (male : female = 1 : 1) ranging in age from 18 to 25 years. According to the National Athletes Skills Standard of China, the subjects in the high sports level group reached the first or above sports level, and the subjects in the medium sports level group reached the second sports level. Those in the low sports level group were ordinary college students. In each group, there were 10 gymnasts, 10 ball players, 10 athletes in track and field, and 10 swimmers, with 20 males and 20 females. All the subjects' visual acuity (including the corrected visual acuity) was above 1.0.

2.2. Experimental Material and Measurement. The stimulus variable was two different sets of graphic materials (Figure 1) controlled and displayed on the screen of a microcomputer.

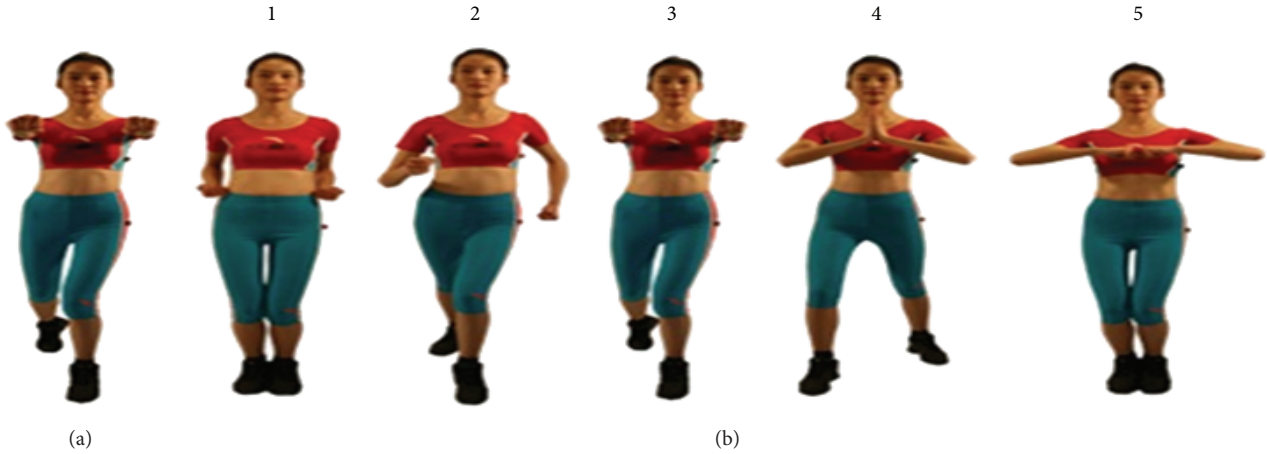

Figure 1: One left picture (a) serving as standard stimulus and a set of 5 numbered right pictures (b) serving as selective stimuli.

The response variable consisted of the reaction time and the number of errors made by the subjects in conducting the experimental tasks, which were automatically recorded by the computer.

In the experiment, the subjects visually focused on the screen of the computer with the dominant hand on the keyboard. One picture (Figure 1(a)) serving as standard stimulus was displayed on the computer screen for 2 seconds. After a 5-second interval, a set of 5 numbered pictures (Figure 1(b)) serving as selective stimuli were displayed. Of the 5 numbered pictures (Figure 1(b)), one was exactly the same as the standard stimulus and the other four were just very similar to the standard stimulus. The subjects were required to make the choice and press the corresponding number on the keyboard as soon as possible. Every subject had 5 trials for practice to be familiar with the operation procedure of the experiment and was then required to take 15 consecutive trials in the test with the reaction time and errors recorded.

All the collected data were processed and analyzed with the help of SPSS 8.0. Data were expressed as mean ± standard deviation. Independent t-tests and one-way ANOVA were carried out, respectively.

3. Results

3.1. Results and the Analysis of the Visual Image Operation of Subjects with Different Sports Levels. Table 1 showed the results of the tests, where the operation speed and accuracy of the visual image operation increased with the improvement of the level of motor skills. The higher the level of motor skills was, the shorter the reaction time was and the fewer the errors were, respectively. The reaction time and errors of the high sports level group were shorter and fewer than those of the medium sports level group, and the reaction time and errors of the medium sports level group were shorter and fewer than those of the low sports level group, respectively. One-way ANOVA showed that there was significant difference among the three experimental groups ($F = 9.56$, $P < 0.01$).

Table 1: Visual image operation performance of subjects with different sports levels.

Group	Reaction time (s)		Error (times)	
	M	SD	M	SD
High sports level	4.56	1.89	3.13	1.43
Medium sports level	4.76	1.95	3.21	1.65
Low sports level	5.23	2.13	3.87	2.01

Notes: M and SD denoted the mean reaction time and standard deviation, respectively.

Table 2: Visual image operation performance of subjects of different gender.

	Male		Female		P
	M	SD	M	SD	
Reaction time (s)	4.82	1.89	4.78	1.94	>0.05
Error (times)	3.43	1.73	3.49	1.89	>0.05

Notes: M and SD denoted the mean reaction time and standard deviation, respectively.

3.2. The Test Results of the Visual Image Operation on Subjects of Different Gender. Table 2 showed that there was no significant difference either on the reaction time or on the errors between the male and female subjects in visual image operation in the present study from independent t-tests of the reaction time and error rates.

3.3. The Test Results of the Visual Image Operation on Subjects of Different Sports Games. Independent t-tests were carried out with the data in Table 3, showing that gymnasts significantly outperformed the ball players, athletes in track and field, and swimmers on the operation speed. The differences were significant. But the differences among the other three types of athletes on the visual image operation which were indicated through the reaction time and errors were not significant.

Table 3: Visual image operation performance of subjects of different sports games.

	Ball players		Gymnasts		Athletes in T and F		Swimmers	
	M	SD	M	SD	M	SD	M	SD
Reaction time (s)	4.87	1.93	4.40	1.89	4.95	1.84	4.94	2.01
Error (times)	3.33	1.56	3.21	1.45	3.35	1.38	3.43	1.42

Notes: M, SD, T, and F denoted the mean reaction time, standard deviation, track, and field, respectively.

4. Discussions

Kida et al. [5] found that the athletic skill level improved the reaction time of Go or No go visual image operation. The present study further found that the athletic skill level improved the operation level of more complicated visual images. These may play a role in a comprehensive and thorough understanding of the interrelationship between motor learning activity and visual image operation.

4.1. Speed-Specific Homeostasis. In many everyday situations, speed is of the essence. Speed is a function of an organism. There may be a speed-specific homeostasis (SeSH), a negative-feedback response of an organism to maintain the speed-specific internal conditions so that the speed is perfectly performed [10, 11]. A speed in/far from its SeSH may be called a normal/dysfunction speed. For a normal speed, fast decision means few mistakes. The higher the speed fitness, the faster the decision and the fewer the mistakes. However, for a dysfunctional speed, fast decision means more mistakes. As the physical fitness can be increased by exercise training, the reaction times can be reduced with appropriate training, within one individual, across a range of tasks, and without compromising accuracy. Dye et al. [3] have reviewed evidence that the very act of playing action video games significantly reduces reaction times without sacrificing accuracy. Critically, this increase in speed is observed across various tasks beyond game situations. Video gaming may therefore provide an efficient training regimen to induce a general speeding of perceptual reaction times without decreases in accuracy of performance. Some studies have also found that motor activities such as baseball and tennis playing [5], volleyball playing and rowing [6], kung fu [8], Suryanamaskar [9] and gymnastics, ball playing, games in track and field, and swimming in this paper also significantly reduce reaction times without sacrificing accuracy.

4.2. The Relationship between Motor Skill Level and Visual Image Operation Level. In the present study, our experiment results showed that there were significant differences among the three experimental groups on visual image operation. The high sports level group significantly outperformed the medium sports level group, and the medium sports level group significantly outperformed the low sports level group. This suggested that the visual image of the subjects was closely related to the motor skill level.

Why did the visual image operation level increase with the motor skill level? One reason might be because both of them are the external activities of the same body. The two activities have shared the same internal functions such as the essential heart functions [12]. Bhavanani et al. [9] found that performance of Suryanamaskar produced immediate decrease in both auditory reaction time and visual reaction time, and heart rate increased significantly following Suryanamaskar compared with both self-control and external-control group. Generally, physical fitness can increase action heart rate but decrease rest heart rate [13] and then decrease the reaction time. On the other hand, sport activity is the essential activity of an athlete according to the scale-free network theory [12]. Visual image operation is his/her nonessential activity, but can be learned in an implicit way. Therefore, the longer the sport training is, the higher the athletic skill level is, and then the higher the visual image operation is. However, the implicit learning in sports training has not been widely studied yet.

The deep reason might be the cross-talking between visual nerves and motor nerves at least through autonomic nervous system (ANS). ANS at rest was found to be partially interlocked with activity of motor brain regions—the caudate nuclei and the motor cortex [14]. Magnetic stimulation of the human motor cortex evokes skin sympathetic nerve activity [15]. Transcutaneous electrical nerve stimulation (TENS), a maneuver used for pain control, has been found to influence cardiovascular responses through ANS reflex and to enhance motor function, visuospatial abilities, postural control, and cognitive function [16, 17]. For example, sympathetic activity increased but parasympathetic activity decreased after flight simulator exposure [17] or during motion sickness (MS) evoked by the conflict among somatosensory, visual, and vestibular input [16], and TENS was effective in reducing the symptoms of MS [16] or simulator sickness developed during or after flight simulator training [16, 17] as well as alleviating cognitive impairment.

4.3. The Relationship between Gender and Visual Image Operation Level. There have been few studies on the comparison of the abilities of male and female in their visual image operation. It was pointed out that there were differences in the ability of spatial image, where the male outperformed the female [18]. This is interpreted as that the male outperformed the female in spatial perception, which leads to the male's advantage in spatial image operation based on it. But some researchers disagreed with this view. They held that image was not simply derivant of perception but was born out of symbolic mechanism or signal function [10, 19]. Image is restricted at least by factors from two aspects: one is the objective material provided by perception and the other is the thinking pattern. So the content and form of image depend on the outside perceptive activities and then

the internalized schema [20]. According to this viewpoint, it is not well grounded to attribute the performance difference in spatial image to the different levels of spatial perception solely. Findings from the present study showed that both the athletes have improved and developed in the visual image level and ability, but the difference in gender is not significant.

4.4. Applications in Obsessive-Compulsive Disorder Treatments. Obsessive-compulsive disorder (OCD) may be treated by phototherapy, but its therapeutic effects depended on its seasonality. The serotonin transporter (HTT) is a candidate gene for OCD that has been associated with anxiety-related traits. The long (l) and short (s) variants of the HTT promoter have different transcriptional efficiencies. Subjects with the l/l and l/s genotypes had significantly higher blood 5-hydroxytryptamine (5-HT) levels than those with the s/s genotype. There was a significant interaction between HTT promoter genotype and seasonal variation in blood 5-HT content, with significant seasonal differences in 5-HT occurring only in the subjects with the l/l genotype [21]. Yoney et al. [22] found that the patients with OCD did not report a greater degree of seasonal variations than normal and no response was seen to bright light therapy in the small number of patients treated. On the other hand, Höflich et al. [23] reported the case of a 40-year-old woman with a seasonal form of OCD which was usually accompanied by obsessions and occurred only in autumn or winter. After a 12-day treatment with full spectrum bright light (3000 lux; 2 hours a day between 9 and 11 am) without changing the long-term antidepressive medication (125 mg amitriptyline/day) there was a complete remission of OCD symptomatology, with no relapse during the next months.

OCD may also be treated by exercise therapy. Half of pediatric-onset OCD cases remit by adulthood, but visuospatial and fine-motor skill deficits are predictive of poor long-term outcome in pediatric-onset OCD [24]. This suggested that exercise may reduce OCD symptoms since our study suggested that fine-motor skill may promote visuospatial skill. Brown et al. [25] enrolled fifteen patients (53% male; mean age = 44.4 years) in a 12-week moderate-intensity exercise intervention. Measures of OCD symptom severity were obtained at baseline, at end of treatment, and at 3- and 6-week and 6-month follow-up. They found a beneficial effect (Cohen's $d = 1.69$) of a 12-week aerobic exercise intervention on reduction in OCD symptom severity. Abrantes et al. [26] further examined acute changes in OCD symptoms after engaging in single exercise sessions during a 12-week exercise intervention for 15 (53% female; mean age = 41.9 years) patients with OCD. Participants reported reductions in negative mood, anxiety, and OCD symptoms at the end of each exercise session relative to the beginning. Changes in the magnitude of the effect of exercise in reducing negative mood and anxiety remained fairly stable while levels of self-reported obsessions and compulsions decreased over the duration of the intervention. Results of this study point toward the promising effect of exercise for acute symptom reduction in patients with OCD.

5. Conclusions

There may be close relationship between sport skill level and the operation level of visual images. The higher the sport skill level is, the higher the operation level may be. The gymnasts may be faster in the operation of visual images than other athletes, but there may be no significant difference among athletes of other sports games in visual image operation. The athletes may achieve great improvement in their ability of visual image, but there may be no significant difference between different genders.

Conflict of Interests

The authors declare that there is no conflict of interests regarding the publication of this paper.

Authors' Contribution

P. Zeng and L. Liu contributed equally to this work.

Acknowledgments

This work was supported by National Science Foundation of China (60878061, 10974061, and 11374107), Doctoral Fund of Ministry of Education of China (20124407110013), and Guangdong Scientific Project (2012B031600004).

References

[1] J. Bo and R. D. Seidler, "Visuospatial working memory capacity predicts the organization of acquired explicit motor sequences," *Journal of Neurophysiology*, vol. 101, no. 6, pp. 3116–3125, 2009.

[2] J. Bo, V. Borza, and R. D. Seidler, "Age-related declines in visuospatial working memory correlate with deficits in explicit motor sequence learning," *Journal of Neurophysiology*, vol. 102, no. 5, pp. 2744–2754, 2009.

[3] M. W. G. Dye, C. S. Green, and D. Bavelier, "Increasing speed of processing with action video games," *Current Directions in Psychological Science*, vol. 18, no. 6, pp. 321–326, 2009.

[4] B. D. Glass, W. T. Maddox, and B. C. Love, "Real-time strategy game training: emergence of a cognitive flexibility trait," *PLoS One*, vol. 8, no. 8, Article ID e70350, 2013.

[5] N. Kida, S. Oda, and M. Matsumura, "Intensive baseball practice improves the Go/Nogo reaction time, but not the simple reaction time," *Cognitive Brain Research*, vol. 22, no. 2, pp. 257–264, 2005.

[6] G. Giglia, F. Brighina, D. Zangla et al., "Visuospatial attention lateralization in volleyball players and in rowers," *Perceptual and Motor Skills*, vol. 112, no. 3, pp. 915–925, 2011.

[7] J. Seo, Y.-T. Kim, H.-J. Song et al., "Stronger activation and deactivation in archery experts for differential cognitive strategy in visuospatial working memory processing," *Behavioural Brain Research*, vol. 229, no. 1, pp. 185–193, 2012.

[8] M. Muiños and S. Ballesteros, "Visuospatial attention and motor skills in kung fu athletes," *Perception*, vol. 42, no. 10, pp. 1043–1050, 2013.

[9] A. B. Bhavanani, M. Ramanathan, R. Balaji, and D. Pushpa, "Immediate effects of Suryanamaskar on reaction time and

heart rate in female volunteers," *Indian Journal of Physiology and Pharmacology*, vol. 57, no. 2, pp. 199–204, 2013.

[10] T. C. Y. Liu, R. Liu, L. Zhu, J. Q. Yuan, M. Wu, and S. H. Liu, "Homeostatic photobiomodulation," *Frontiers of Optoelectronics in China*, vol. 2, no. 1, pp. 1–8, 2009.

[11] T. C. Y. Liu, Y. Y. Liu, E. X. Wei, and F. H. Li, "Photobiomodulation on stress," *International Journal of Photoenergy*, vol. 2012, Article ID 628649, 11 pages, 2012.

[12] T. C. Y. Liu, L. Liu, J. G. Chen, P. Zeng, and X. B. Yang, "Action-dependent photobiomodulation on health, suboptimal health and disease," *International Journal of Photoenergy*, vol. 2014, Article ID 832706, 11 pages, 2014.

[13] M. T. Jensen, P. Suadicani, H. O. Hein, and F. Gyntelberg, "Elevated resting heart rate, physical fitness and all-cause mortality: a 16-year follow-up in the Copenhagen Male Study," *Heart*, vol. 99, no. 12, pp. 882–887, 2013.

[14] P. Schlindwein, H.-G. Buchholz, M. Schreckenberger, P. Bartenstein, M. Dieterich, and F. Birklein, "Sympathetic activity at rest and motor brain areas: FDG-PET study," *Autonomic Neuroscience: Basic and Clinical*, vol. 143, no. 1-2, pp. 27–32, 2008.

[15] D. H. Silber, L. I. Sinoway, U. A. Leuenberger, and V. E. Amassian, "Magnetic stimulation of the human motor cortex evokes skin sympathetic nerve activity," *Journal of Applied Physiology*, vol. 88, no. 1, pp. 126–134, 2000.

[16] H. Chu, M. H. Li, S. H. Juan, and W. Y. Chiou, "Effects of transcutaneous electrical nerve stimulation on motion sickness induced by rotary chair: a crossover study," *Journal of Alternative and Complementary Medicine*, vol. 18, no. 5, pp. 494–500, 2012.

[17] H. Chu, M. H. Li, Y. C. Huang, and S. Y. Lee, "Simultaneous transcutaneous electrical nerve stimulation mitigates simulator sickness symptoms in healthy adults: a crossover study," *BMC Complementary and Alternative Medicine*, vol. 13, no. 1, article 84, 2013.

[18] W. Hidetoshi and Y. M. Chen, "Intelligence differences between men and women," *Information on Psychological Sciences*, vol. 6, pp. 56–58, 1981.

[19] R. H. Cox, *Sport Psychology: Concepts and Applications*, McGraw-Hall, 6th edition, 2007.

[20] Y. S. Lei, *Comments on Epistomology of Piaget*, People's Publishing House, Beijing, China, 1987.

[21] G. L. Hanna, J. A. Himle, G. C. Curtis et al., "Serotonin transporter and seasonal variation in blood serotonin in families with obsessive-compulsive disorder," *Neuropsychopharmacology*, vol. 18, no. 2, pp. 102–111, 1998.

[22] T. H. Yoney, T. A. Pigott, F. L'Heureux, and N. E. Rosenthal, "Seasonal variation in obsessive-compulsive disorder: preliminary experience with light treatment," *The American Journal of Psychiatry*, vol. 148, no. 12, pp. 1727–1729, 1991.

[23] G. Höflich, S. Kasper, and H. J. Möller, "Successful treatment of seasonal compulsive syndrome with phototherapy," *Der Nervenarzt*, vol. 63, no. 11, pp. 701–704, 1992.

[24] M. H. Bloch, D. G. Sukhodolsky, P. A. Dombrowski et al., "Poor fine-motor and visuospatial skills predict persistence of pediatric-onset obsessive-compulsive disorder into adulthood," *Journal of Child Psychology and Psychiatry and Allied Disciplines*, vol. 52, no. 9, pp. 974–983, 2011.

[25] R. A. Brown, A. M. Abrantes, D. R. Strong et al., "A pilot study of moderate-intensity aerobic exercise for obsessive compulsive disorder," *Journal of Nervous and Mental Disease*, vol. 195, no. 6, pp. 514–520, 2007.

[26] A. M. Abrantes, D. R. Strong, A. Cohn et al., "Acute changes in obsessions and compulsions following moderate-intensity aerobic exercise among patients with obsessive-compulsive disorder," *Journal of Anxiety Disorders*, vol. 23, no. 7, pp. 923–927, 2009.

Hindawi Publishing Corporation
International Journal of Photoenergy
Volume 2014, Article ID 832706, 11 pages
http://dx.doi.org/10.1155/2014/832706

Review Article

Action-Dependent Photobiomodulation on Health, Suboptimal Health, and Disease

Timon Cheng-Yi Liu,[1] Long Liu,[2] Jing-Gang Chen,[1] Peng Zeng,[1] and Xiang-Bo Yang[1,3]

[1] *Laboratory of Laser Sports Medicine, South China Normal University, University Town, Guangzhou 510006, China*
[2] *Department of Chemistry and Biology, College of Science, National University of Defense Technology, Changsha 410073, China*
[3] *MOE Key Laboratory of Laser Life Science and Institute of Laser Life Science, College of Biophotonics, South China Normal University, Guangzhou 510631, China*

Correspondence should be addressed to Timon Cheng-Yi Liu; liutcy@scnu.edu.cn

Received 22 February 2014; Accepted 29 March 2014; Published 24 April 2014

Academic Editor: Quan-Guang Zhang

The global photobiomodulation (PBM) on an organism was studied in terms of function-specific homeostasis (FSH) and scale-free functional network in this paper. A function can be classified into a normal function in its FSH and a dysfunctional function far from its FSH. An FSH-specific stress (FSS) disrupting an FSH can also be classified into a successful stress in its FSS-specific homeostasis (FSSH) and a chronic stress far from its FSSH. The internal functions of an organism can be divided into essential, special nonessential, and general nonessential functions. Health may be defined as a state of an organism in which all the essential and special nonessential functions are normal or their stresses are successful. Suboptimal health may be defined as a state of a disease-free organism in which only some special nonessential functions are dysfunctional in comparison with its healthy state. Disease may be defined as a state of an organism which is not in both health and suboptimal health. The global PBM of health, suboptimal health, or disease suggested that the PBM may depend on the organism action.

1. Introduction

Unsustainable cost increases threaten the global health care system, and further progress is stymied more by societal than technological factors [1]. Conventional medical practice has been "reactive" (doctor takes part when disease appears). However, Sobradillo et al. [2] found that the theoretical (scale-free networks and complex systems), technological (high efficiency "omic" technologies), and conceptual (biology systems) advances throughout the last decade allowed us to anticipate in the transition to an "anticipatory" medicine known as "P4 medicine" (standing for personalized, predictive, preventive and participatory medicine). In fact, both the functional medicine [3] and traditional Chinese medicine (TCM) [4, 5] are also "anticipatory" medicines mainly from the functional viewpoint [6]. Constitution-based TCM strategies [7] and photobiomodulation (PBM) [8] in disease prevention and treatment are consistent with the current proposed P4 medical mode. At its foundation, P4 medicine is about quantifying health and demystifying disease [1]. However, the current definition of health is vague and incomplete [1]. The exact definitions of health, suboptimal health, and disease and their PBM mechanism are examined in this paper from the viewpoints of functions and scale-free networks.

2. Functional Negative Feedback

Negative feedback is common in biological processes and acts to optimize the activity of a circuit in the presence of alleles with altered activities [9], which can maintain a system's stability to internal and external perturbations. Function-specific homeostasis (FSH) is a negative-feedback response of a biosystem to maintain the function-specific conditions inside the biosystem so that the function is perfectly performed [8, 10–12]. The quality of an FSH may be called a functional fitness of the maintained normal function.

The fitness has been used to discuss function performance by Nowak et al. [13], but the functional fitness was not defined. A function in and far from its FSH is called a "normal/dysfunctional function," respectively. The transition of a dysfunctional function to a normal function is called "to be normalized." A normal function is better performed than all the dysfunctional functions so that the normal function is locally the best performed function. These phenomena can be explained by using the Arndt-Schulz law [14] when, after an initial peak response, the marginal efficacy declines as dosage increases. FSH can finely extend this curve into a plateau.

A functional fitness is maintained by its normal function. Endurance exercise is any activity that uses large muscle groups can be performed continuously and is rhythmic and aerobic in nature. To maintain a cardiovascular fitness, this exercise should be performed at a frequency of 3 to 5 days per week, at an intensity of 60% to 90% of maximum heart rate (HRmax) or 50% to 85% of HRmax reserve, and at a duration of 20 to 60 min [15]. An inverse relationship exists between physical fitness and resting heart rate, body weight, percent body fat, serum cholesterol, triglycerides, glucose, and systolic blood pressure. In addition, exercise training increases the high-density lipoprotein portion of total cholesterol.

A normal function can resist internal/external disturbance under its threshold. It is resilient or robust. Higher functional fitness offers higher threshold. Using skill level as an example, Hancock [16] examined the effect of individual skill level on task performance in transient extreme heat and found that individuals who were skillful at the task were better able to withstand the detrimental effect of the stress exposure than their unskilled counterparts.

An FSH can be disrupted by an FSH-specific stress (FSS). The FSS is also a function of a biosystem [11, 12]. A normal/dysfunctional FSS is called a "successful/chronic stress," respectively and has been referred to as being "antifragile/fragile" by Taleb [17]. Taleb [17] hypothesized that the antifragileness should be beyond the resilience or robustness of a normal function. The resilience resists shocks and stays the same, but the antifragileness gets better and better. Moreover, hormetic (in small doses) stress [17, 18] is another kind of successful stress. A successful stress upgrades a normal function, but a chronic stress destroys a normal function. These phenomena are explained by the Arndt-Schulz Law [14], the Yerkes-Dodson law in psychology [19], or nonlinear relationships commonly described as being U- or J-shaped or inverted U- or J-shaped [18].

The simplest, most obvious, and best appreciated mechanism for buffering genetic variation is redundancy [9]. Redundancy can play an important role in hormesis [20] and antifragileness [17]. It also enhances performance. As an example, elite athletes often undertake altitude training to improve sea-level athletic performance. Robertson et al. [21] found that a combined approach of live high/train low plus train high elicited greater enhancements in physiological capacities when compared with the train high approach. Taleb [17] illustrated the redundancy-mediated antifragileness with a barbell-style approach. His preferred strategy was to be both hyperconservative and hyperaggressive at the same time. Instead of doing steady and moderate exercise daily, he suggested that it should be better to do a low-effort exercise such as walking slowly most of the time, while occasionally expending extreme effort. Redundancy enhances the cellular function [11, 12]. The m genes performing the same function, respectively, are called redundant genes with one another. Each redundant gene may activate a normal function-specific signal transduction (NSP) [12]. The m NSPs are called redundant pathways with one another. As it has been hypothesized [12], the full activation of each NSP may maintain the first-order normal function in its NSP-specific microenvironment (NSM), and the synergistic full activation of one NSP and its n-1 redundant pathways may maintain the nth-order normal function ($n = 2, 3, \ldots, m$) in its NSM.

Let Q be the quality of a FSH or the functional fitness of a normal function. An organism has many kinds of functions which include internal functions and external activities. Their normal ones are being maintained by their respective FSH $\{\text{FSH}_i,\ i = 1, 2, \ldots, n\}$ and their respective quality $\{\mathbf{Q}_i,\ i = 1, 2, \ldots, n\}$. Their performance is accompanied by various rhythms; higher functional fitness gives higher rhythm fitness. Janiak and kedziora [22] investigated the effect of exercise on the diurnal changes of electromechanical systolic time (QS2) in healthy men with different physical fitness and found that the effect of exercise on the circadian rhythm of QS2 was dependent on the level of physical fitness. After exercise, the circadian rhythm QS2 was presented in the human with higher physical fitness, whereas it was not evident in human with lower physical fitness. On the other hand, the enhancement of normal rhythms can upgrade the related normal functions or activities. Zhao et al. [23] found that, when a PBM improved sleep and melatonin, it also enhanced endurance performance.

Let $Q\max = \max\{Q_i,\ i = 1, 2, \ldots, l$. Let $F\max$ and $F\text{maxSH}$ denote the corresponding function/activity and its homeostasis, respectively. The $Q\max$ increases when a person grows but decreases when the person ages. The age at which the $Q\max$ is the highest, Qp, is called the prime age h. As growing and aging are symmetrical with each other, the most possible lifespan y of a person may be $2h + 1$ [8, 24]. Obviously, the higher the Qp and/or the slower the increase in Q max, the longer the expected lifespan.

3. Scale-Free Networks

Many complex systems can be viewed as networks, in which nodes represent system elements and edges correspond to interactions between those elements. Many results suggest that networks from different domains but in the same category may be more similar to one another than previously thought [25]. Among the popular networks, the scale-free networks are extremely heterogeneous, their topology being dominated by a few highly connected nodes (essential nodes) which link the rest of the less connected nodes (nonessential nodes) to the system [2]. A network diameter is defined as the shortest pathway averaged over all pairs of nodes. To investigate whether networks displayed a similar error tolerance, Jeong et al. [26] performed computer simulations

on the metabolic network of *E. coli*. Upon removal of the essential nodes the diameter increased rapidly, illustrating the special role of these nodes in maintaining a constant metabolic network diameter. However, when randomly chosen nonessential nodes were removed—mimicking the consequence of random mutations of catalysing enzymes—the average distance between the remaining nodes was not affected, indicating a striking insensitivity to random errors. Indeed, *in silico* and *in vivo* mutagenesis studies indicated remarkable fault tolerance upon removal of a substantial number of metabolic enzymes from the *E. coli* metabolic network [27].

All scale-free networks are sparse [28]. It suggested that their essential nodes should be sparse. A cell far from its FSH has many partially activated signal transduction pathways, but a cell in its FSH has sparse fully activated signal transduction pathways [29] so that there are NSPs [12]. There are many factors that contribute to maintaining a FSH state, but FSH-essential factors are very sparse [8]. Examples are a wide range of reprogramming of biological systems using overexpression of only one to five transcription factors [30] and a white-collar worker performing normal office work with very little brain material [31]. As shown in the next section, an organism has five essential internal functions and only one essential external activity.

4. Function Network

The scale-free networks dominate all aspects of human health and disease [2]. Generally, the nodes are genes, proteins, cells, or organisms. As presented in this paper the nodes are functions in the internal body or activities in the external body. Either the internal functions or external activities of an organism can be essential or nonessential according to the scale-free network properties. It depends on its importance in lifespan. The essential ones play important roles in healthy lifespan. The nonessential ones do not significantly affect the healthy lifespan under their respective threshold. They are further classified into the special nonessential ones which significantly affect the lifespan of nonhealthy body and the general nonessential ones which do not significantly affect the lifespan of nonhealthy body under their respective threshold.

4.1. Internal Functions. Western mainstream medicine including P4 medicine studies an organism mainly from anatomical viewpoint, but functional medicine [3] and TCM [6] study an organism mainly from the functional viewpoint. The internal function network has often been discussed from the TCM [4, 5] viewpoint.

An organism has many internal functions [3–5]. Among them, the five *yin zang* functions, *heart* function, *liver* function, *spleen* function, *lung* function, and *kidney* function, should be essential functions according to TCM. Navarrete et al. [32] analyzed organ mass data for 100 mammalian species, including 23 primates. They found that, controlling for fat-free body mass, there was significant positive mass correlation between heart and lungs or liver, between lungs and kidneys, liver, or spleen, between kidneys and liver or spleen, or between liver and spleen. In TCM, the heart rate belongs to the essential *heart* function. Jensen et al. [33] have done a prospective cohort study, the Copenhagen Male Study, a longitudinal study of healthy middle-aged employed men, and found that elevated resting heart rate was a risk factor for mortality independent of physical fitness, leisure-time physical activity, and other major cardiovascular risk factors. Xiong et al. [34] investigated physiological parameters during practicing simplified 24-form **T'ai chi ch'uan** (TCC) in 10 young high-level male TCC athletes and 10 ordinary-level male TCC practitioners with similar age and body size. They found significantly higher energy expenditure, heart rate, oxygen uptake, and tidal volume in the high-level group than the ordinary-level group during TCC performance. In TCM, gamma glutamyltransferase (GGT) and alkaline phosphatase (ALP) belong to the essential *liver* function. Kunutsor et al. [35] conducted a systematic review and meta-analysis of published prospective cohort studies evaluating the associations of baseline levels of these enzymes with all-cause mortality in general populations. Nineteen unique cohort studies with aggregate data on over 9.24 million participants and 242, 953 all-cause mortality outcomes were included. They found that the pooled relative risks (95% confidence intervals) for all-cause mortality per 5 U/L increment in GGT and ALP levels were 1.07 (1.04–1.10) and 1.03 (1.01–1.06), respectively. In TCM, forced expiratory volume in 1 second (FEV1) and peripheral blood leukocyte count belong to the essential *lung* and *spleen* functions. Weiss et al. [36] explored the relation of leukocyte count and FEV1 to total mortality in the Normative Aging Study population in the Boston, Massachusetts, area. The sample for the current analysis consisted of 1,956 men who underwent the baseline Normative Aging Study examination during 1961–1969. Subjects ranged in age from 21 to 80 years of age at the time of entry. A total of 170 deaths occurred over the 30 years of follow-up. They found that age, FEV1, and peripheral blood leukocyte count were the three most important predictors of increased mortality in this cohort, independent of cigarette smoking. In TCM, plasma fibrinogen belongs to the essential *kidney* function. Stack et al. [37] identified 9, 184 subjects at the age of 40 years and over from the Third National Health and Nutrition Examination Survey (1988–1994) with vital status assessed through 2006. They found that the adjusted hazard ratio (HR) per 1 μmol/L (34 mg/dL) increase in fibrinogen was 1.07 (95% confidence interval (CI) 1.04–1.09) for total mortality and 1.06 (95% CI 1.03–1.09) for cardiovascular mortality in multivariate analysis.

Qi function, *blood* function, *body fluid* functions, *meridian* functions, *acupoint* functions, and the six *yang fu* functions, *gallbladder* function, *stomach* function, *small intestine* function, *large intestine* function, *bladder* function, and *triple energizer* function, should be special nonessential functions according to TCM. In TCM, haemoglobin belongs to the nonessential *blood* function. Skjelbakken et al. [38] examined 6541 men aged between 20 and 49 years in 1974 in a prospective, population-based study from the municipality of Tromsø, Northern Norway, for 20 years of follow-up and found a U-shaped relationship between quintiles of haemoglobin and total mortality. In the above-mentioned

cohort of Weiss et al. [36], other covariates examined included forced vital capacity, height, body mass index, systolic and diastolic blood pressure, and total cholesterol, but age, FEV1, and peripheral blood leukocyte count were the three most important predictors of increased mortality.

The extraordinary *fu* functions such as *brain* function, *marrow* function, *bone* functions, *blood vessel* functions, *gallbladder* function, *uterus* function, *pericardium* function, *life gate* function, and *essence chamber* function should be general nonessential functions according to TCM. In TCM, brain mass belongs to the general nonessential *brain* function. Navarrete et al. [32] analyzed brain size and organ mass data for 100 mammalian species, including 23 primates. They found that, controlling for fat-free body mass, brain size was not negatively correlated with the mass of the digestive tract or any other expensive organ. In TCM, reproduction belongs to the general nonessential *essence chamber* function. Castration, which removes the source of male sex hormones, prolongs male lifespan in many animals [39]. Min et al. [40] studied the genealogy records of Korean eunuchs and determined the lifespan of 81 eunuchs and found that the average lifespan of eunuchs was 70.0 ± 1.76 years, which was 14.4–19.1 years longer than the lifespan of noncastrated men of similar socioeconomic status.

In TCM, the neurological functions except consciousness belong to the general nonessential *brain* function. Feuillet et al. [31] reported the case of an anatomically "brainless" white-collar worker who functioned much better than could be expected with so little brain material. The 44-year-old worker presented a 2-week history of mild left leg weakness. At the age of 6 months, he had undergone a ventriculoatrial shunt, because of postnatal hydrocephalus of unknown cause. When he was 14 years old, he developed ataxia and paresis of the left leg, which resolved entirely after shunt revision. His neurological development and medical history were otherwise normal. He was a married father of two children and worked as a civil servant. On neuropsychological testing, he proved to have an intelligence quotient (IQ) of 75: his verbal IQ was 84 and his performance IQ was 70. Computer tomography (CT) showed severe dilatation of the lateral ventricles. Magnetic resonance imaging revealed massive enlargement of the lateral, third, and fourth ventricles, a very thin cortical mantle and a posterior fossa cyst. Feuillet et al. [31] diagnosed a noncommunicating hydrocephalus, with probable stenosis of Magendie's foramen. The leg weakness improved partly after neuroendoscopic ventriculocisternostomy but soon recurred; however, after a ventriculoperitoneal shunt was inserted, the findings on neurological examination became normal within a few weeks. The findings on neuropsychological testing and CT did not change.

4.2. External Activities. A person may have many external activities [41, 42]. An average adult's personal F max as discussed in Section 2 should be his/her occupational work [43]. Li [43] has collected 104 dead scientists or celebrities and found that the Pearson correlation coefficients of the prime occupation age with the lifespan and the prime age h discussed in Section 2 were 0.901 and 0.906, respectively, and there was a positive linear relationship between the prime occupation age and the lifespan. Moreover, the higher the Qp or/and the slower the increases in Q max, the longer the expected lifespan. Therefore, the occupational work should be the only essential activity. While studying engagement outcomes worldwide, Gallup [44] discovered a correlation between employees' engagement levels at work and their physical health. Low engagement may lead to low skill level [45]. In another study by Tjepkema et al. [46], a 15% sample of 1991 Canadian Census respondents aged 25 years or older was linked to 16 years of mortality data (1991–2006). The study analyzed 2.3 million people aged 25 to 64 years at cohort inception, among whom there were 164, 332 deaths during the follow-up period, and found that mortality gradients by occupational skill level were evident for most causes of death.

The observations have been directly supported by butterfly experiments conducted by Niitepõld and Hanski [47]. They analyzed the repeatability of measurements of peak flight metabolic rate (MR (peak)) throughout the life of the Glanville fritillary butterfly (*Melitaea cinxia*). They found that measurements of MR (peak) showed significant repeatability and there was a significant positive correlation between MR (peak) and lifespan in all three experiments: in the laboratory, under field conditions, and in a laboratory experiment with repeated flight treatments.

These findings are also supported by a study on competitive sports by Teramoto and Bungum [48]. They reviewed elite endurance (aerobic) athletes and mixed-sports (aerobic and anaerobic) athletes and found that they survive longer than the general population, as indicated by lower mortality and higher longevity. For example, a former career elite athlete would be protected from both type 2 diabetes and impaired glucose tolerance in later life [49] and an athlete doing high- but not low-intensity cycling may resist diesel exhaust exposure [50].

Wiseman [51] suggested that physical actions may be the quickest, easiest, and most powerful way to instantly change how one thinks and feels. This suggested that subjective well-being (SWB) should be a nonessential activity. There is a longstanding idea that happiness causes people to live longer, healthier lives. However, convincing evidence that SWB contributes to longevity and health has not been available [52]. Chida and Steptoe [53] have reviewed systematically prospective, observational cohort studies of the association between positive well-being and mortality using meta-analytic methods and suggested that positive psychological well-being has a favorable effect on survival in both healthy and diseased populations. Many other kinds of studies also concluded that happiness has a positive causal effect on longevity and physiological health [52]. However, other studies did not support it. Wiest et al. [54] have examined differential effects of life satisfaction (LS), positive affect (PA), and negative affect (NA) on mortality in a conjoint analysis using data of German adults between the ages of 40 and 85 years ($N = 3,124$). They found that LS and PA predicted mortality over and above sociodemographic factors and physical health. However, this effect diminished when it included self-rated health and physical activity. NA was not associated with mortality. Although PA predicted mortality in older adults (65+) even after controlling for self-rated health

and physical activity, no SWB indicator predicted mortality when controlling for covariates in middle-aged participants.

The nonessential activities can be further classified into the special ones and the general ones. Kahneman et al. [41] have assessed the range of mean enjoyment ratings for the lowest and highest levels of selected person and job characteristics after controlling for other job features or for other personal features for 909 employed women in USA. The ranges of both constant pressure to work quickly (definitely yes or definitely not) work episodes and sleep quality (very bad or very good) home episodes ranked the first. The ones of requires specialized education/training (definitely yes or definitely not) work episodes, importance of religion (not at all or very important) home episodes, and household income (less than $30,000 or more than $90,000) home episodes ranked the second. The ones of constant pressure to work quickly (definitely yes or definitely not) home episodes, at risk of being laid off (definitely yes or definitely not) work episodes, and marital status (divorced or married) home episodes ranked the third. These findings paralleled the observation that life circumstances have surprisingly little influence on global reports of life satisfaction [41]. These results suggested that sleep, one of the first rank activities, should be a special nonessential activity, but the other activities of second or third rank should be general nonessential ones. The nonessential sleep was supported by the U-shaped relationship between survival and actigraphically measured sleep durations [55] and between the hazard ratios for all-cause mortality and sleep duration [56]. It has been found that melatonin administration during daytime does not have any acute (1-2 h) effects either on the maximal jumping ability of adult men or on the maximal strength [57] and daily locomotor activity levels were similar between wild-type and circadian Clock mutant mice throughout the training protocol [58]. Moreover, sleep may be a special nonessential activity. Garde et al. [59] found that short sleep duration is a risk factor for ischemic heart disease mortality among middle-aged and elderly men, particularly those using tranquilizers/hypnotics on a regular or even a rare basis, but not among men not using tranquilizers/hypnotics.

SWB can be represented by health-related quality of life (HRQOL) [60]. HRQOL can be also represented by the Euro-Qol questionnaire (EQ-5D) [61]. Healthy Japan 21 (Japanese National Health Promotion in the 21st Century) was started in 2000 to promote extension of healthy life expectancy and improve HRQOL. Fujikawa et al. [61] described HRQOL of Japanese subjects using the EQ-5D and investigated the influence of social background, health-related behaviors, and chronic conditions on HRQOL using representatives in Takamatsu, Japan. They found that EQ-5D scores decreased with age, particularly for respondents who were unemployed or retired. Adjusting to sex and age, the results showed that age, unemployment/retirement, feeling severe stress, and musculoskeletal and gastrointestinal diseases were significantly associated with decreased HRQOL. Conversely, sufficient sleep (7-8 h/day) and having a hobby were significantly associated with increased HRQOL. It should be pointed out that there was no significant association between exercise and HRQOL although exercise is one of hobby activities. These results supported the special nonessential nature of sleep and suggested that a hobby is a special nonessential activity.

In TCM, nutrition corresponds to the nutritive *qi* function which belongs to a special nonessential function, and it should be a special nonessential activity. Many studies have found that there was a U-shaped relationship between body mass index (BMI) and mortality, morbidity, hazard risk, medical costs, physical fitness, subjective well-being, job strain, health-related quality of life, or other health-related outcomes. Goyal et al. [62] evaluated all-cause, cancer, and cardiovascular mortality risks associated with quintiles (Q1–Q5) of serum antioxidant (vitamins C and E, β-carotene, and selenium) and vitamin A levels, in 16,008 adult participants of The Third National Health and Nutrition Examination Survey (NHANES III; 1988–1994) and found that both vitamins A and E had U-shaped associations with all-cause mortality.

5. Organism Photobiomodulation

There are two kinds of PBM [11, 12], direct and indirect PBM (dPBM and iPBM). A dPBM can promote the normalization of a dysfunctional function [11] by promoting the activation of one partially activated NSP [12]. An iPBM can upgrade a normal function [11] maintaining a fully activated NSP by promoting the activation of one or more redundant pathways of the NSP and then the synergistic action of all the fully activated redundant NSPs [12]. Their mechanisms on health, suboptimal health, and disease were discussed in this section.

5.1. Health Promotion. Health is a state of complete physical, mental, and social well-being and not merely the absence of disease or infirmity according to the World Health Organization. Health is the state of an organism with undisturbed functional dynamic homeostasis providing optimum performance of organism functions to the extent necessary for productive relations of the organism with the environment according to Kryzhanovsky [63]. When discussing health, Taleb [17] thought that antifragileness should play an important role. As it has been pointed out in Section 2, the so-called antifragileness was just successful stress. In terms of FSH, FSSH, and scale-free functional network, health may be defined as a state of an organism in which its essential and special non-essential functions are normal or their stresses are successful. Its general nonessential functions may be dysfunctional or their stresses may be chronic. In this context, health can be of different levels because its normal functions can be of different levels and the phase transition of health can be discussed in view of the phase transition of its normal functions as discussed in our previous paper [12]. The higher the functional fitness of one of the essential or special nonessential functions is, the higher the health level is. In TCM, consciousness belongs to the essential five *yin zang* functions. Through kinesiological testing, Hawkins [64] has estimated the various levels of consciousness.

A global PBM can enhance health level by upgrading a normal function or activity in an iPBM way or normalizing a dysfunctional function or activity in a dPBM way. The work of an athlete is doing sports. His/her performance represents

his/her health level. Zhao et al. [23] have globally irradiated elite Chinese female basketball players wearing swimsuits with red light at 658 nm and 30 J/cm^2 for 30 min every night during 14 routine days including 12 training days with the following specifications: 2 hours of morning training, 2 hours of afternoon training, and no training on Sunday. They found that the 14-day whole-body irradiation improved sleep, serum melatonin level, and endurance performance. Leal-Junior et al. [65] have performed a systematic review with meta-analysis to investigate the effects of the PBM applied before exercises. They found that 12 randomized controlled trials (RCTs) irradiated phototherapy before exercise among which 10 RCTs reported significant improvement in the main outcome measures related to performance. The time until exhaustion increased significantly compared to placebo by 4.12 s and the number of repetitions increased by 5.47 after phototherapy. They concluded that the PBM improved muscular performance and accelerated recovery mainly when applied before exercise.

Based on the theory of constitution in TCM, the human health can be classified into nine constitutions including a balanced constitution and eight unbalanced constitutions, *yang*-deficiency, *yin*-deficiency, *qi*-deficiency, *phlegm-wetness*, *wetness-heat*, stagnant *blood*, depression, and inherited special constitutions [66, 67]. For the balanced constitution, the functional fitness of normal essential and special nonessential functions matches with one another. For the unbalanced constitution, the functional fitness of some normal functions is lower than the balanced one so that the functional fitness of normal essential and special nonessential functions does not match with one another. A global PBM can enhance health level by upgrading a normal function in an iPBM way so that it can transform unbalanced constitutions into the balanced constitution. We have analyzed the published epidemiological investigation of nine constitutions in nine provinces in China [68] according to province latitudes and found that sunlight may transform the unbalanced constitutionssuch as *qi*-deficiency, *yang*-deficiency, *yin*-deficiency, *phlegm-wetness,* or depression into the balanced constitution. Obviously, the skin-decayed sunlight can play an iPBM role so that it can enhance the functional fitness.

5.2. Suboptimal Health Rehabilitation. Although suboptimal health has been mentioned as early as in 1979 [69], its exact definition has been left unresolved. In terms of FSH, FSSH, and scale-free functional network, the suboptimal health may be defined as a state of disease-free organism in which some special nonessential functions are lightly dysfunctional or their stresses are lightly chronic in comparison with health definition.

Suboptimal health is often self-limited [11, 70]. Health can resist low-level disturbance under the threshold, but high-level disturbance of some special nonessential functions above their respective threshold may result in suboptimal health. Suboptimal health can be completely self-recovered if the high-level disturbance is eliminated. A dPBM can promote the normalization of dysfunctional special nonessential functions and possibly even at the high-level disturbance. For example, intranasal low-intensity laser therapy (ILILT) has been used in health care applications for hyperlipidemia, blood hyperviscosity, and insomnia [8]. In a study, it treated high blood coagulation status in healthy pregnant women at term [8].

The SWB or HRQOL of an organism in suboptimal health is lower than the one in health. The higher the health level is, the higher the SWB or HRQOL is. Jia and Lubetkin [71] have examined a 1993–2006 monthly behavioral risk factor surveillance system (BRFSS) random sample and found that the worst physical health was during the winter and the best physical health was during the summer. Oswald and Wu [72] have examined a 2005–2008 BRFSS random sample of 1.3 million U.S. citizens and found that southern citizens were averagely happier than northern citizens. It might partially be due to the intensity of southern or summer sunlight being high enough for the skin-decayed sunlight to promote the rehabilitation of citizens in suboptimal health in a dPBM way or enhance the health level of citizens in health in an iPBM way. Of the sample of 7979 individuals, being representative of the Finnish general population aged 30 and over, Grimaldi et al. [73] found that the HRQoL was influenced by both the seasonal changes in mood and behavior and the illumination experienced indoors. Greater seasonal changes and poor illumination indoors were associated with more severe mental ill-being.

5.3. Disease Treatment. According to Kryzhanovsky [63], disease is a state of an organism with disturbed functional dynamic homeostasis and inability to perform to a necessary extent, with the functions providing productive relations with the environment. In this paper, the disease may be defined as a state far from its health or suboptimal health. It may be classified into two kinds, the essential and nonessential disease. The essential disease such as myocardial infarction is a state of an organism in which some of the essential functions are dysfunctional or their stresses are chronic. A nonessential disease such as diabetes is a state of an organism in which some special nonessential functions are heavily dysfunctional or their stresses are heavily chronic so that the functional fitness of some nonessential functions is too low for healthy survival.

The initial phase of a disease is often self-limited [11, 70]. Health can resist low-level disturbance, but high-level disturbance may result in disease. The initial phase of a disease can be completely self-recovered if the high-level disturbance is eliminated. A dPBM can promote the normalization of one dysfunctional function if the self-recovery process is delayed. For example, ILILT has positive clinical applications in mild cognitive impairment, Alzheimer's disease, Parkinson's disease, schizophrenia, pain relief, stroke, depression, inflammation, coronary heart disease, myocardial infarction, and cerebral palsy [8], and potential applications in hypertension, vascular dementia, cancer, diabetes, influenza, olfactory dysfunction, myopia, withdrawal symptoms, and renal failure [8], and its possible applications in upper respiratory tract infection, asthma, osteoarthritis, exercise-induced muscle damage, wound, traumatic brain injury, and osteoporosis [74].

The network of condition-specific functions of a patient with a disease which cannot be self-limited is also a scale-free network. The functions can be classified into the essential and nonessential functions. The dysfunctional nonessential function may be self-limited, but the dysfunctional essential function cannot be self-limited and its normalization may be promoted with a dPBM. For fibrosis [75], the nonessential oxidative stress or inflammation may be self-limited, but the delayed essential tissue self-regeneration can be promoted with a dPBM.

5.4. Action-Dependent Organism Photobiomodulation. Cellular functions and their PBM on cells are decided by their microenvironment [12]. For example, mitotic cells in their respective proliferation-specific homeostasis inactivate DNA double-strand break repair [76]. A PBM on the irradiated tissue should be decided by the tissue essential functions. For example, a dPBM on fibrosis can promote the delayed essential tissue self-regeneration [75]. A global PBM on an organism should be decided by the organism action, especially the normal action in its action-specific homeostasis (ASH). A PBM may modulate any functions. As actions may be the quickest, easiest, and most powerful way to instantly change how one thinks and feels [51], the organism action or its ASH would inhibit function PBM, a PBM which modulate a function, unless the function PBM is needed for action normalization, ASH maintenance, or its fitness enhancement. The higher the ASH fitness is, the stronger the resistance of the ASH is. For example, an athlete doing high- but not low-intensity cycling may resist diesel exhaust exposure [50]. Therefore, a global PBM on an organism may promote the normalization of a dysfunctional action in a dPBM way or upgrade the normal action in an iPBM way and then modulate organism health, suboptimal health, and disease.

The PBM modulated actions may be circadian rhythms. Circadian rhythms prepare an organism for daily external activities or internal functions. The fitness enhancement of circadian rhythms can upgrade the related normal activities or functions. A PBM on circadian rhythm recovery or enhancement may promote the recovery or enhancement. The circadian rhythm protein period 2 (Per2) has been implicated in cardiac adaptation to limited oxygen availability. Eckle et al. [77] found that recovery of Per2 in the heart by exposing mice to bright light resulted in the transcriptional induction of glycolytic enzymes and Per2-dependent cardioprotection from ischemia. Melatonin entrains many aspects of the biological clock via activation of specific G-protein-coupled integral membrane melatonin receptors [78]. ILILT promoted melatonin recovery has found its applications in treating Alzheimer's disease, Parkinson's disease, poststroke depression and insomnia [8, 74] and its possible applications in treating wound, traumatic brain injury, and osteoporosis [74].

The PBM modulated actions may be sleep, preactivity warming, or postactivity cooling. Anafi et al. [79] found that sleep enhanced organ-specific molecular functions and that it had a ubiquitous role in reducing cellular metabolic stress in both brain and peripheral tissues. Their data suggested a novel role for sleep in synchronizing transcription in peripheral tissues. Night time is the due time for melatonin increase, which is triggered by the circadian rhythms [80]. Warm-up exercise may increase physical fitness [81]. Therefore, the iPBM enhancement of the circadian rhythms fitness during night time [23] or warming time [65] can enhance exercise performance as has been discussed in Section 5.1.

The PBM modulated actions may be exercise. Ng et al. [82] found that successful aging in multivariate models was significantly associated with age (OR = 0.90), female gender (OR = 1.37), ≥6 years of education (OR = 2.31), better housing (OR = 1.41), religious or spiritual beliefs (OR = 1.64), physical activities and exercise (OR = 1.90), and low or no nutritional risk (OR = 2.16). Liu et al. [83] found that treadmill exercise enhanced learning and memory function not only in wild-type mice but also in APP/PS1 transgenic mouse model of Alzheimer's disease paralleled by long-term potentiation. ILILT may be directly used to treat aging persons or patients with Alzheimer's disease [8] and may also be used to treat exercising elders or exercising patients with Alzheimer's disease, and the therapeutic effects of the latter approach may be better than the ones of the former approach.

The recoveries of suboptimal health or disease need cellular factors by circadian rhythms. They also need cells, especially mesenchymal stem cells (MSCs), which has been supported by widely used cell therapy. The MSCs can be transplanted. They can also be increased *in situ* with a PBM [84]. Sprague-Dawley rats underwent experimental myocardial infarction (MI). Tuby et al. [84] have compared the tibia irradiation with heart irradiation of low-intensity laser irradiation (Ga-Al-As diode laser, power density 10 mW/cm^2, for 100 seconds). They found that the tibia irradiation was more effective than heart irradiation. They further found that the tibia irradiation was mediated by bone marrow-derived MSCs.

6. Discussions

In the above-mentioned studies, the health, suboptimal health, and disease of an organism have been defined in terms of FSH, FSSH, and scale-free functional network, and their global PBM have been discussed, respectively. The global PBM on an organism may depend on the organism action, but the corresponding studies are very preliminary.

A patient or animal usually does nothing else while doing suboptimal health or disease treatment with a PBM. The therapeutic effects may be enhanced if the patient or animal does something to aid the PBM treatment. For example, the patient can sleep, listen to music, draw a picture, read materials, or exercise. The best alternative may be to be at his/her F max as discussed in Section 2. The F max is often achieved while performing the occupational work [43], the unique essential external activity as discussed in Section 4.2. As Tjepkema et al. [46] have found, mortality gradients by occupational skill level were evident for most causes of death. The higher the occupational skill level is, the lower the mortality for most causes of death is. In this context, the therapeutic effects of the global PBM on an organism may be

mediated and enhanced by its modulation on the organism action. The laser device for *in situ* activity modulation may be ILILT, wrist low-intensity laser therapy, or interdigital low-intensity laser therapy.

Among other therapies offering global PBM, sunlight is the simplest. The skin-decayed sunlight may play an important role in outdoor effects on action performance according to the action-dependent mechanism of a global PBM. The hypothesis that there are added beneficial effects to be gained from performing physical activity outdoors in natural environments is very appealing and has generated considerable interest [85]. Compared with exercising indoors, exercising in natural environments has been associated with greater feelings of revitalization and positive engagement, decreases in tension, confusion, anger, and depression, and increased energy. Participants also reported greater enjoyment and satisfaction with outdoor activity and declared a greater intent to repeat the activity at a later date [85]. Athletes' times in 200 m indoor races are greater than in outdoor races [86]. The outdoor effects have been also observed in many animals or birds. Chen et al. [87] have investigated the effects of outdoor access on the growth performance and meat quality of broiler chickens and found that outdoor access had no effect on growth performance and yield traits but could improve the meat quality; birds reared with outdoor access from 36 d of age had better appearance and meat quality than those with outdoor access from 71 d of age.

The skin-decayed bright light may also play an important role in bright light intensification of affective responses [88] according to the action-dependent mechanism of a global PBM. Across six experiments, Xu et al. [88] found that light increased people's perception of ambient warmth, which in turn activates their hot emotional system, leading to intensified affective reactions—positive and negative—to different kinds of stimuli. Across different domains, ranging from feelings towards words to judgments of ad scripts and ad models for aggressiveness and sexiness, and to choice of food spiciness levels and consumptions of drinks, they found that light intensified both experienced and anticipated affective reactions, and consequently, influenced judgment and choice in a variety of contexts. Importantly, the awareness of a potential influence of ambient brightness on affective response did not result in a correction of its influence. The reality, based on their data, however, is that bright light intensifies positive or negative affective responses. For example, the participants consumed more of the favorable juice in bright rather than dimmed light, but less of the unfavorable juice; bright-light compared to dim light enhanced positive feelings toward the favorable drink and enhanced negative feelings toward the unfavorable drink; ambient brightness amplified affective reaction which impacts consumption; and people consumed more of favorable drinks and less of unfavorable drinks in bright light.

7. Conclusions

The health, suboptimal health, and disease of an organism may be defined in terms of FSH, FSSH, and scale-free functional network. Their global PBM may depend on the organism action so that the PBM modulated action may modulate PBM therapeutic effects.

Conflict of Interests

The authors declare that there is no conflict of interests regarding the publication of this paper.

Authors' Contribution

Timon Cheng-Yi Liu, Long Liu, and Jing-Gang Chen contributed equally to this work.

Acknowledgments

This work was supported by National Science Foundation of China (60878061, 10974061, and 11374107), Doctoral Fund of Ministry of Education of China (20124407110013), and Guangdong Scientific Project (2012B031600004).

References

[1] L. Hood and N. D. Price, "Demystifying disease, democratizing health care," *Science Translational Medicine*, vol. 6, no. 225, Article ID 225ed5, 2014.

[2] P. Sobradillo, F. Pozo, and Á. Agustí, "P4 medicine: the future around the corner," *Archivos de Bronconeumologia*, vol. 47, no. 1, pp. 35–40, 2011.

[3] D. S. Jones, *Textbook of Functional Medicine*, The Institute for Functional Medicine, Gig Harbor, Wash, USA, 2006.

[4] Z. Xie, *On the Standard Nomenclature of Traditional Chinese Medicine*, Foreign Languages Press, Beijing, China, 2003.

[5] P. C. Leung, C. C. Xue, and Y. C. Cheng, Eds., *A Comprehensive Guide to Chinese Medicine*, World Scientific, River Edge, NJ, USA, 2003.

[6] M. A. Hyman, "Systems of correspondence: functionality in traditional Chinese medicine and emerging systems biology," *Alternative Therapies in Health and Medicine*, vol. 12, no. 2, pp. 10–11, 2006.

[7] J. Wang, Q. Wang, L. Li et al., "Phlegm-dampness constitution: genomics, susceptibility, adjustment and treatment with traditional Chinese medicine," *The American Journal of Chinese Medicine*, vol. 41, no. 2, pp. 253–262, 2013.

[8] T. C.-Y. Liu and P. Zhu, *Intranasal Low Intensity Laser Therapy*, People's Military Medical Press, Beijing, China, 2009.

[9] J. L. Hartman IV, B. Garvik, and L. Hartwell, "Cell biology: principles for the buffering of genetic variation," *Science*, vol. 291, no. 5506, pp. 1001–1004, 2001.

[10] T. C.-Y. Liu, R. Liu, L. Zhu, J. Q. Yuan, M. Hu, and S. H. Liu, "Homeostatic photobiomodulation," *Frontiers of Optoelectronics in China*, vol. 2, no. 1, pp. 1–8, 2009.

[11] T. C.-Y. Liu, Y. Y. Liu, E. X. Wei, and F. H. Li, "Photobiomodulation on stress," *International Journal of Photoenergy*, vol. 2012, Article ID 628649, 11 pages, 2012.

[12] T. C.-Y. Liu, D. Wu, L. Zhu, P. Zeng, L. Liu, and X. Yang, "Microenvironment dependent photobiomodulation on function-specific signal transduction pathways," *International Journal of Photoenergy*, vol. 2014, Article ID 904304, 8 pages, 2014.

[13] M. A. Nowak, M. C. Boerlijst, J. Cooke, and J. M. Smith, "Evolution of genetic redundancy," *Nature*, vol. 388, no. 6638, pp. 167–170, 1997.

[14] F. Martius, "Das amdt-schulz grandgesetz," *Munchener Medizinische Wochenschrift*, vol. 70, pp. 1005–1006, 1923.

[15] L. T. Braun, "Exercise physiology and cardiovascular fitness," *Nursing Clinics of North America*, vol. 26, no. 1, pp. 135–147, 1991.

[16] P. A. Hancock, "The effect of skill on performance under an environmental stressor," *Aviation, Space, and Environmental Medicine*, vol. 57, no. 1, pp. 59–64, 1986.

[17] N. N. Taleb, *Antifragile: Things That Gain from Disorder*, Random House Press, New York, NY, USA, 2012.

[18] E. J. Calabrese, K. A. Bachmann, A. J. Bailer et al., "Biological stress response terminology: integrating the concepts of adaptive response and preconditioning stress within a hormetic dose-response framework," *Toxicology and Applied Pharmacology*, vol. 222, no. 1, pp. 122–128, 2007.

[19] R. M. Yerkes and J. D. Dodson, "The relation of strength of stimulus to rapidity of habit-formation," *Journal of Comparative Neurology and Psychology*, vol. 18, no. 5, pp. 459–482, 1908.

[20] A. I. Yashin, "Hormesis against aging and diseases: using properties of biological adaptation for health and survival improvement," *Dose-Response*, vol. 8, no. 1, pp. 41–47, 2010.

[21] E. Y. Robertson, P. U. Saunders, D. B. Pyne, C. J. Gore, and J. M. Anson, "Effectiveness of intermittent training in hypoxia combined with live high/train low," *European Journal of Applied Physiology*, vol. 110, no. 2, pp. 379–387, 2010.

[22] A. Janiak and J. Kedziora, "Exercise effect on the circadian rhythm of left ventricular systole in healthy men with higher and lower physical fitness," *Acta Physiologica Polonica*, vol. 33, no. 4, pp. 345–351, 1982.

[23] J. Zhao, Y. Tian, J. Nie, J. Xu, and D. Liu, "Red light and the sleep quality and endurance performance of Chinese female basketball players," *Journal of Athletic Training*, vol. 47, no. 6, pp. 673–678, 2012.

[24] T. C.-Y. Liu, L. Zhu, and X. B. Yang, "Longevity chance," *Journal of Innovative Optical Health Sciences*, vol. 7, no. 2, Article ID 1330006, 6 pages, 2013.

[25] J. P. Onnela, "Physics: flow of control in networks," *Science*, vol. 343, no. 6177, pp. 1325–1326, 2014.

[26] H. Jeong, B. Tombor, R. Albert, Z. N. Oltval, and A.-L. Barabásl, "The large-scale organization of metabolic networks," *Nature*, vol. 407, no. 6804, pp. 651–654, 2000.

[27] J. S. Edwards and B. O. Palsson, "The *Escherichia coli* MG1655 in silico metabolic genotype: its definition, characteristics, and capabilities," *Proceedings of the National Academy of Sciences of the United States of America*, vol. 97, no. 10, pp. 5528–5533, 2000.

[28] C. I. del Genio, T. Gross, and K. E. Bassler, "All scale-free networks are sparse," *Physical Review Letters*, vol. 107, no. 17, Article ID 178701, 4 pages, 2011.

[29] T. C.-Y. Liu, L. Zhu, and X. B. Yang, "Photobiomodulation-mediated pathway diagnostics," *Journal of Innovation in Optical Health Science*, vol. 6, no. 1, Article ID 133000, 11 pages, 2013.

[30] F.-J. Müller and A. Schuppert, "Few inputs can reprogram biological networks," *Nature*, vol. 478, no. 7369, pp. E4–E5, 2011.

[31] L. Feuillet, H. Dufour, and J. Pelletier, "Brain of a white-collar worker," *The Lancet*, vol. 370, no. 9583, p. 262, 2007.

[32] A. Navarrete, C. P. van Schaik, and K. Isler, "Energetics and the evolution of human brain size," *Nature*, vol. 480, no. 7375, pp. 91–93, 2011.

[33] M. T. Jensen, P. Suadicani, H. O. Hein, and F. Gyntelberg, "Elevated resting heart rate, physical fitness and all-cause mortality: a 16-year follow-up in the Copenhagen Male Study," *Heart*, vol. 99, no. 12, pp. 882–887, 2013.

[34] K. Xiong, H. He, and G. X. Ni, "Effect of skill level on cardiorespiratory and metabolic responses during Tai Chi training," *European Journal of Sport Science*, vol. 13, no. 4, pp. 386–391, 2013.

[35] S. K. Kunutsor, T. A. Apekey, D. Seddoh, and J. Walley, "Liver enzymes and risk of all-cause mortality in general populations: a systematic review and meta-analysis," *International Journal of Epidemiology*, vol. 43, no. 1, pp. 187–201, 2014.

[36] S. T. Weiss, M. R. Segal, D. Sparrow, C. Wager, R. J. Crowell, and J. M. Samet, "Relation of FEV1 and peripheral blood leukocyte count to total mortality: the Normative Aging Study," *American Journal of Epidemiology*, vol. 142, no. 5, pp. 493–503, 1995.

[37] A. G. Stack, U. Donigiewicz, A. A. Abdalla et al., "Plasma fibrinogen associates independently with total and cardiovascular mortality among subjects with normal and reduced kidney function in the general population," *Quarterly Journal of Medicine*, 2014.

[38] T. Skjelbakken, T. Wilsgaard, O. H. Førde, E. Arnesen, and M.-L. Løchen, "Haemoglobin predicts total mortality in a general young and middle-aged male population. The Tromsø Study," *Scandinavian Journal of Clinical & Laboratory Investigation*, vol. 66, no. 7, pp. 567–576, 2006.

[39] H. M. Brown-Borg, "Hormonal regulation of longevity in mammals," *Ageing Research Reviews*, vol. 6, no. 1, pp. 28–45, 2007.

[40] K. J. Min, C. K. Lee, and H. N. Park, "The lifespan of Korean eunuchs," *Current Biology*, vol. 22, no. 18, pp. R792–R793, 2012.

[41] D. Kahneman, A. B. Krueger, D. A. Schkade, N. Schwarz, and A. A. Stone, "A survey method for characterizing daily life experience: the day reconstruction method," *Science*, vol. 306, no. 5702, pp. 1776–1780, 2004.

[42] M. A. Killingsworth and D. T. Gilbert, "A wandering mind is an unhappy mind," *Science*, vol. 330, no. 6006, p. 932, 2010.

[43] J. Li, *The study of scientist lifespan based on the function-specific homeostasis theory [M.S. of science thesis]*, South China Normal University, 2012.

[44] State of the Global Workplace, http://www.gallup.com/strategicconsulting/164735/state-global-workplace.aspx?utm_source=WWW&utm_medium=csm&utm_campaign=syndicationutm.

[45] P. Belchior, M. Marsiske, S. Sisco, A. Yam, and W. Mann, "Older adults' engagement with a video game training program," *Activities, Adaptation & Aging*, vol. 36, no. 4, pp. 269–279, 2012.

[46] M. Tjepkema, R. Wilkins, and A. Long, "Cause-specific mortality by occupational skill level in Canada: a 16-year follow-up study," *Chronic Diseases and Injuries in Canada*, vol. 33, no. 4, pp. 195–203, 2013.

[47] K. Niitepõld and I. Hanski, "A long life in the fast lane: positive association between peak metabolic rate and lifespan in a butterfly," *The Journal of Experimental Biology*, vol. 216, no. 8, pp. 1388–1397, 2013.

[48] M. Teramoto and T. J. Bungum, "Mortality and longevity of elite athletes," *Journal of Science and Medicine in Sport*, vol. 13, no. 4, pp. 410–416, 2010.

[49] M. K. Laine, J. G. Eriksson, U. M. Kujala et al., "A former career as a male elite athlete—does it protect against type 2 diabetes in later life?" *Diabetologia*, vol. 57, no. 2, pp. 270–274, 2014.

[50] L. V. Giles, J. P. Brandenburg, C. Carlsten, and M. S. Koehle, "Physiological responses to diesel exhaust exposure are modified by cycling intensity," *Medicine & Science in Sports & Exercise*, 2014.

[51] R. Wiseman, *Rip It up: The Radically New Approach to Changing Your Life*, Conville & Walsh Press, London , UK, 2012.

[52] B. S. Frey, "Happy people live longer," *Science*, vol. 331, no. 6017, pp. 542–543, 2011.

[53] Y. Chida and A. Steptoe, "Positive psychological well-being and mortality: a quantitative review of prospective observational studies," *Psychosomatic Medicine*, vol. 70, no. 7, pp. 741–756, 2008.

[54] M. Wiest, B. Schüz, N. Webster, and S. Wurm, "Subjective well-being and mortality revisited: differential effects of cognitive and emotional facets of well-being on mortality," *Health Psychology*, vol. 30, no. 6, pp. 728–735, 2011.

[55] D. F. Kripke, R. D. Langer, J. A. Elliott, M. R. Klauber, and K. M. Rex, "Mortality related to actigraphic long and short sleep," *Sleep Medicine*, vol. 12, no. 1, pp. 28–33, 2011.

[56] Y. Yeo, S. H. Ma, S. K. Park et al., "A prospective cohort study on the relationship of sleep duration with all-cause and disease-specific mortality in the Korean Multi-Center Cancer Cohort Study," *Journal of Preventive Medicine and Public Health*, vol. 46, no. 5, pp. 271–281, 2013.

[57] A. A. Mero, M. Vähälummukka, J. J. Hulmi, P. Kallio, and A. von Wright, "Effects of resistance exercise session after oral ingestion of melatonin on physiological and performance responses of adult men," *European Journal of Applied Physiology*, vol. 96, no. 6, pp. 729–739, 2006.

[58] S. Pastore and D. A. Hood, "Endurance training ameliorates the metabolic and performance characteristics of circadian Clock mutant mice," *Applied Physiology*, vol. 114, no. 8, pp. 1076–1084, 2013.

[59] A. H. Garde, Å. M. Hansen, A. Holtermann, F. Gyntelberg, and P. Suadicani, "Sleep duration and ischemic heart disease and all-cause mortality: prospective cohort study on effects of tranquilizers/hypnotics and perceived stress," *Scandinavian Journal of Work, Environment & Health*, vol. 39, no. 6, pp. 550–558, 2013.

[60] R. A. Cummins, "Fluency disorders and life quality: subjective wellbeing vs. health-related quality of life," *Journal of Fluency Disorders*, vol. 35, no. 3, pp. 161–172, 2010.

[61] A. Fujikawa, T. Suzue, F. Jitsunari, and T. Hirao, "Evaluation of health-related quality of life using EQ-5D in Takamatsu, Japan," *Environmental Health and Preventive Medicine*, vol. 16, no. 1, pp. 25–35, 2011.

[62] A. Goyal, M. B. Terry, and A. B. Siegel, "Serum antioxidant nutrients, vitamin a, and mortality in US adults," *Cancer Epidemiology, Biomarkers & Prevention*, vol. 22, no. 12, pp. 2202–2211, 2013.

[63] G. N. Kryzhanovsky, "Some categories of general pathology and biology: health, disease, homeostasis, sanogenesis, adaptation, immunity: new approaches and notions," *Pathophysiology*, vol. 11, no. 3, pp. 135–138, 2004.

[64] D. R. Hawkins, *Power versus Force*, Hay House, Carlsbad, Calif, USA, 2002.

[65] E. C. Leal-Junior, A. A. Vanin, E. F. Miranda, P. D. de Carvalho, S. dal Corso, and J. M. Bjordal, "Effect of phototherapy (low-level laser therapy and light-emitting diode therapy) on exercise performance and markers of exercise recovery: a systematic review with meta-analysis," *Lasers in Medical Science*, 2013.

[66] Q. Wang and S. Yao, "Molecular basis for cold-intolerant yang-deficient constitution of traditional chinese medicine," *The American Journal of Chinese Medicine*, vol. 36, no. 5, pp. 827–834, 2008.

[67] J. Wang, Y. Li, C. Ni, H. Zhang, L. Li, and Q. Wang, "Cognition research and constitutional classification in chinese medicine," *The American Journal of Chinese Medicine*, vol. 39, no. 4, pp. 651–660, 2011.

[68] Q. Wang and Y. Zhu, "Epidemiological investigation of constitutional types of Chinese medicine in general population: base on 21,948 epidemiological investigation data of nine provinces in China," *China Journal of Traditional Chinese Medicine and Pharmacy*, vol. 24, no. 1, pp. 7–12, 2009 (Chinese).

[69] R. G. Farmer and W. M. Michener, "Prognosis of Crohn's disease with onset in childhood or adolescence," *Digestive Diseases and Sciences*, vol. 24, no. 10, pp. 752–757, 1979.

[70] J. Bigelow, *A Discourse on Self-Limited Diseases (1835)*, Kessinger, Whitefish, Mont, USA, 1999.

[71] H. Jia and E. I. Lubetkin, "Time trends and seasonal patterns of health-related quality of life among US adults," *Public Health Reports*, vol. 124, no. 5, pp. 692–701, 2009.

[72] A. J. Oswald and S. Wu, "Objective confirmation of subjective measures of human well-being: evidence from the USA," *Science*, vol. 327, no. 5965, pp. 576–579, 2010.

[73] S. Grimaldi, T. Partonen, S. I. Saarni, A. Aromaa, and J. Lönnqvist, "Indoors illumination and seasonal changes in mood and behavior are associated with the health-related quality of life," *Health and Quality of Life Outcomes*, vol. 6, article 56, 2008.

[74] T. C.-Y. Liu, D.-F. Wu, Z.-Q. Gu, and M. Wu, "Applications of intranasal low intensity laser therapy in sports medicine," *Journal of Innovative Optical Health Sciences*, vol. 3, no. 1, pp. 1–16, 2010.

[75] X. E. Li, L. Zhu, and T. C. Y. Liu, "Fibrosis inhibition of photobiomodulation promoted regeneration," *Photomedicine and Laser Surgery*, vol. 31, no. 10, pp. 505–506, 2013.

[76] A. Orthwein, A. Fradet-Turcotte, S. M. Noordermeer et al., "Mitosis inhibits DNA double-strand break repair to guard against telomere fusions," *Science*, 2014.

[77] T. Eckle, K. Hartmann, S. Bonney et al., "Adora2b-elicited *Per2* stabilization promotes a HIF-dependent metabolic switch crucial for myocardial adaptation to ischemia," *Nature Medicine*, vol. 18, no. 5, pp. 774–782, 2012.

[78] A. F. Wiechmann and J. A. Summers, "Circadian rhythms in the eye: the physiological significance of melatonin receptors in ocular tissues," *Progress in Retinal and Eye Research*, vol. 27, no. 2, pp. 137–160, 2008.

[79] R. C. Anafi, R. Pellegrino, K. R. Shockley, M. Romer, S. Tufik, and A. I. Pack, "Sleep is not just for the brain: transcriptional responses to sleep in peripheral tissues," *BMC Genomics*, vol. 14, article 362, 2013.

[80] C. Cajochen, C. Jud, M. Münch, S. Kobialka, A. Wirz-Justice, and U. Albrecht, "Evening exposure to blue light stimulates the expression of the clock gene *PER2* in humans," *European Journal of Neuroscience*, vol. 23, no. 4, pp. 1082–1086, 2006.

[81] S. A. Zeno, D. Purvis, C. Crawford, C. Lee, P. Lisman, and P. A. Deuster, "Warm-ups for military fitness testing: rapid evidence assessment of the literature," *Medicine & Science in Sports & Exercise*, vol. 45, no. 7, pp. 1369–1376, 2013.

[82] T. P. Ng, B. F. P. Broekman, M. Niti, X. Gwee, and E. H. Kua, "Determinants of successful aging using a multidimensional

definition among chinese elderly in singapore," *The American Journal of Geriatric Psychiatry*, vol. 17, no. 5, pp. 407–416, 2009.

[83] H.-L. Liu, G. Zhao, K. Cai, H.-H. Zhao, and L.-D. Shi, "Treadmill exercise prevents decline in spatial learning and memory in APP/PS1 transgenic mice through improvement of hippocampal long-term potentiation," *Behavioural Brain Research*, vol. 218, no. 2, pp. 308–314, 2011.

[84] H. Tuby, L. Maltz, and U. Oron, "Induction of autologous mesenchymal stem cells in the bone marrow by low-level laser therapy has profound beneficial effects on the infarcted rat heart," *Lasers in Surgery and Medicine*, vol. 43, no. 5, pp. 401–409, 2011.

[85] J. T. Coon, K. Boddy, K. Stein, R. Whear, J. Barton, and M. H. Depledge, "Does participating in physical activity in outdoor natural environments have a greater effect on physical and mental wellbeing than physical activity indoors? A systematic review," *Environmental Science & Technology*, vol. 45, no. 5, pp. 1761–1772, 2011.

[86] A. Ferro and P. Floria, "Differences in 200-m sprint running performance between outdoor and indoor venues," *The Journal of Strength and Conditioning Research*, vol. 27, no. 1, pp. 83–88, 2013.

[87] X. Chen, W. Jiang, H. Z. Tan et al., "Effects of outdoor access on growth performance, carcass composition, and meat characteristics of broiler chickens," *Poultry Science*, vol. 92, no. 2, pp. 435–443, 2013.

[88] A. J. Xu and A. A. Labroo, "Incandescent affect: turning on the hot emotional system with bright light," *Journal of Consumer Psychology*, vol. 24, no. 2, pp. 207–216, 2014.

Hindawi Publishing Corporation
International Journal of Photoenergy
Volume 2014, Article ID 898752, 7 pages
http://dx.doi.org/10.1155/2014/898752

Research Article

Photobiomodulation on KATP Channels of Kir6.2-Transfected HEK-293 Cells

Fu-qing Zhong,[1] Yang Li,[2] and Xian-qiang Mi[1,3,4]

[1] *College of Medical Device and Food Engineering, University of Shanghai for Science and Technology, Shanghai 200093, China*
[2] *CAS Key Laboratory of Receptor Research, Shanghai Institute of Materia Medica, Chinese Academy of Sciences, Shanghai 201203, China*
[3] *Key Laboratory of System Biology, Chinese Academy of Sciences, Shanghai 201210, China*
[4] *Laboratory of System Biology, Shanghai Advanced Research Institute, Chinese Academy of Sciences, Shanghai 201210, China*

Correspondence should be addressed to Yang Li; liyang@simm.ac.cn and Xian-qiang Mi; mixq@sari.ac.cn

Received 9 January 2014; Accepted 15 February 2014; Published 6 April 2014

Academic Editor: Timon Cheng-Yi Liu

Background and Objective. ATP-sensitive potassium (KATP) channel couples cell metabolism to excitability. To explore role of KATP channels in cellular photobiomodulation, we designed experiment to study effect of low intensity 808 nm laser irradiation on the activity of membrane KATP channel. *Study Design/Materials and Methods*. Plasmids encoding Kir6.2 was constructed and heterologously expressed in cultured mammalian HEK-293 cells. The patch-clamp and data acquisition systems were used to record KATP channel current before and after irradiation. A laser beam of Ga-As 808 nm at 5 mW/cm^2 was used in experiments. A one-way ANOVA test followed by a *post hoc* Student-Newman-Keuls test was used to assess the statistical differences between data groups. *Results*. Obvious openings of KATP channels of Kir6.2-transfected HEK-293 cells and excised patches were recorded during and after low intensity 808 nm laser irradiation. Compared with the channels that did not undergo irradiation, open probability, current amplitude, and dwell time of KATP channels after irradiation improved. *Conclusions*. Low intensity 808 nm laser irradiation may activate membrane KATP channels of Kir6.2-transfected HEK-293 cells and in excised patches.

1. Introduction

It has been demonstrated that irradiation of specific infrared wavelengths is able to penetrate scalp and skull and can reach superficial layers of the cerebral cortex [1]. A recent research confirmed that transcranial laser stimulation (TLS) with low intensity near-infrared laser (NIR) can modulate the excitability of the motor cortex [2]. As constant fluctuation of excitability is a fundamental characteristic of neurons in both central and peripheral nervous system and the homeostatic regulation of neuronal excitability is mainly effected through the mechanisms involved in maintenance of the membrane potential, these findings give further insights into the mechanisms of TLS effects in the human cerebral cortex.

ATP-sensitive potassium (KATP) channels are widely expressed in cytoplasmic membranes of neurons and are the marker of cellular energy metabolism [3]. They link the membrane potential to the metabolic state of the cell and can regulate neuronal excitability. KATP channels may mediate a potential neuroprotective role which may be achieved by membrane hyperpolarization and reduction of excitability in response to hypoxia, ischemia or metabolic stress. Using UV photoirradiation stimulation, the effects of cell stress on KATP channels were studied and the linkage between KATP channels and cellular stress has been confirmed [4]. Nevertheless, there has been no study published so far on effects of low intensity infrared laser irradiation on KATP channel.

Here, we designed experiment to study effect of low intensity infrared laser irradiation on the activity of KATP channels. Molecular cloning of KATP channels was constructed into plasmid and was overexpressed in HEK293 cells. By using patch clamp electrophysiology techniques, we investigated the KATP channels activities under low intensity 808 nm laser irradiation. We found that infrared low intensity laser irradiation activated KATP channels of Kir6.2-transfected HEK-293 cells and in excised patches directly.

2. Materials and Methods

2.1. Construction of Plasmids Encoding Kir6.2. A truncated form of the Kir6.2 subunit, Kir6.2ΔC35, was constructed using a PCR-based site-directed mutagenesis kit, ExSite (Stratagene, CA, USA), in a mammalian expression vector, pcDNA3.1 (Invitrogen, CA, USA). The Kir6.2ΔC35 sequence was also subcloned into a yeast expression vector, pYES2/NT (Invitrogen), containing a GAL1 promoter for high-level inducible protein expression by galactose and repression by glucose, for expression with a $(His)_6$-Xpress tag at its N-terminus for affinity purification and antibody recognition. Kir6.2ΔC35 without SUR subunits expresses functional ATP-sensitive channels in mammalian and yeast cells. For simplicity, in this study Kir6.2ΔC35 is referred to as Kir6.2.

2.2. Heterologous Expression in Cultured Mammalian Cells (HEK-293 Cells). The pcDNA3.1-Kir6.2 vector was introduced into HEK-293 cells. A HEK-293 cells cell line was maintained in continuous culture. Kir6.2 in mammalian expression vectors was transiently transfected with an Effectene transfection kit (Qiangen, Hiden, Germany). The channels were expressed in the absence of sulfonylurea receptor (SUR) regulatory subunits. Channel expression usually peaked 36–48 hours after transfection, at which time the cells were used for patch-clamp experiments.

2.3. Chemicals. Inside-out single or multiple channel currents were recorded with an intracellular solution containing 140 mM KCl, 5.5 mM HEPES, and 2 mM EGTA (pH 7.4) and an extracellular solution containing 130 mM NaCl, 10 mM KCl, 1.8 mM CaCl2, 0.48 mM MgCl2, and 5.5 mM HEPES (pH 7.4). In some experiments, NaCl in the extracellular solution was replaced with 130 mM KCl.

2.4. Electrophysiological Recording. The patch-clamp and data acquisition systems used were Axopatch 200B amplifier with a Digidata 1440A and pCLAMP10.2 software (Axon Instruments, USA) running on a PC. Solution changes in the bath (membrane side of channel in excised patches) were achieved within 100 ms by means of a rapid solution exchange system (RSC-200, Bio-Logic Science Instruments, Claix, France). All current recordings were filtered at 1 kHz and digitized at 10 kHz. Outward currents are shown as upward deviations from the closed level. The current traces were plotted after being manually corrected for baseline shift and filtered with a low-pass digital filter at a cut-off frequency of 500 Hz. Unless specified, currents were recorded at a membrane potential of 0 mV. B150-86-10HP Glass Micropipette and P-97 Flaming/Brown Micropipette Puller (Sutter Instrument Company, USA). The pipettes required 1~2 micron tip and 5~10 M Ω of resistance.

2.5. Laser Irradiation. A laser beam of Ga-As 808 nm from semiconductor laser (SHENZHEN LAMPLICSCIENCECO-.LTD) was used in experiments. The laser power density was kept constant at 5 mW cm^{-2} measured by power meter (Lasercheck, Coherent). The distance is 15 cm; the angle is 75°.

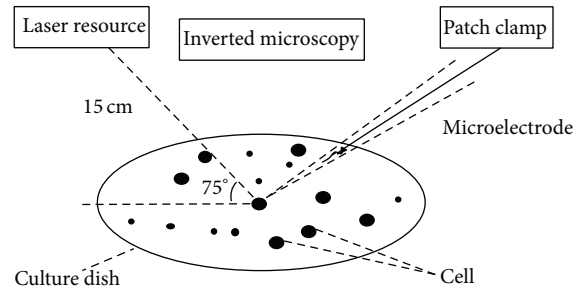

Figure 1: The sketch of laser irradiation system.

The laser beam was delivered to samples in dishes with the 3 mm diameter of irradiation spot (Figure 1). The phenomena of cells being irradiated by red light from laser system can be observed under the inverted microscopy.

2.6. Analysis of Single-Channel Data. Direct P_O (opening probability) measurement is used as a quick indicator of channel activity. The value of P_O has a biological interpretation. For cells that demonstrate an action potential, the action potential is the sum of the single-channel current through many ion channel. The P_O was measured over a large number of channels. $P_O = t_O/T$, T is the total recording time and t_O is the open time. In macropatch recordings containing more than five active channels, the apparent open probability (NP_O) was used, where N is the number of channels, an unknown parameter in a macropatch; then $(NP_O) = T_O/NT$, and $T_O = \sum_{L=1}^{N} t_{OL}$, L is the level of channel open; $L = 1, 2, 3, \ldots$. t_{OL} is the open time of different levels. Although ion channels state transits suddenly, the dwell time of an ion channel at a given conductance level is long enough to be observed with electrophysiological recording techniques. The investigator can identify channel transitions (openings and closings) in the recorded data. The result is an "event table" describing each transition of an idealized data trace. This process is also called "event detection." According to the opening probability resulting from ligand concentration, the dose-response curves can be made. In general, the horizontal axis uses a logarithmic scale ($\log[A]$), and the vertical axis indicates open probability ($P_O/P_{\max}$); $P_{\max}$ is the maximal open probability. The concentration of ATP ([ATP]) producing half-maximal inhibition (IC_{50}) and the Hill coefficient (H) were obtained by fitting the measured open probability data with the expression: $P_O/P_{\max} = 1 - A^H/(A^H + IC_{50}{}^H)$.

2.7. Statistical Analysis. Experimental data are presented as Mean ± S.E.M. A one-way ANOVA test followed by a *post hoc* Student-Newman-Keuls test was used to assess the statistical differences between data groups. Student's t-test was used wherever two groups of data were compared.

3. Results

3.1. Activation of KATP Channels. For the HEK-293 cells without KATP channels, no current was recorded in attached

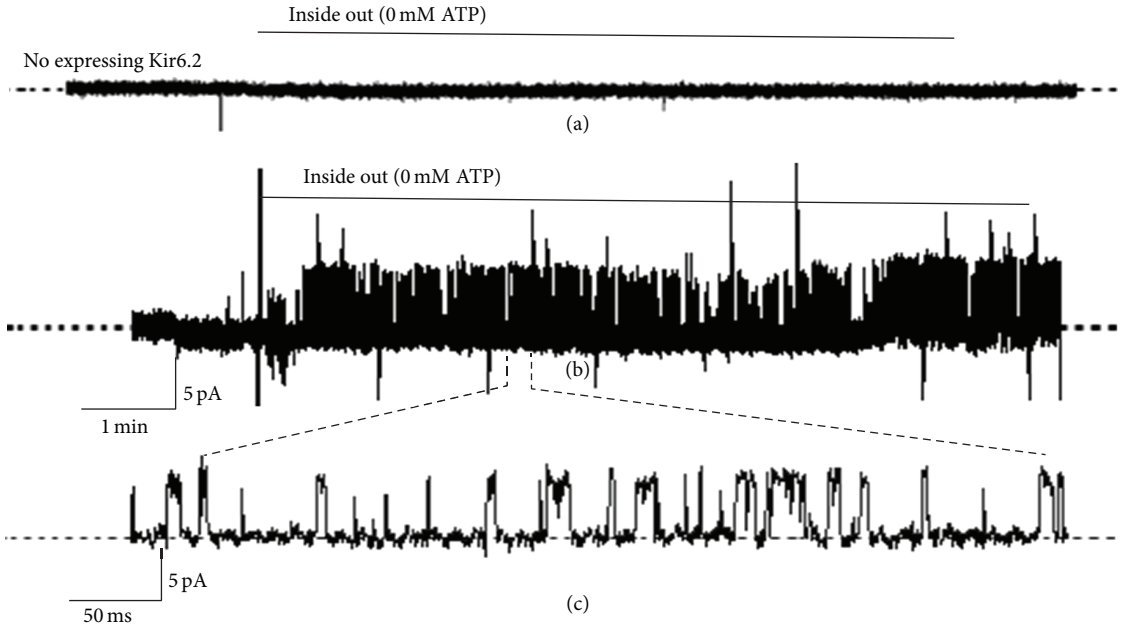

Figure 2: Activation of potassium channels in Kir6.2-transfected HEK-293 cells. (a) HEK-293 cells not expressing Kir6.2. No current was recorded in attached and inside-out patch clamp. (b) HEK-293 cells expressing Kir6.2. The patch membrane was excised at the time marked inside out. The cell was bathed in extracellular solution without ATP, and the patch membrane was held at 0 mV throughout the recording period. (c) A specific time domain was displayed.

and inside-out patch clamp (Figure 2(a)). A significant channel current was recorded from the patch membrane of Kir6.2-transfected HEK-293 cells (the cell was bathed in extracellular solution without ATP, the patch membrane was held at 0 mV throughout the recording period, and the patch membrane was excised at the time marked inside out). Channel current of a specific time domain was displayed in Figure 2(c).

3.2. Effect of ATP on the KATP Channels. As shown in the recording trace in Figure 3(a), the patch membrane was excised from the cell, and the sensitivity of the channels to inhibition by ATP was measured. Upon excision of the patch membrane into a solution with an ATP concentration ([ATP]) of 1 μM, outward KATP channel currents were recorded in all of the successful patch excisions. The ATP sensitivity was obtained by varying [ATP] in the intracellular solution. Changes in [ATP] were made by a series of both increasing and decreasing concentration steps of 10–20 s (this protocol has been shown to be effective at minimizing possible errors caused by run-down of the channels). Relationships between concentration and the ATP inhibition of KATP channels were shown in Figure 3(b).

3.3. Effect of Photobiomodulation on the Opening of KATP Channel. 808 nm laser irradiation on KATP channels was examined in HEK-293 cells expressing Kir6.2. Figure 4 illustrates an experimental recording of a patch containing multiple channels initially recorded in the cell-attached configuration on a HEK-293 cells expressing Kir6.2. After establishment of the cell-attached patch-clamp configuration, the cell was exposed to a spectrum of 5 mW/cm^2 at 808 nm via the microscope; the exposure lasted 1-2 min, obvious openings of KATP channels were recorded during and after irradiation, and the current amplitude improved (Figure 4(a)). In 8 cells tested, 5 exhibited clear openings of KATP channels after the irradiation was started. After inside out, the ATP sensitivity was obtained by varying [ATP] in the intracellular solution. Changes in [ATP] were made by a series of both increasing and decreasing concentration steps of 10–20 s. In these experiments, laser irradiation was applied to excised patch membranes while KATP channel currents were recorded in the inside-out patch-clamp configuration during perfusion with intracellular solution containing modulators of channel activity. Irradiation induced a significant increase in the maximal open probability of the active channels. Channel current of a specific time domain was displayed in Figure 4(b).

3.4. Effect of Photobiomodulation on Single KATP Channel. The photobiomodulation on KATP channels was further analyzed kinetically in two patches that contained only a single active channel. An experimental recording of the photobiomodulation on single KATP channels was illustrated. In the example given in Figure 5, a Kir6.2 channel was active from the beginning of the experiment when the excised patch was perfused without ATP. It shows that open probability, current amplitude, and dwell time of KATP channel improved after the irradiation.

Compared with the channels that did not undergo irradiation, the current amplitude and dwell time of KATP channel improved after irradiation (Table 1). The improvement of current amplitude and dwell time distributions after irradiation

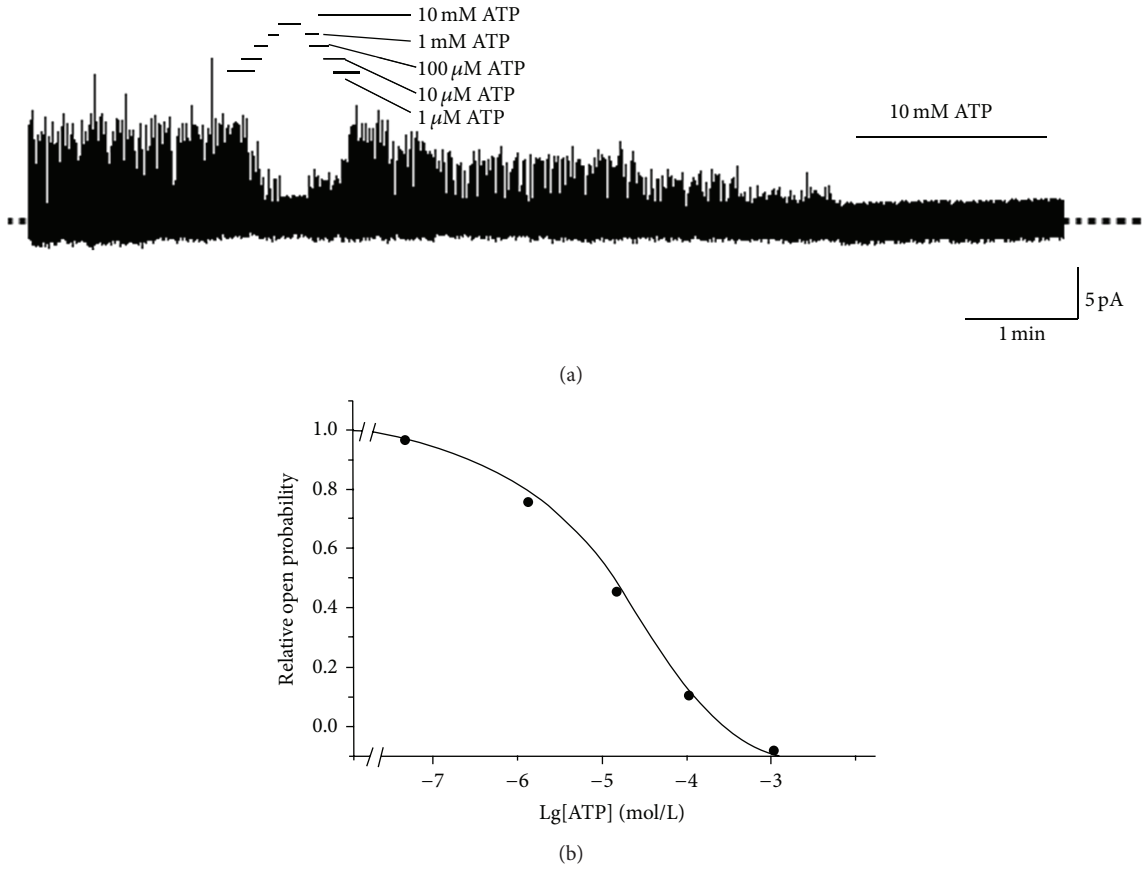

Figure 3: Different concentrations of ATP on the KATP channel effects. (a) The potassium current increased in response to 0 mM ATP (inside out) and decreased in response to 10 mM ATP. No open channel event in 1 mM ATP was observed. HEK-293 cells expressing Kir6.2 was bathed in extracellular solution, and the patch membrane was held at 0 mV throughout the recording period. (b) Relationships between concentration and the ATP inhibition of KATP channels.

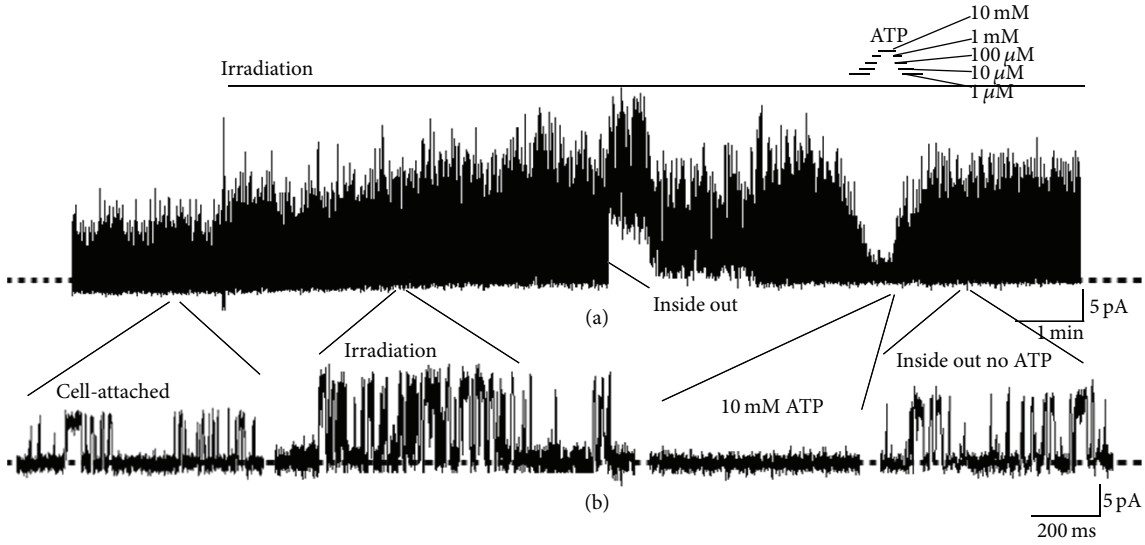

Figure 4: Opening of KATP channels by photobiomodulation in a Kir6.2-transfected HEK-293 cell. The current was initially recorded in the cell-attached configuration. The patch membrane was excised at the time marked Inside out. The cell was bathed in extracellular solution, and the patch membrane was held at 0 mV throughout the recording period. ATP was applied at the concentrations indicated by the bars above the current trace. Irradiation indicates the period during which the patched cell was exposed to photobiomodulation (see text for details of photobiomodulation treatment). In this and subsequent figures, the dotted line through the current recording indicates the closed channel level.

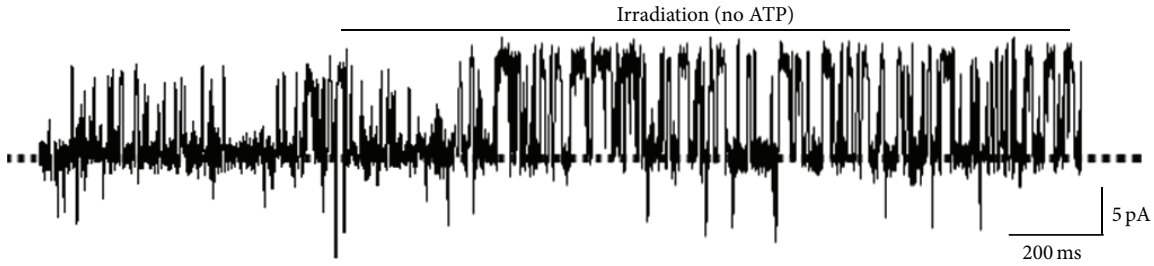

Figure 5: Photobiomodulation-induced activation of single-channel current recorded from a Kir6.2-transfected HEK-293 cell. The membrane was held at 0 mV. The open probability, current amplitude, and dwell time of KATP channel have changed after irradiation.

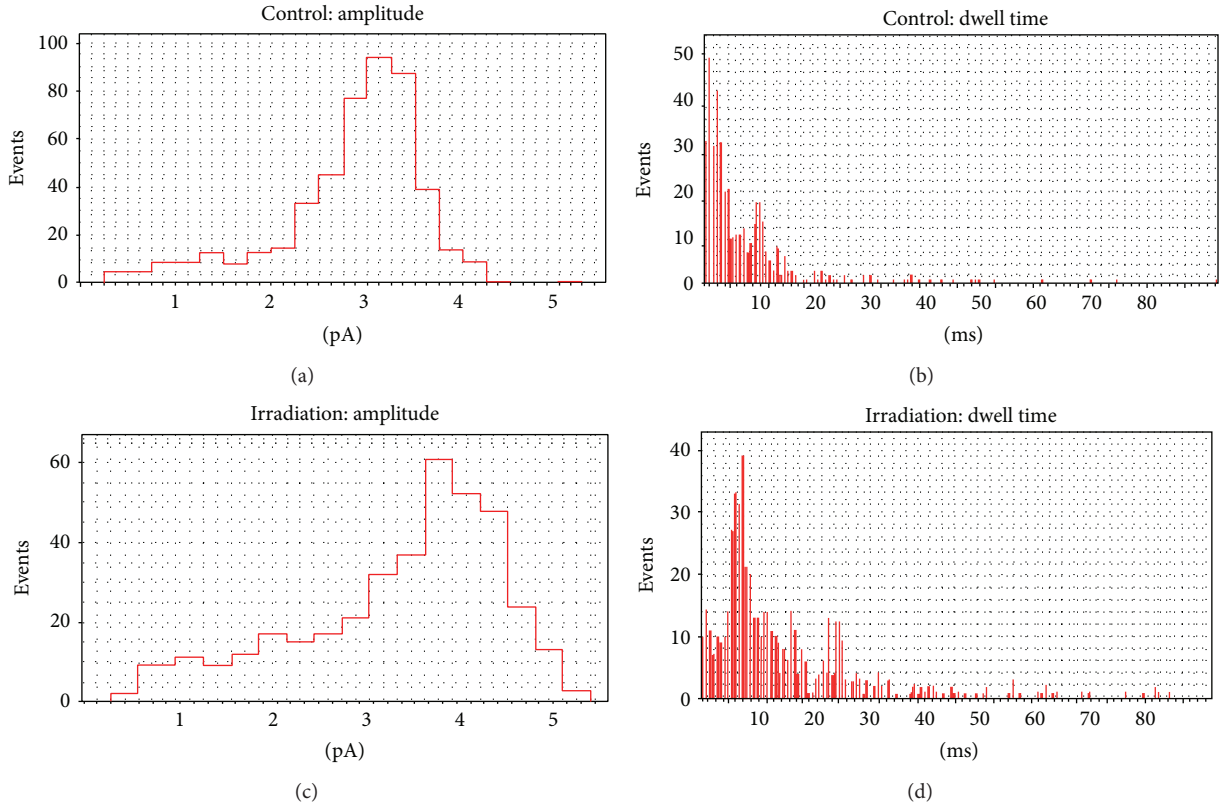

Figure 6: Photobiomodulation on amplitude and dwell time. The Kir6.2-transfected HEK-293 cell was bathed in extracellular solution without ATP, and the patch membrane was held at 0 mV throughout the recording period.

Table 1: Effects of irradiation on closed and open time distributions.

	Amplitude	Dwell time	Count
Control	3.1583 ± 0.5371	6.4813 ± 3.3475	972
Irradiation	3.9406 ± 0.6147**	10.7639 ± 4.7935**	1047

**$P < 0.01$. Control: before irradiation, irradiation: after irradiation.

can also be seen from the histograms from the single-channel current of patch excised from a Kir6.2 channel (Figure 6).

Maximal open probability (P_{max}) has statistically been confirmed to increase after irradiation. Under control conditions, no open channel event in 1 mM ATP was observed. In contrast, open channel events could be identified clearly after irradiation. This result indicates that irradiation reduces the ATP sensitivity. A quantitative measure of the ATP sensitivity change is presented as the half-inhibitory [ATP] (IC_{50}) and Hill coefficient (H) (Table 2) from the fit of a Hill saturation function to the relationship between ATP inhibition and [ATP] (Figure 7). The maximal open probability and IC_{50} both increased significantly after irradiation (Table 2). The changes in these parameters might have been involved in the increased channel activity observed in both cell-attached and excised patches.

4. Discussion

In this study, we report that infrared low intensity laser irradiation activated KATP channels of Kir6.2-transfected

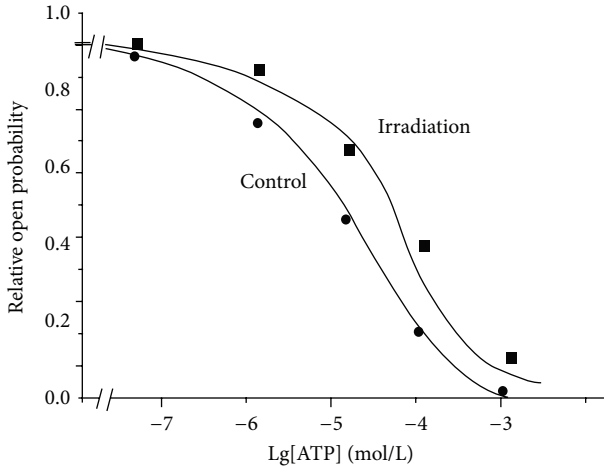

Figure 7: Activation of KATP channels by photobiomodulation. Effect of irradiation on the concentration-dependent inhibition of KATP channels by ATP. ● and ■ data collected before and after irradiation, respectively.

Table 2: Irradiation-induced activation of KATP channels.

	P_{max} (NO ATP)	IC_{50}	H
Control	0.204569	78.6 ± 6.3	1.1 ± 0.2
Irradiation	0.247436**	103.7 ± 9.2**	1.2 ± 0.2*

**$P < 0.01$; *$P < 0.05$.

P_{max}: maximal open probability. The concentration of ATP ([ATP]) producing half-maximal inhibition (IC_{50}) and the Hill coefficient (H) were obtained by fitting the measured open probability data with the expression $P_O/P_{max} = 1 - A^H/(A^H + {IC_{50}}^H)$.

HEK-293 cells and excised patches directly. A prominent increase in KATP channel activity was perceived during and after irradiation and the current amplitude improved (Figure 4). An experimental recording of the photobiomodulation on single KATP channels showed that a Kir6.2 channel was active from the beginning of the experiment when the excised patch was perfused without ATP and the open probability, current amplitude, and dwell time of KATP channel improved after the irradiation (Figure 5). Compared with the channels that did not undergo irradiation, the current amplitude and dwell time of KATP channel improved after irradiation (Table 2, Figure 6). In excised patches, the activation of a KATP channel can be dissected into three major components: (1) an increase in maximal open probability, (2) a decrease in ATP sensitivity, and (3) an increase in dwell time of a KATP channel. The reduced ATP sensitivity in patches excised from cells exposed to irradiation indicated a change in the intrinsic KATP channel sensitivity which is at least a partial cause of channel activation (Figure 4).

Using UV photoirradiation stimulation on KATP channels of rat heart and recombinant KATP channels composed of SUR2 and Kir6.2 in intact cells and in excised patches, it was found that the modification favoring channel opening triggered by UV photoirradiation affects KATP channel activity partly by regulating membrane phosphoinositide levels [4]. It was also found that free radical scavengers retarded irradiation induced activation of KATP channel [4]. As free radicals have been shown to increase the opening of cardiac KATP channels by increasing the open probability and reducing the ATP sensitivity [5–7], It was proposed that the upstream step that transforms UV irradiation energy into stimulation of enzymatic production of phosphoinositides is the production of ROS [4, 8]. The results of our electrophysiological study on low intensity infrared laser irradiation on KATP channel are very similar with the results of Fan's electrophysiological study on UV irradiation on KATP channel. In order to interact with the living cell, light has to be absorbed by intracellular chromophores. There is a growing body of evidence that suggests cytochrome c oxidase is the primary photoacceptor of nucleated cells which can absorb the light energy [9–12]. Here, we infer that cytochrome c oxidase may play a similar role as UV irradiation in KATP channel. We propose that cytochrome c oxidase may absorb the photons from low intensity infrared laser irradiation, produce ROS, and thus stimulate the production of phosphoinositides, while our data do not totally exclude other effects such as direct structural modification of membrane KATP channels of neuron.

Many physical and chemical stimuli such as photoirradiation, photochemical treatment, and osmotic stress share an array of common or closely related signal cascades to evoke a cellular response. So our results have the similar physiological implications in terms of the response of KATP channels to other physical stimuli of cell stresses [13].

In this study, we only observed some interesting phenomena, and much more work like the relationship among infrared low intensity laser irradiation with changes in membrane phosphoinositide and KATP channels should be explored later.

The use of TLS which involves photobiomodulation on neurological functions has gained significant interest in recent years [14, 15]. TLS has shown significant beneficial and sustained effects in animal stroke models [15] and human trial (the NEST-1 and the NEST-2) [16, 17] for stroke. It shows photobiomodulation may be an alternative intervention modality for ischemic stroke. It is well known that there exists an "ischemic penumbra" around the infarct area in the acute ischemic stroke. How to save the neuron in the cerebral ischemia penumbra area is the key to improve the cure rate of acute ischemic stroke. Membrane KATP channels are the marker of cellular energy metabolism which links the membrane potential to the metabolic state of the cell as reflected by the levels of nucleoside triphosphates and diphosphates. As it was reported that activation of KATP channels plays a protective effect on hypoxic ischemic neurons [18], the phenomena we observed that low intensity laser irradiation can active membrane KATP channels may help to reveal the protection mechanism of low intensity 808 nm laser irradiation on ischemic hypoxic neurons.

5. Conclusions

Low intensity 808 nm laser irradiation at 5 mW/cm^2 may activate membrane KATP channels of Kir6.2-transfected HEK-293 cells and in excised patches.

Conflict of Interests

The authors declare that there is no conflict of interests regarding the publication of this paper.

Acknowledgments

This study had the financial support of the National Natural Science Foundation of China (no. 61078071), the Natural Science Foundation of Shanghai (no. 09ZR1422500), the State Key Development Program for Basic Research of China (no. 2013CB91060101), and The 2013 "Innovation Action Plan" from Science and Technology Commission of Shanghai Municipality (no. 13DZ1940200).

References

[1] Q. Zhang, H. Ma, S. Nioka, and B. Chance, "Study of near infrared technology for intracranial hematoma detection," *Journal of Biomedical Optics*, vol. 5, no. 2, pp. 206–213, 2000.

[2] L. M. Konstantinovic, M. B. Jelic, A. Jeremic, V. B. Stevanovic, S. D. Milanovic, and S. R. Filipovic, "Transcranial application of near-infrared low-level laser can modulate cortical excitability," *Lasers in Surgery and Medicine*, vol. 45, no. 10, pp. 648–653, 2013.

[3] H. Yokoshiki, M. Sunagawa, T. Seki, and N. Sperelakis, "ATP-sensitive K+ channels in pancreatic, cardiac, and vascular smooth muscle cells," *American Journal of Physiology—Cell Physiology*, vol. 274, no. 1, part 1, pp. C25–C37, 1998.

[4] Z. Fan and R. A. Neff, "Susceptibility of ATP-sensitive K+ channels to cell stress through mediation of phosphoinositides as examined by photoirradiation," *Journal of Physiology*, vol. 529, part 3, pp. 707–721, 2000.

[5] K. Tokube, T. Kiyosue, and M. Arita, "Openings of cardiac KATP channel by oxygen free radicals produced by xanthine oxidase reaction," *American Journal of Physiology—Heart and Circulatory Physiology*, vol. 271, no. 2, part 2, pp. H478–H489, 1996.

[6] K. Tokube, T. Kiyosue, and M. Arita, "Effects of hydroxyl radicals on K(ATP) channels in guinea-pig ventricular myocytes," *Pflugers Archiv European Journal of Physiology*, vol. 437, no. 1, pp. 155–157, 1998.

[7] K. Ichinari, M. Kakei, T. Matsuoka, H. Nakashima, and H. Tanaka, "Direct activation of the ATP-sensitive potassium channel by oxygen free radicals in guinea-pig ventricular cells: its potentiation by MgADP," *Journal of Molecular and Cellular Cardiology*, vol. 28, no. 9, pp. 1867–1877, 1996.

[8] Y. Kabuyama, M. Hamaya, and Y. Homma, "Wavelength specific activation of PI 3-kinase by UVB irradiation," *FEBS Letters*, vol. 441, no. 2, pp. 297–301, 1998.

[9] N. R. Sims and M. F. Anderson, "Mitochondrial contributions to tissue damage in stroke," *Neurochemistry International*, vol. 40, no. 6, pp. 511–526, 2002.

[10] M. T. T. Wong-Riley, H. L. Liang, J. T. Eells et al., "Photobiomodulation directly benefits primary neurons functionally inactivated by toxins: role of cytochrome c oxidase," *Journal of Biological Chemistry*, vol. 280, no. 6, pp. 4761–4771, 2005.

[11] J. T. Eells, M. M. Henry, P. Summerfelt et al., "Therapeutic photobiomodulation for methanol-induced retinal toxicity," *Proceedings of the National Academy of Sciences of the United States of America*, vol. 100, no. 6, pp. 3439–3444, 2003.

[12] P. A. Lapchak and L. de Taboada, "Transcranial near infrared laser treatment (NILT) increases cortical adenosine-5′-triph osphate (ATP) content following embolic strokes in rabbits," *Brain Research*, vol. 1306, pp. 100–105, 2010.

[13] T. C. Y. Liu, Y. Y. Liu, E. X. Wei, and F. H. Li, "Photobiomodulation on stress," *International Journal of Photoenergy*, vol. 2012, Article ID 628649, 11 pages, 2012.

[14] A. Oron, U. Oron, J. Chen et al., "Low-level laser therapy applied transcranially to rats after induction of stroke significantly reduces long-term neurological deficits," *Stroke*, vol. 37, no. 10, pp. 2620–2624, 2006.

[15] P. A. Lapchak, J. Wei, and J. A. Zivin, "Transcranial infrared laser therapy improves clinical eating scores after embolic strokes in rabbits," *Stroke*, vol. 35, no. 8, pp. 1985–1988, 2004.

[16] J. A. Zivin, G. W. Albers, N. Bornstein et al., "Effectiveness and safety of transcranial laser therapy for acute ischemic stroke," *Stroke*, vol. 40, no. 4, pp. 1359–1364, 2009.

[17] Y. Lampl, J. A. Zivin, M. Fisher et al., "Infrared laser therapy for ischemic stroke: a new treatment strategy—results of the NeuroThera Effectiveness and Safety Trial-1 (NEST-1)," *Stroke*, vol. 38, no. 6, pp. 1843–1849, 2007.

[18] X.-L. Sun and G. Hu, "ATP-sensitive potassium channels: a promising target for protecting neurovascular unit function in stroke," *Clinical and Experimental Pharmacology and Physiology*, vol. 37, no. 2, pp. 243–252, 2010.

Hindawi Publishing Corporation
International Journal of Photoenergy
Volume 2014, Article ID 971491, 5 pages
http://dx.doi.org/10.1155/2014/971491

Research Article

Photobiomodulation for Cobalt Chloride-Induced Hypoxic Damage of RF/6A Cells by 670 nm Light-Emitting Diode Irradiation

Shuang Li,[1] Qiang-Li Wang,[2] Xin Chen,[1] and Xian-qiang Mi[1,3,4]

[1] *College of Medical Device and Food Engineering, University of Shanghai for Science and Technology, Shanghai 200093, China*
[2] *Shanghai University of Traditional Chinese Medicine, Shanghai 201203, China*
[3] *Key Laboratory of System Biology, Chinese Academy of Sciences, Shanghai 201210, China*
[4] *Laboratory of System Biology, Shanghai Advanced Research Institute, Chinese Academy of Sciences, Shanghai 201210, China*

Correspondence should be addressed to Xian-qiang Mi; mixq@sari.ac.cn

Received 26 December 2013; Accepted 18 February 2014; Published 1 April 2014

Academic Editor: Timon Cheng-Yi Liu

Objective. The goal of this study was to investigate the therapeutic efficacy of 670 nm light-emitting diode (LED) irradiation on the diabetic retinopathy (DR) using hypoxic rhesus monkey choroid-retinal (RF/6A) cells as the model system. *Background Data*. Treatment with light in the spectrum from red to near-infrared region has beneficial effect on tissue injury and 670 nm LED is currently under clinical investigation for retinoprotective therapy. *Methods*. Studies were conducted in the cultured cells under hypoxia treated by cobalt chloride ($CoCl_2$). After irradiation by 670 nm LED with different power densities, cell viability, cytochrome C oxidase activity, and ATP concentration were measured. *Results*. The irradiation of 670 nm LED significantly improved cell viability, cytochrome C oxidase activity, and ATP concentration in the hypoxia RF/6A cells. *Conclusion*. 670 nm LED irradiation could recover the hypoxia damage caused by $CoCl_2$. Photobiomodulation of 670 nm LED plays a potential role for the treatment of diabetic retinopathy.

1. Introduction

Diabetic retinopathy (DR) is one of the most serious diabetic microvascular complications affecting large number of patients. DR causes retinal capillary damage [1] and ultimately leads to blindness. Despite the wide-spread applications of retinal laser photocoagulation in the treatment of DR, there are serious side effects as the treatment itself is a pathological process. New treatment methods for DR are being actively explored and photobiomodulation for DR is one of the most promising therapies.

Photobiomodulation has been demonstrated to be able to modulate various biological processes in cell culture and animal models [2] including accelerating wound healing, improving mitochondrial function, and attenuating degeneration in the injured optic nerve [3–6]. Low level laser or light emitting diodes (LEDs) are the most common light sources for photobiomodulation. Compared with laser, LED shows more promising future as it has less heat production and toxic side effects.

Previous studies have provided evidence for the therapeutic benefit of LED treatment at 670 nm in improvement of oxidative metabolism of mitochondria *in vitro* and functional recovery of retinal after acute injury by the mitochondrial toxin *in vivo* [4, 7]. It indicates that cytochrome C oxidase which plays an important role in generating ATP is a primary photoreceptor of light in the red to near-IR region of the spectrum [8–10].

Here, we demonstrate that the protective effect of 670 nm LED on RF/6A cells results from the stimulation of cellular events associated with the enhancement of cytochrome C oxidase activity, further improves oxidative metabolism of mitochondria, and provides protection against hypoxic damage. We employed cytochrome c oxidase activity and ATP content

as the sensitive indicators after hypoxic caused by $CoCl_2$ and demonstrated the efficacy of 670 nm LED treatment delivered one time per day. We proposed that photobiomodulation of LED represents an innovative and noninvasive therapeutic approach for the treatment of diabetic retinopathy.

2. Materials and Methods

2.1. Materials. LED device was obtained from Shenzhen Lamplic Technology Company Limited. The retinal vascular endothelial cell line RF/6A was obtained from Cell Bank, Chinese Academy of Sciences. MTT and $CoCl_2$ were obtained from Sigma-Aldrich Corporation (mainland). Mitochondria cytochrome C oxidase activity kit was purchased from Genmed Scientifics Inc., USA. Mitochondria isolation kit, BCA protein concentration determination kit, and ATP Assay Kit were purchased from Shanghai Beyotime Institute of Biotechnology.

2.2. Cell Cultures. RF/6A cells were cultured in DMEM containing 10% fetal bovine serum (1% streptomycin and penicillin) under 5% CO2, 37∘C, and passaged per 2-3 d.

2.3. Hypoxic Model System Induced by $CoCl_2$. Hypoxic model system was produced by the rhesus monkey choroid-retinal (RF/6A) cells incubated with $CoCl_2$ for 24 h. Controls group was the RF/6A cells without cobalt chloride.

2.4. LED Treatment. RF/6A cells with $CoCl_2$ treatment were irradiated for 71 seconds in the dark with 670 nm LED once a day for 3 days.

2.5. Cell Viability. Cell viability was determined by MTT assay. Cells in good conditions was transferred to cell suspension and then added to 96-well plates at 5×10^4/mL (100 μL each well). MTT solution (5 mg/m1, 20 μL) was added to each well and then cultured in CO_2 incubator for 4 h. After the medium was removed, 200 μL DMSO was added and shaked 10 min. OD value was obtained by ELISA Reader.

2.6. Cytochrome C Oxidase Assays. Cytochrome C oxidase activity was determined by the change of light absorption value with colorimetry by spectrophotometer at 550 nm. 30 μL mitochondrial lysate was added to split mitochondria. Guided by Mitochondria Cytochrome C Oxidase Activity Kit Introductions provided by manufacturer, samples were prepared. After buffer and samples were added, OD values were measured by spectrophotometer. Cytochrome C oxidase activity of samples was calculated and normalized based on OD values and protein concentration.

2.7. ATP Assay Kit. The assay is based on the firefly luciferase-catalyzed oxidation of D-luciferin in the presence of ATP and oxygen, whereby the amount of ATP is quantified by the amount of light (hv) produce. Cultured cells were rinsed with cold phosphate-buffered saline, harvested from the cover slips by means of a cell scraper, and then centrifuged at 4°C, 12000 g for 8 min with supernatant left. 100 μL ATP testing reagent was added and incubated at room temperature for 3–5 min to exhaust the ATP in background. Then mixed with the luciferase ATP assay and assayed with a luminometer.

2.8. Statistical Analysis. All values are expressed as means ± SEM. A one way ANOVA was used in SPSS13.0 to determine whether any significant differences existed among groups. In all cases, the minimum level of significance was taken as $P < 0.05$.

3. Result

3.1. The Determinant of the Optimal $CoCl_2$ Concentration. The RF/6A model cells were divided into control group and hypoxia groups induced by different concentration of $CoCl_2$ (100, 200, 300, 400, and 500 μmol/L). Cell viability was measured by MTT method. It showed that cell viability decreased in a power density dependent manner (Figure 1). There is significant difference among cell viability of 200 μmol/L, 300 μmol/L, 400 μmol/L, and 500 μmol/L $CoCl_2$ damaged groups and control group. Here, 200 μmol/L $CoCl_2$ was chosen for the following up experiments.

3.2. The Determinant of the Optimal LED Power Density. It demonstrated that, compared with the control group, the cell viability of both the RF/6A model cell damaged by 200 μmol/L $CoCl_2$ alone group and the RF/6A model cells damaged by 200 μmol/L $CoCl_2$ then irradiated by LED at 7 mW/cm^2, 14 mW/cm^2, and 28 mW/cm^2 groups decreased significantly. But the cell viability of RF/6A model cells damaged by 200 μmol/L $CoCl_2$ and irradiated by LED at 21 mW/cm^2 had no significant difference compared with the control group. Compared with 200 μmol/L $CoCl_2$ alone group, cell viability of RF/6A model cells damaged by 200 μmol/L $CoCl_2$ and irradiated by LED with power intensity of 7, 14, 21, and 28 mW/cm^2 increased significantly. Here, 21 mW/cm^2 was chosen as the optimum power density for the following up experiment (Figure 2).

3.3. Effect of LED Treatment on Cytochrome C Oxidase Activity. As shown in Figure 3, compared with control group, cytochrome C oxidase activity of cells damaged by 200 μmol/L $CoCl_2$ decreased significantly and cytochrome C oxidase activity of RF/6A model cells damaged by 200 μmol/L, $CoCl_2$ for 24 h and irradiated by 21 mW/cm^2 LED decreased significantly. There are no significant differences between the cytochrome C oxidase activity of RF/6A model cells treated by 21 mW/cm^2 LED and control group. However, compared with 200 μmol/L $CoCl_2$ alone group, cytochrome C oxidase activity of RF/6A model cells damaged by 200 μmol/L $CoCl_2$ and irradiated by 21 mW/cm^2 LED increased significantly although it did not completely reverse the cytochrome C oxidase to the level of control group. There is significantly difference between the cytochrome C oxidase activity of RF/6A model cells irradiated by 21 mW/cm^2

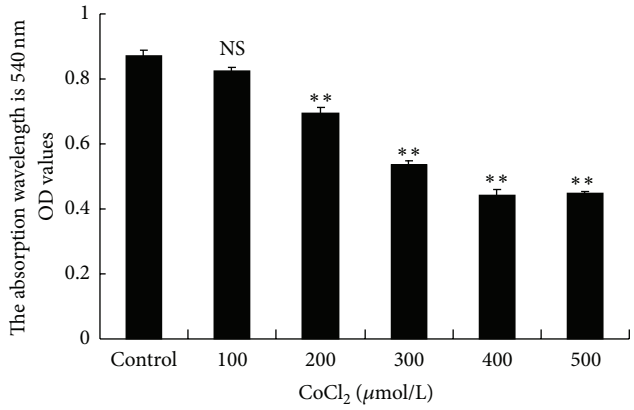

Figure 1: Effect of $CoCl_2$ with various concentrations on cell viability of RF/6A model cell. $^{**}P < 0.01$ indicates comparison with control group.

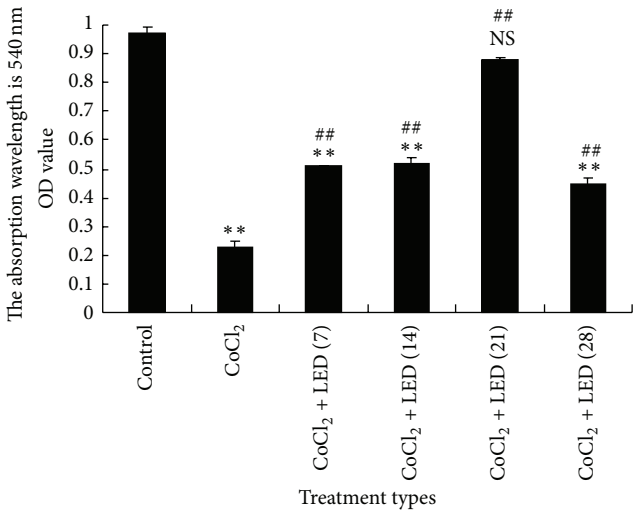

Figure 2: Effects of 670 nm LED irradiation with various power densities on cell viability of RF/6A cells incubated with $CoCl_2$ at 200 μM for 24 h. Data are means ± SEM. $^{**}P < 0.01$ indicates comparison with control group. NS indicates no significance; $^{\#\#}P < 0.01$ indicates comparison with 200 μmol/L $CoCl_2$ group.

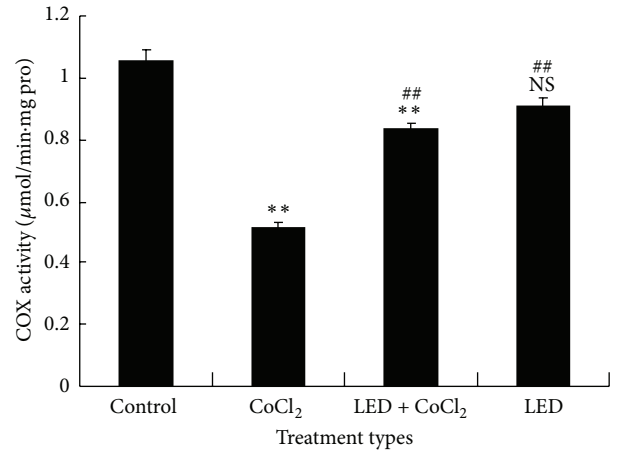

Figure 3: Effect of 21 mW/cm^2 670 nm LED treatment on cytochrome C oxidase activity. Data are means ± SEM. $^{**}P < 0.01$ indicates comparison with control group. NS indicates no significance compared with control group. $^{\#\#}P < 0.01$ indicates comparison with 200 μmol/L $CoCl_2$ group.

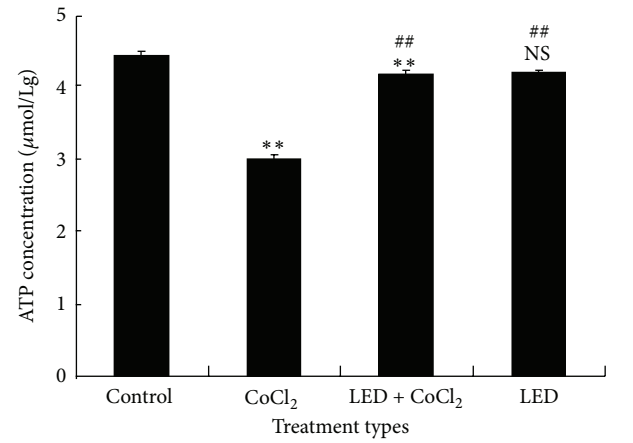

Figure 4: Effects of 21 mW/cm^2 670 nm LED treatment on ATP content. Data are means ± SEM. $^{**}P < 0.01$ indicates comparison to control group. NS indicates no significantly difference compared with control group. $^{\#\#}P < 0.01$ indicates comparison to $CoCl_2$ group.

670 nm LED treatment alone group and 200 μmol/L $CoCl_2$ alone group.

3.4. Effect of LED Treatment on ATP Content. It was seen that, compared with control group, the ATP content of RF/6A model cells damaged by 200 μ mol/L, $CoCl_2$ for 24 h was reduced significantly (Figure 4); the ATP content of RF/6A model cells damaged by 200 μmol/L, $CoCl_2$ for 24 h and irradiated by 21 mW/cm^2 LED decreased significantly. There are no significant differences between the ATP content of RF/6A model cells treated by 21 mW/cm^2 LED and control group. But compared with 200 μmol/L $CoCl_2$ alone group, ATP content of RF/6A model cells damaged by 200 μmol/L $CoCl_2$ and irradiated by LED with power intensity of 21 mW/cm^2 increased significantly. There is significant difference between the ATP content of RF/6A model cells irradiated by 21 mW/cm^2 670 nm LED alone and 200 μmol/L $CoCl_2$ treatment alone.

4. Discussion

Diabetes produces retinal abnormalities that result in damage to the vasculature and neurons, and in severe cases, loss of vision itself. The pathogenesis of DR remains to be elucidated, although reduction in hyperglycemia has been shown to exert positive effects on the development and progression of

diabetic retinopathy. Nevertheless, achievement and maintenance of glycemic control have been difficult or impossible in many patients; therefore effective therapies are explored to inhibit the retinopathy. An alternative approach would be to identify innovative noninvasive treatment modalities that act by multiple potential mechanisms. Light in the spectrum from red to near-infrared region (630–1000 nm) has been reported to be beneficial in the treatment of infected, ischemic, and hypoxic wounds and other soft tissue injuries.

High-energy light has been used as a treatment option for ophthalmic diseases, such as in laser photocoagulation for age-related macular degeneration or diabetic retinopathy. In the present study, however, we demonstrated that photobiomodulation using low-intensity light can recover the damage of hypoxia caused by cobalt chloride. We found that low-intensity 670 nm LED irradiation for 3 days improved cell viability, cytochrome C oxidase activity, and ATP content of hypoxic RF/6A cells damaged by $CoCl_2$ exposure. Our data demonstrated the recovery role of LED irradiation on hypoxia damage of RF/6A cells caused by cobalt chloride. Moreover, it has no effect on normal RF/A6 cells, indicating that there is no side effect of 670 nm LED irradiation, which means low-intensity LED irradiation only plays a recovery role on the cells under pathological state, as Liu et al. have pointed out [11]. Further study for the mechanisms that LED only has effect on the pathological cells but has no effect on normal cells should have been further studied.

Cytochrome C oxidase complex has the antioxidant effect. It is the last enzyme in the respiratory electron transport chain of mitochondria. It receives an electron from each of four cytochrome c molecules and transfers them to one oxygen molecule. As a primary photoreceptor of light in the spectrum from the red to near-IR region, cytochrome C oxidase plays an important role in LED treatment for retina. In the present study, we explored the effects of low-intensity 670 nm LED irradiation on the proliferation, cytochrome C oxidase activity, and ATP concentration for hypoxic RF/6A model cells demonstrating the possible mechanisms underlying photobiomodulation of cell energy metabolism. Even though 670 nm LED irradiation can completely recover the proliferation of hypoxic RF/6A cells to the level of normal RF/6A cells, the cytochrome C oxidase activity and ATP concentration can only partially recover. It suggested that the pathway [12] maintaining proliferation of normal RF/6A cells and the one maintaining LED completely recovered proliferation of the RF/6A cells exposed on $CoCl_2$ were different from each other, but they maintained the same proliferation. Those two pathways are well-known redundant pathways [11].

It was shown that photoreceptors are the most metabolically active cells in the body and the energy required for phototransduction is derived primarily from oxidative metabolism. These signaling events may include the activation of immediate early genes, transcription factors, cytochrome oxidase subunit gene expression, and a host of other enzymes and pathways related to increased oxidative metabolism [13, 14]. Our study shows that low-intensity 670 nm LED treatment could modulate the oxidative metabolism of retina and improve the retinal function via increasing the activity of cytochrome C oxidase which plays a role in inhibiting the development of diabetic retinopathy. Because photobiomodulation has been found to be associated with minimal risk, noninvasive, inexpensive, and easy to administer, it may be a simple adjunct therapy to help inhibit the development of diabetic retinopathy.

5. Conclusions

Our study presented that the hypoxia damage of RF/6A caused by $CoCl_2$ can be completely recovered by low-intensity LED 670 nm irradiation. Photobiomodulation of 670 nm LED may be a new effective method for DR treatment.

Conflict of Interests

The authors declare that there is no conflict of interests regarding the publication of this paper.

Acknowledgments

This study had the financial support of the National Natural Science Foundation of China (no. 61078071), the Natural Science Foundation of Shanghai, (09ZR1422500), and The 2013 "Innovation Action Plan" from Science and Technology Commission of Shanghai Municipality (no. 13DZ1940200).

References

[1] D. S. Fong, L. Aiello, T. W. Gardner et al., "Diabetic retinopathy," *Diabetes Care*, vol. 26, no. 1, pp. 226–229, 2003.

[2] T. Karu, "High-tech helps to estimate cellular mechanisms of low power laser therapy," *Lasers in Surgery and Medicine*, vol. 34, no. 4, pp. 298–299, 2004.

[3] H. T. Whelan, R. L. Smits Jr., E. V. Buchman et al., "Effect of NASA light-emitting diode irradiation on wound healing," *Journal of Clinical Laser Medicine and Surgery*, vol. 19, no. 6, pp. 305–314, 2001.

[4] M. T. T. Wong-Riley, X. Bai, E. Buchmann, and H. T. Whelan, "Light-emitting diode treatment reverses the effect of TTX on cytochrome oxidase in neurons," *NeuroReport*, vol. 12, no. 14, pp. 3033–3037, 2001.

[5] D. S. Fong, F. B. Barton, and G. H. Bresnick, "Impaired color vision associated with diabetic retinopathy: Early Treatment Diabetic Retinopathy Study Report No. 15," *American Journal of Ophthalmology*, vol. 128, no. 5, pp. 612–617, 1999.

[6] M. T. T. Wong-Riley, H. L. Liang, J. T. Eells et al., "Photobiomodulation directly benefits primary neurons functionally inactivated by toxins: role of cytochrome c oxidase," *Journal of Biological Chemistry*, vol. 280, no. 6, pp. 4761–4771, 2005.

[7] J. T. Eells, M. M. Henry, P. Summerfelt et al., "Therapeutic photobiomodulation for methanol-induced retinal toxicity," *Proceedings of the National Academy of Sciences of the United States of America*, vol. 100, no. 6, pp. 3439–3444, 2003.

[8] T. Karu, "Primary and secondary mechanisms of action of visible to near-IR radiation on cells," *Journal of Photochemistry and Photobiology B: Biology*, vol. 49, no. 1, pp. 1–17, 1999.

[9] W. Yu, J. O. Naim, M. McGowan, K. Ippolito, and R. J. Lanzafame, "Photomodulation of oxidative metabolism and

electron chain enzymes in rat liver mitochondria," *Photochemistry and Photobiology*, vol. 66, no. 6, pp. 866–871, 1997.

[10] D. Pastore, M. Greco, and S. Passarella, "Specific helium-neon laser sensitivity of the purified cytochrome c oxidase," *International Journal of Radiation Biology*, vol. 76, no. 6, pp. 863–870, 2000.

[11] T. C. Y. Liu, Y. Y. Liu, E. X. Wei, and F. H. Li, "Photobiomodulation on stress," *International Journal of Photoenergy*, vol. 2012, Article ID 628649, 11 pages, 2012.

[12] T. C. Y. Liu, L. Zhu, and X. B. Yang, "Photobiomodulation-mediated pathway diagnostics," *Journal of Innovative Optical Health Sciences*, vol. 6, Article ID 133001, 11 pages, 2013.

[13] M. T. T. Wong-Riley, X. Bai, E. Buchmann, and H. T. Whelan, "Light-emitting diode treatment reverses the effect of TTX on cytochrome oxidase in neurons," *NeuroReport*, vol. 12, no. 14, pp. 3033–3037, 2001.

[14] C. Zhang and M. T. T. Wong-Riley, "Depolarizing stimulation upregulates GA-binding protein in neurons: a transcription factor involved in the bigenomic expression of cytochrome oxidase subunits," *European Journal of Neuroscience*, vol. 12, no. 3, pp. 1013–1023, 2000.

Hindawi Publishing Corporation
International Journal of Photoenergy
Volume 2014, Article ID 585934, 5 pages
http://dx.doi.org/10.1155/2014/585934

Research Article

Effect and Mechanism of 808 nm Light Pretreatment of Hypoxic Primary Neurons

Xin Chen,[1] Qiang-Li Wang,[2] Shuang Li,[1] and Xian-qiang Mi[1,3,4]

[1] *College of Medical Device and Food Engineering, University of Shanghai for Science and Technology, Shanghai 200093, China*
[2] *Shanghai University of Traditional Chinese Medicine, Shanghai 201203, China*
[3] *Key Laboratory of System Biology, Chinese Academy of Sciences, Shanghai 201210, China*
[4] *Laboratory of System Biology, Shanghai Advanced Research Institute, Chinese Academy of Sciences, Shanghai 201210, China*

Correspondence should be addressed to Xian-qiang Mi; mixq@sari.ac.cn

Received 9 January 2014; Accepted 29 January 2014; Published 11 March 2014

Academic Editor: Timon Cheng-Yi Liu

This study investigated the effect of low intensity 808 nm light pretreatment of hypoxic primary neurons. Cobalt chloride ($CoCl_2$) has been used to induce hypoxic injury in primary mouse cortical neurons. Low intensity 808 nm light was from light-emitting diode (LED). Cells were randomly divided into 4 groups: normal control group, $CoCl_2$-induced group, $CoCl_2$-induced group with 808 nm light irradiation pretreatment, and normal group with 808 nm light irradiation pretreatment. Effect of low intensity 808 nm light on neuronal morphology has been observed by microscope. MTT colorimetric assay has been used to detect the effect of low intensity 808 nm light on neuronal activity. Adenosine triphosphate (ATP) concentration and cytochrome C oxidase (COX) activity has been detected to study the effect of low intensity 808 nm light on neuronal mitochondria function. The results indicated that low intensity 808 nm light pretreatment alone did not affect cell viability, COX activity, and ATP content of neurons and low intensity 808 nm light pretreatment promoted the cell viability, COX activity, and ATP content of neurons with $CoCl_2$ exposure; however, low intensity 808 nm light pretreatment did not completely recover COX activity and cellular ATP content of primary neurons with $CoCl_2$ exposure to the level of the normal neurons.

1. Introduction

Stroke, known medically as a cerebral vascular accident, could cause the rapid loss of brain function due to disturbance in the blood supply to the brain [1]. The high incidence and mortality of stroke have brought serious harm to people's health [2]. Currently, thrombolytic therapy is used commonly, but it has a strict time window constraint; meanwhile it has the risk of secondary hemorrhage [3]. A number of new and efficient methods are being explored. Among them, the transcranial near-infrared laser therapy (TLT) has been demonstrated to be effective and safe [4–6]. TLT is based on the effect of photobiomodulation of far- or near-infrared light. Biological effect of photobiomodulation using low intensity 808 nm LED light [7] irradiation showed no significant difference with low intensity laser irradiation, but with lower cost. Here, we investigated the biological effect of low intensity 808 nm LED light irradiation on neurons and explored its mechanisms. Our study observed the effect of low intensity 808 nm LED light pretreatment on the cell morphology, cell viability, COX activity, and ATP level of primary neurons with $CoCl_2$ exposure. This study demonstrated the protective function of low intensity 808 nm LED light pretreatment on anoxia injury neurons from the cellular level, which may be useful for the development of nondrug therapy modality of the acute ischemic stroke (AIS).

2. Materials and Methods

2.1. Culture of Primary Neurons. Postnatal Sprague-Dawley rats were brought from Shanghai Laboratory Animal Resources Center. After cutting the skull and removing the brain,

cortical neurons derived from newborn rats (24 h) were dissociated in DMEM/F12 with 10% fetal bovine serum and 10% horse serum and then plated on poly-L-Lysine coated 24-well plates (2×10^5/mL). Cultures were kept at 37°C in a humidified CO_2 incubator. Nonneuronal cell division was halted by exposure to 5 μM Cytarabine for one day. Subsequently, partial medium replacement was carried out every two or three days. After cultured for 7 days, neurons were used for the follow-up experiments.

2.2. Design of the Study. Neurons were divided into four groups:

control group: neurons without any treatment;

$CoCl_2$ group: neurons without any treatment for 3 days then exposed to 100 μM/L-$CoCl_2$ for 12 hours;

LED + $CoCl_2$ group: neurons irradiated for 80 seconds in the dark with 25 mW/cm^2 808 nm LED light, once a day for 3 days, then exposed to 100 μM/L-$CoCl_2$ for 12 hours;

LED group: neurons were irradiated by 25 mW/cm^2 808 nm LED light for 3 days then exposed for 12 hours without 100 μM/L-$CoCl_2$ treatment.

2.3. Cellular Morphology. Cellular morphology was observed by inverted microscopy (Olympus ZX71).

2.4. Cell Viability. Cell viability was determined by the typical MTT assay [8]. The brief process is as follows: cells in good conditions were incubated on 96-well plates, 100 μL each well; MTT working solution was filtered through a 0.22 μm filter and added 20 μL each well. After cultivation in incubator at 37°C for 4 h, the culture medium was removed and then 200 μL of DMSO was added after 10 min shaking. The cells were transferred to ELISA Reader and the cell viabilities were measured by optical density values at 570 nm.

2.5. COX Assays. COX was determined according to the instruction of mitochondrial cytochrome C oxidase activity assay kit. After the cells being digested and collected, mitochondria isolation assay was added, containing protein inhibitor. Stand for 15 minutes after mixing, cells were homogenized using ultrasound. After being centrifuged (600 g) for 10 minutes at 4°C, supernatant was collected. After being centrifuged (11000 g) at 4°C for 10 min, the precipitation was collected. Mitochondrial lysate was added into the prepared mitochondria to obtain the samples. After the addition of sample into the reaction system including cytochrome C and then mixed quickly, the activity of COX was tested by the OD values in 0 s and 60 s from spectrophotometer at 550 nm and then calculated by the protein concentration of samples.

2.6. ATP Content Assays. Using a modification of the luminescence method of Strehler [9], ATP content was measured as follows: after lysis of neuron cells being placed on ice and centrifuged (12000 g) at 4°C for 8 min, supernatant was collected. Some samples were placed in the ice box and the corresponding BCA solution was prepared. The dissolved standard proteins were added to the standard hole of 96-hole plate. An appropriate volume of samples was also added to the same hole and then diluted to 20 μL with PBS solution. Working solution prepared previously was added. The volume of each hole is 200 μL. After being put at 37°C for 30 minutes, the protein concentration of each sample was calculated. 100 μL ATP testing reagent was added into the testing wells and then put at room temperature for 3–5 min so as to exhaust the ATP in background. Then, ATP content can be calculated by liquid scintillation counter and standard curve made previously.

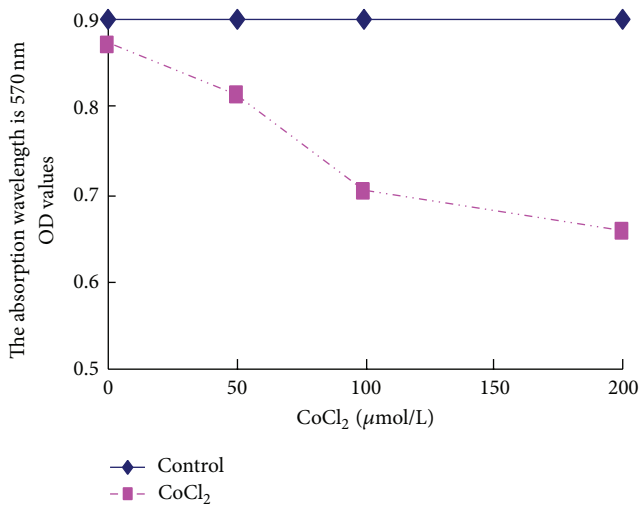

Figure 1: Effects of $CoCl_2$ with various concentrations on cell viability in cultured neurons.

2.7. Statistical Analysis. All light-emitting diode irradiation experiments and biochemical assays associated with measuring changes as a result of light irradiation were performed six times ($n = 6$). All values are expressed as means ± SEM. A one way ANOVA was used in SPSS13.0 to determine whether any significant differences existed among groups. In all cases, the minimum level of significance was taken as $P < 0.05$.

3. Results

3.1. To Determine the Optimal Concentration of $CoCl_2$. Figure 1 shows the cell viability of neurons affected by $CoCl_2$ with different concentration. Compared with normal control group (without any treatment), cell viability began to decrease under exposure to $CoCl_2$ at the concentration of 50 μM/L. Cell viability was 80% of the control group at the concentration of 100 μM/L-$CoCl_2$. Cell viability was less than 50% at the concentration of 200 μM/L-$CoCl_2$. Hence, 100 μM/L-$CoCl_2$ was chosen to produce cell injury in the follow-up experiments.

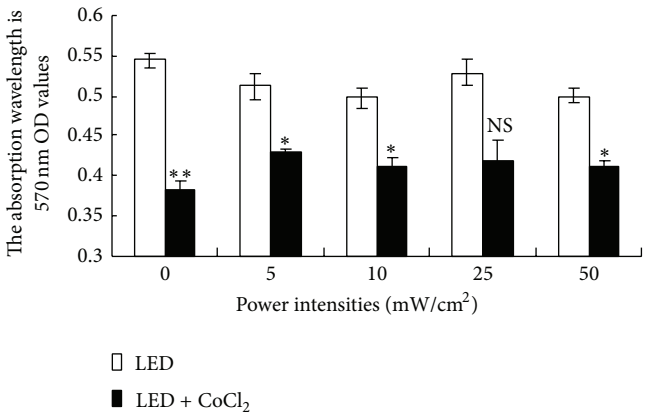

Figure 2: Effect of 808 nm LED light pretreatment with various power densities on cell viability in cultured neurons with 100 μM/L-$CoCl_2$. Neurons were cultured in incubator at 37°C for 4 h, the culture medium was removed, and then 200 μL of DMSO was added after 10 min shaking before cell viability was measured. The power intensities chosen were 5, 10, 25, and 50 mW/cm^2. Data are Means ± SEM. ** means that this group was highly significantly different from control group ($P < 0.01$). * means that this group has statistical difference with control group ($P < 0.05$).

3.2. To Determine the Optimal LED Power Density. The effect of LED light pretreatment with various power densities on cell viability of cultured neurons with $CoCl_2$ is shown in Figure 2. Among the four power densities (5, 10, 25, and 50 mW/cm^2) of LED light pretreatment groups there was nonsignificant difference between cell viability of 25 mW/cm^2 LED light pretreatment group alone and the 25 mW/cm^2 LED light pretreatment with 100 μM/L-$CoCl_2$ group. It means that LED light pretreatment with power intensity of 25 mW/cm^2 has the best capacity of inhibiting the damage induced by $CoCl_2$. The optimal power density for increasing cell viability was 25 mW/cm^2. Thus, the dose of 25 mW/cm^2 was chosen for the following experiment.

3.3. Effect of LED Light Treatment on Neuronal Morphology. The typical morphology of neurons which were irradiated at the optimal power density of 25 mW/cm^2 could be observed (Figure 3). The neuronal soma of control group was full and surrounded by halos; the neuritis were slender and interrelated to a network (Figure 3(a)). The cell body of neuron exposed to 100 μM/L-$CoCl_2$ had serious shrinkage, the neuritis was fractured and the network disappeared, and even the cell died after ruptures (Figure 3(b)). The morphology of the neurons treated with low intensity 808 nm LED light pretreatment with $CoCl_2$ was improved obviously (Figure 3(c)) and the neurons only treated with 808 nm LED light grew in good condition (Figure 3(d)).

3.4. Effect of LED Light Pretreatment on COX Activity. Compared with the control group, the COX activity of $CoCl_2$ group decreased very significantly ($P < 0.01$) and LED + $CoCl_2$ group decreased significantly ($P < 0.05$). There is no significant difference between the COX activity of LED group with control group. Compared with 100 μM/L-$CoCl_2$ group, COX activity of both LED + $CoCl_2$ group and LED group increased significantly ($P < 0.01$) (Figure 4).

3.5. Effects of LED Light Treatment on Cellular ATP Content. Compared with the control group, the cellular ATP content of $CoCl_2$ group decreased very significantly ($P < 0.01$) and LED + $CoCl_2$ group decreased significantly ($P < 0.05$). There is no significant difference between the cellular ATP of LED group with control group. Compared with 100 μM/L-$CoCl_2$ group, COX activity of both LED + $CoCl_2$ group and LED group increased significantly ($P < 0.01$) (Figure 5).

4. Discussion

$CoCl_2$ has been demonstrated to induce the hypoxia damages of cells *in vitro* [10]. It demonstrated that the $CoCl_2$-induced hypoxic injury neurons model could be used for AIS research. Our results showed that low intensity 808 nm light pretreatment promotes the cell viability, COX activity, and ATP content of neurons with $CoCl_2$ exposure. It means that low intensity 808 nm light pretreatment has the capacity to protect against the hypoxia damage of neurons. It might be due to indirect photobiomodulation of low intensity 808 nm light pretreatment according to Liu et al. [11]. However, there was no significant difference about the cell viability, COX activity, and ATP content between the LED group and control group. This suggested that more parameters need to be further assessed.

As a primary biological photoreceptor in the red to near-IR spectrum, COX plays an important role in photobiomodulation [12]. Our research showed that the cellular ATP content of primary neurons rises or falls in concert with the activity of COX. However, low intensity 808 nm LED light pretreatment could not completely recover COX activity and cellular ATP content of primary neurons exposed to $CoCl_2$ to the level of the normal neurons. It suggested that the pathway maintaining proliferation of normal neurons and the one maintaining proliferation of neurons by LED light T pretreatment then exposed to $CoCl_2$ were different from each other, but they maintained the same proliferation [13]. Those two pathways are well-known redundant pathways [11, 14]. Of course, it should be further studied.

5. Conclusion

Under the conditions in which this study was carried out, it was possible to conclude that low intensity 808 nm LED light pretreatment has the capacity to promote mitochondrial energy metabolism and protect against the hypoxia damage of neurons. Low intensity 808 nm LED light pretreatment can improve and restore the neuron function of ischemic penumbra in patients with AIS. Our findings provided experimental evidences for clinical application of low intensity 808 nm LED device.

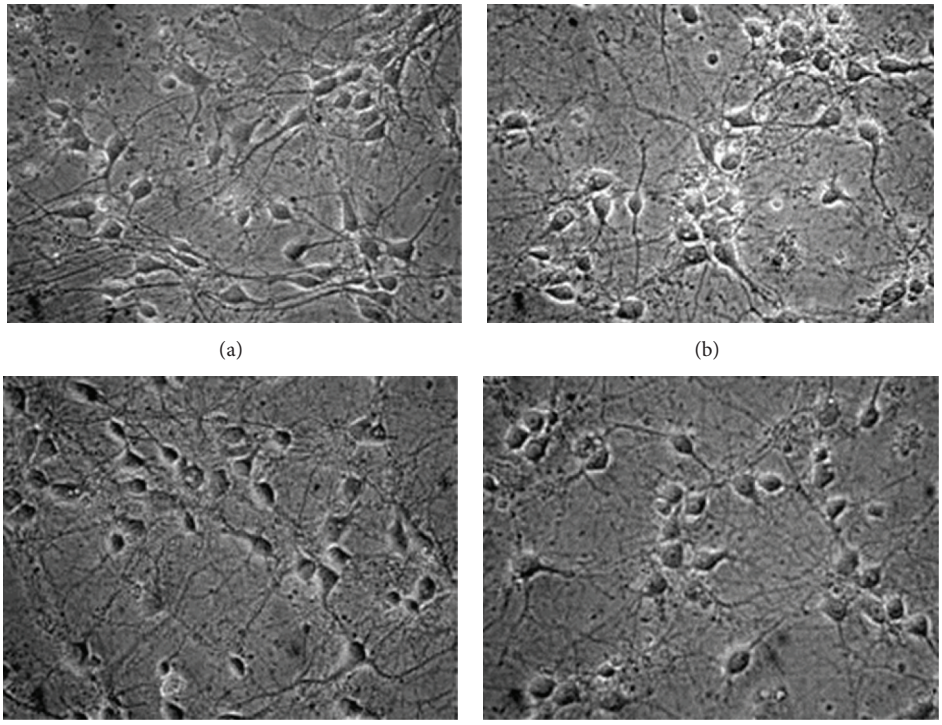

Figure 3: Morphology of the primary cortical neurons in culture (400X). (a) Control, (b) Neurons without any treatment for 3 days then exposed to 100 μM/L-$CoCl_2$ for 12 hours. (c) Neurons irradiated for 80 seconds in the dark with 25 mW/cm^2 808 nm LED light, once a day for 3 days, then exposed to 100 μM/L-$CoCl_2$ for 12 hours. (d) Neurons were irradiated by 25 mW/cm^2 808 nm LED light for 3 days then exposed for 12 hours without 100 μM/L-$CoCl_2$ treatment. Images shown are representative of several plates for each group.

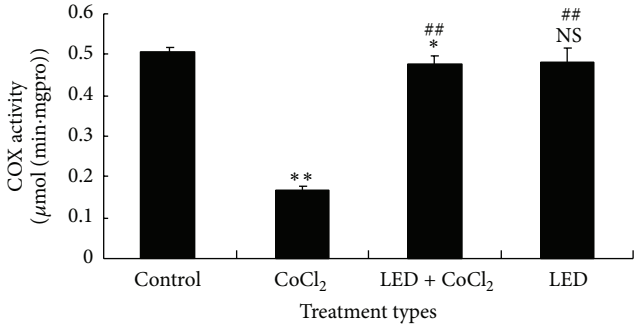

Figure 4: Effect of 25 mW/cm^2 808 nm LED light pretreatment on COX activity. After cultured neuron cells being digested and collected, mitochondria isolation assay was added. 15 minutes later, cells were homogenized. After being centrifuged (600 g) for 10 minutes, supernatant was collected. After being centrifuged (11000 g) for 10 minutes, the precipitation was collected. Mitochondrial lysate was added to obtain the samples. Then COX was measured. Data are Means ± SEM. $^{**}(P < 0.01)$ and $^{*}(P < 0.05)$ mean compared with control group; $^{\#\#}(P < 0.01)$ and $^{\#}(P < 0.05)$ mean compared with 100 μM/L $CoCl_2$ group.

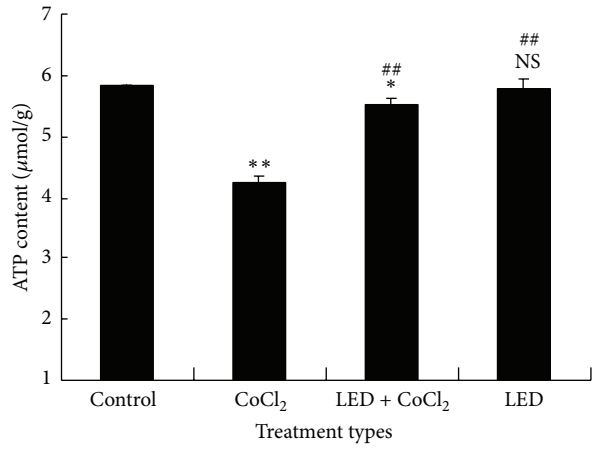

Figure 5: Effect of 25 mW/cm^{2}808 nm LED light pretreatment on cellular ATP content. After the lytic neuron cells were placed on ice and centrifuged for 8 min, its supernatant was collected. After treatment and putting at 37°C for 30 minutes, protein concentration of each sample was calculated. After 100 μL ATP testing reagent was added into the testing wells and put at room temperature for 3–5 min, ATP content was calculated. Data are Means ± SEM. $^{**}(P < 0.01)$ and $^{*}(P < 0.05)$ mean compared with control group and $^{\#\#}(P < 0.01)$ and $^{\#}(P < 0.05)$ mean compared with 100 μM/L-$CoCl_2$ group.

Conflict of Interests

The authors declare that there is no conflict of interests regarding the publication of this paper.

Acknowledgments

This study had the financial support of the National Natural Science Foundation of China (no. 61078071), the Natural Science Foundation of Shanghai (no. 09ZR1422500), and the 2013 "Innovation Action Plan" from Science and Technology Commission of Shanghai Municipality (no. 13DZ1940200).

References

[1] N. R. Sims and H. Muyderman, "Mitochondria, oxidative metabolism and cell death in stroke," *Biochimica et Biophysica Acta*, vol. 1802, no. 1, pp. 80–91, 2010.

[2] X.-Q. Mi, J. Chen, R. Chen, S. Zheng, and L.-W. Zhou, "Mechanism of low power laser irradiation on red blood cell deformability," *Chinese Optics Letters*, vol. 3, supplement 1, pp. S182–S184, 2005.

[3] P. A. Lapchak, J. Wei, and J. A. Zivin, "Transcranial infrared laser therapy improves clinical eating scores after embolic strokes in rabbits," *Stroke*, vol. 35, no. 8, pp. 1985–1988, 2004.

[4] Y. Lampl, J. A. Zivin, M. Fisher et al., "Infrared laser therapy for ischemic stroke: a new treatment strategy—results of the NeuroThera Effectiveness and Safety Trial-1 (NEST-1)," *Stroke*, vol. 38, no. 6, pp. 1843–1849, 2007.

[5] A. Oron, U. Oron, J. Chen et al., "Low-level laser therapy applied transcranially to rats after induction of stroke significantly reduces long-term neurological deficits," *Stroke*, vol. 37, no. 10, pp. 2620–2624, 2006.

[6] J. A. Zivin, G. W. Albers, N. Bornstein et al., "Effectiveness and safety of transcranial laser therapy for acute ischemic stroke," *Stroke*, vol. 40, no. 4, pp. 1359–1364, 2009.

[7] S. M. Potter and T. B. DeMarse, "A new approach to neural cell culture for long-term studies," *Journal of Neuroscience Methods*, vol. 110, no. 1-2, pp. 17–24, 2001.

[8] T. Mosmann, "Rapid colorimetric assay for cellular growth and survival: application to proliferation and cytotoxicity assays," *Journal of Immunological Methods*, vol. 65, no. 1-2, pp. 55–63, 1983.

[9] B. L. Strehler, "Bioluminescence assay: principles and practice," in *Methods of Biochemical Analysis*, vol. 16, pp. 99–181, 1968.

[10] G. L. Wang and G. L. Semenza, "Purification and characterization of hypoxia-inducible factor 1," *The Journal of Biological Chemistry*, vol. 270, no. 3, pp. 1230–1237, 1995.

[11] T. C.-Y. Liu, Y.-Y. Liu, E.-X. Wei, and F.-H. Li, "Photobiomodulation on stress," *International Journal of Photoenergy*, vol. 2012, Article ID 628649, 11 pages, 2012.

[12] M. T. Wong-Riley, H. L. Liang, J. T. Eells et al., "Photobiomodulation directly benefits primary neurons functionally inactivated by toxins: role of cytochrome c oxidase," *The Journal of Biological Chemistry*, vol. 280, no. 6, pp. 4761–4771, 2005.

[13] T. C.-Y. Liu, L. Zhu, and X.-B. Yang, "Photobiomodulation-mediated pathway diagnostics," *Journal of Innovative Optical Health Sciences*, vol. 6, no. 1, Article ID 1330001, 11 pages, 2013.

[14] T. C.-Y. Liu, F. H. Li, E.-X. Wei, and L. Y. Deng, "Redundant pathway mediated photobiomodulation enhancement on a myoblast proliferation in its proliferation-specific homeostasis," *Lasers in Surgery and Medicine*, vol. 45, supplement 25, p. 53, 2013.

Hindawi Publishing Corporation
International Journal of Photoenergy
Volume 2014, Article ID 904304, 8 pages
http://dx.doi.org/10.1155/2014/904304

Review Article

Microenvironment Dependent Photobiomodulation on Function-Specific Signal Transduction Pathways

Timon Cheng-Yi Liu,[1] De-Feng Wu,[1] Ling Zhu,[1] P. Peng,[1] Long Liu,[2] and Xiang-Bo Yang[1,3]

[1] *Laboratory of Laser Sports Medicine, South China Normal University, University Town, Guangzhou 510006, China*
[2] *Department of Chemistry and Biology, College of Science, National University of Defense Technology, Changsha 410073, China*
[3] *MOE Key Laboratory of Laser Life Science and Institute of Laser Life Science, College of Biophotonics, South China Normal University, Guangzhou 510631, China*

Correspondence should be addressed to Timon Cheng-Yi Liu; liutcy@scnu.edu.cn

Received 7 January 2014; Accepted 28 January 2014; Published 9 March 2014

Academic Editor: Quan-Guang Zhang

Cellular photobiomodulation on a cellular function has been shown to be homeostatic. Its function-specific pathway mechanism would be further discussed in this paper. The signal transduction pathways maintaining a normal function in its function-specific homeostasis (FSH), resisting the activation of many other irrelative signal transduction pathways, are so sparse that it can be supposed that there may be normal function-specific signal transduction pathways (NSPs). A low level laser irradiation or monochromatic light may promote the activation of partially activated NSP and/or its redundant NSP so that it may induce the second-order phase transition of a function from its dysfunctional one far from its FSH to its normal one in a function-specific microenvironment and may also induce the first-order functional phase transition of the normal function from low level to high level.

1. Introduction

Cellular photobiomodulation (PBM) is a modulation of laser irradiation or monochromatic light (LI) on cells in vitro or in vivo or ex vivo, which stimulates or inhibits cellular functions but does not result in irreducible damage. The LI intensity is in the range of about 10–1000 mW/cm^2 [1, 2]. As we have classified [3–5], the LI used in PBM is always a low intensity LI (LIL), ~10 mW/cm^2, which includes the LI used in the so-called ultra-low-level laser therapy [6], but moderate intensity LI (MIL), 0.10~1.0 W/cm^2, is of PBM if the irradiation time is not so long that it irreducibly damages organelles or cells. The PBM of LIL and MIL are denoted as LPBM and MPBM, respectively. The MIL with short irradiation time and LIL are two kinds of well-known low level LI (LLL).

Many studies have focused on signal transduction pathway mediated cell-autonomous mechanisms of PBM. By contrast, we proposed that the cellular microenvironment confers the response of cellular signal transduction pathways to LLL. Many cellular signal transduction pathways may be modulated by LLL, but which signal transduction pathway can be modulated has been left to be resolved. Many studies suggested that the modulated signal transduction pathway may depend on the microenvironment in which cells live. It would be reviewed in this paper.

2. Function-Specific Homeostasis

Negative feedback is common in biological processes and acts to optimize the activity of a circuit in the presence of alleles with altered activities [7], which can maintain a system's stability to internal and external perturbations. Function-specific homeostasis (FSH) is a negative-feedback response of a biosystem to maintain the function-specific conditions inside the biosystem so that the function is perfectly performed [3, 4, 8, 9]. A function in/far from its FSH is called a normal/dysfunctional function. A normal function is better performed than all the dysfunctional functions so that the normal function is locally the best performed function.

The phenomena are the well-known "Arndt-Schulz Law" or the J-shaped curves. Moreover, the normal function can resist external perturbations so that the peak of Arndt-Schulz Law or the J-shaped curve can be extended to a plateau so that it is called Arndt-Schulz Plateau Law or the U-shaped curve. In 10% fetal bovine serum (FBS), it has been found that there are the normal glucose (nG) at about 22.5 mM, in which many cell lines such as C2C12 [10, 11] and C3H10 T1/2 [12] proliferate at its optimal rate, and the low/high glucose (lG/hG) whose concentration was lower/higher than the one of nG and in which the cell lines proliferate at a rate lower than the optimal rate. In other words, the cells in nG and 10% FBS are in their respective proliferation-specific homeostasis (PlSH).

A normal function can resist external/internal disturbance under its threshold. Straussman et al. [13] have studied the effects of twenty-two cytokines, each at five concentrations, on six melanoma cell lines in their respective PlSH, respectively. They found that only hepatocyte growth factor (HGF) upgraded the normal proliferation but all the other twenty-one cytokines cannot affect the normal proliferation. That is suggested that only HGF was allowed to activate its signal transduction pathway, but all the other twenty-one cytokines were not allowed to activate their pathways, respectively.

The experimental reproducibility in a PlSH is intrinsic. In a recent analysis, Haibe-Kains et al. [14] reported that the measured drug response data are highly discordant for the two large-scale pharmacogenomic studies, the Cancer Genome Project (CGP), and the Cancer Cell Line Encyclopedia (CCLE). CGP and CCLE cells were grown in Roswell Park Memorial Institute (RPMI) or Dulbecco's Modified Eagle's Medium (DMEM)/F12 medium with 5% and 10% FBS, respectively. This suggested that each CGP cell line was far from its respective PlSH and its IC_{50} (concentration in micromolar at which the drug inhibited 50% of the maximum cellular growth) against one antidrug cannot be reproducible. As reported by the CGP, there was only a fair correlation between camptothecin IC_{50} measurements generated at two sites using matched cell line collections and identical experimental protocols. On the other hand, each CCLE cell line may be in its respective PlSH and its IC_{50} value against one antidrug can be reproducible. This was why there were more than one IC_{50} value of each CGP cell line against one antidrug for each CCLE IC_{50} value and the vast majority of drugs and gene-drug associations then yielded poor concordance for IC_{50} and AUC (area under the activity curve measuring dose response).

3. Microenvironments

Cells may have many functions. Which function may be perfectly performed depends on the microenvironment in which cells live. Cells in a serum-free medium may become apoptotic and can be modulated by a LLL [15], but they cannot proliferate, attach, or migrate, so that the PBM on their proliferation [16, 17], attachment [16], or migration [16] could not be observed. Many studies have focused on cell-autonomous mechanisms of drug resistance, but Straussman et al. [13] found that the tumor microenvironment conferred innate resistance to therapy. They found that stromal cell secretion of HGF resulted in activation of the HGF receptor MET, reactivation of the mitogen-activated protein kinase (MAPK) and phosphatidylinositol-3-OH kinase- (PI3K-) AKT signaling pathways, and immediate resistance to RAF inhibition.

A cell may only perform the function in a function-specific microenvironment. Eduardo et al. [18] have studied human dental pulp stem cell (DPSC) proliferation in 5%, 10%, 12.5%, and 15% FBS, respectively, and found that there was no significant difference of the proliferation in 10% FBS from the one in 12.5% FBS after 24 h, both of which were significantly smaller than the one in 15% FBS, but larger than the one in 5% FBS. It indicated that the proliferation in 10% or 12.5% FBS was in its PlSH, resisting FBS change. For many cell lines in 10% FBS, only proliferation can be performed and the medium is called a proliferation-specific microenvironment (PSM). For many cell lines, proliferation in 10% FBS and nG is in its PlSH in nG (nPlSH), and the microenvironment is called a PlSH-specific microenvironment (PlSM). If the C3H10 T1/2 cells were cultivated in 10% FBS and lG such as 0 or 5 mmol/L glucose or hG such as 100, 200, or 300 mmol/L glucose for 3 or 6 h and then cultivated in a PlSM for 8 days, the modulated proliferation would become the normal proliferation [12].

A cell may become apoptotic in a PSM or a differentiation-specific microenvironment (DSM). A LLL can inhibit apoptosis by promoting proliferation in a PSM [19] or promoting differentiation in a DSM [20]. Many groups have studied the proliferation-mediated apoptosis inhibition, but only Zhu et al. [20] have studied the differentiation-mediated apoptosis inhibition. Moreover, the latter inhibition was more effective than the former inhibition. As a fact, the in vivo neurons are mostly differentiated. The differentiation-mediated apoptosis inhibition of PBM should be widely studied.

4. Function-Specific Pathways

Signal transduction pathways are always signal-dependent. However, it may not work when the cells are in their FSH [13]. Cancer cells in their respective PlSH eliminate various signaling pathways, especially apoptotic, permitting their surviving, spreading, and thriving in "foreign" organs [21]. It suggested that the negative feedback of the cellular FSH not only resists internal/external disturbance but also resists the activation of many other irrelative signal transduction pathways. The signal transduction pathways are always found by destroying the FSH with serum deprivation or starvation or other stresses. For a cell far from its FSH, many signal transduction pathways have been partially activated [22]. One can alternatively find one of them so that one signal may have many alternative signal transduction pathways. The signal transduction pathways were studied from the viewpoint of functions in this section.

4.1. Normal Function-Specific Signal Transduction Pathways. The activation of one signal transduction pathway can not only be directly promoted, but also be indirectly promoted by inhibiting the activation of other pathways. For example, insulin-like growth factor- (IGF-) 1 can restore dexamethasone- (DEX-) induced heart growth arrest in rats [23], and DEX can promote the IGF-1 promotion on skeletal muscle cell proliferation [24] and the IGF binding protein (IGFBP) 1 production of rat hepatocytes [25] in serum-free medium. The signal transduction pathway activation of a cell may also be inhibited by its FSH. The negative feedback of the cellular FSH can resist the activation of many other irrelative signal transduction pathways so that some signal transduction pathways may be left to be fully activated. It has been found that the best pathways for a dysfunctional function to become normal or a normal function to become upgraded are sparse [9]. Straussman et al. [13] found that the normal proliferation was maintained by full activation of the platelet-derived growth factor (PDGF) pathway, BRAF, MAPK kinase (MEK), and extracellular signal-regulated kinase (ERK), which not only resisted the proliferation effects of twenty-one cytokines, each at five concentrations, but also resisted their signal transduction pathway activation. At this point, it is reasonable to suppose that there may be normal function-specific signal transduction pathways (NSPs) so that the FSH can maintain the full activation of the NSPs but resist the activation of other irrelative signal transduction pathways. The PDGF pathway is the NSP of the normal proliferation of the six melanoma cell lines according to [13].

4.2. Redundant Signal Transduction Pathways. One normal function may have N possible NSPs. Genetic redundancy means that N genes are performing the same function and that inactivation of one of these N genes has little or no effect on the biological phenotype [26]. The N genes performing the same function are called redundant genes with one another [8]. Each redundant gene may have its NSP in its NSP-specific microenvironment (NSM). The full activation of each NSP can maintain its normal function in its NSM. The N NSPs of the same normal function are called redundant NSPs (rNSPs) with one another. Straussman et al. [13] found that HGF upgraded its normal proliferation of the six melanoma cell lines and further found that the proliferation enhancements were mediated by full activation of HGF pathway, PI3K, AKT or RAF1, MEK, and ERK and then by the synergistic full activation of both PDGF pathway and HGF pathway. The HGF pathway and the PDGF pathway are the two ones among the N NSPs of the normal proliferation of the six melanoma cell lines.

Whether NSP of a normal function actually maintains the normal function depends on the microenvironment. For a dysfunctional function, many signal transduction pathways have been partially activated [22]. While a dysfunctional function becomes a normal function, only sparse signal transduction pathways are left to be fully activated [9], but other irrelative signal transduction pathways are completely inhibited. The sparse signal transduction pathways are always one NSP. Liu et al. [9, 10] have studied the effects of hG at 90 mM and the LIL at 640 nm on the messenger ribonucleic acid (mRNA) of 6 genes of C2C12 cells in their nPlSH and found that hG decreased the proliferation and the mRNA expression of sirtuin 1 and manganese superoxide dismutase (MnSOD) but increased the mRNA expression of IGF-1, forkhead box O family (FOXO) 3a, Bcl-2 interacting mediator of cell death (Bim), and p27 and that LIL further increased IGF-1 mRNA expression but decreased Bim mRNA expression until it was lower than the one of C2C12 cells in nG and completely recovered the proliferation and the mRNA expression of the other 4 genes so that the PlSH in hG (hPlSH) was established. IGF-1 inhibits the mRNA of Bim [27, 28]. Obviously, IGF-1 pathway is the hG activated NSP (hNSP) of C2C12 myoblasts although the nG activated NSP (nNSP) has not been found yet. Both nPlSH and hPlSH maintain the same normal proliferation of C2C12 myoblasts, but nNSP/hNSP maintains nPlSH/hPlSH in 10% FBS and nG/hG.

4.3. Functional Phase Transitions. The normal DPSC proliferation in 10% FBS is maintained by its NSP. Eduardo et al. [18] found that MIL could not affect the normal DPSC proliferation in 15% FBS but upgraded the one in 10% FBS, and the upgraded one in 10% FBS was still significantly smaller than the one in 15% FBS. This suggested that the one in 15% FBS may at least be maintained by the synergistic integration of NSP and one of its rNSPs. Generally, the full activation of each NSP maintains the first-order normal function in its NSM, and the synergistic full activation of one NSP and its $n-1$ rNSPs maintains the nth-order normal function ($n = 2, 3, \ldots, N$) in its NSM. The phase transition from a dysfunctional function to the first-order normal function is just the second-order functional phase transition, but the one from the $(n-1)$th-order normal function to the nth-order normal function is just the first-order functional phase transition. In our experiments [11], serum-shocked C2C12 myoblasts were cultivated in nG and FBS at different concentrations. As FBS concentration increased, the dysfunctional proliferation becomes normal, and then the order of the normal proliferation becomes higher. Here, FBS induced a proliferation phase transition from the second-order one to the first-order one. In the experiments of Straussman et al. [13], PDGF pathway maintained the first-order normal proliferation in its PDGF pathway-specific medium, and the synergistic full activation of both PDGF pathway and HGF pathway maintained the second-order normal proliferation in its PDGF pathway-specific medium. Here, HGF induced a first-order proliferation phase transition of six melanoma cell lines in its PDGF pathway-specific medium.

4.4. Pathway-Mediated Photobiomodulation. There were many theories on precise molecular mechanism of PBM. Among them, the cytochrome c oxidase (COX) theory was very popular [2, 29]. Cytochrome c and COX represent the terminal step of the electron transport chain, the proposed rate-limiting reaction in mammals. Cytochrome c and COX show unique regulatory features including allosteric regulation, isoform expression, and regulation through cell signaling pathways [30]. The COX theory of PBM was

proposed by Karu and Afanas'eva [31, 32]. It suggested that COX in mitochondria was the primary photoacceptor upon LLL exposure of cells, and PBM was mediated by LLL increased COX activity. According to the COX theory, LLL can increase nitric oxide (NO) production [2]. However, many studies [33–35] found that LIL may decrease the NO production. For example, Montoro et al. [35] found that LIL may decrease the NO production of FBS-deprived human dental pulp cells (HDPCs) without lipopolysaccharide (LPS) and FBS-deprived HDPCs with LPS. Moreover, Wu et al. [36] demonstrated that the initial reaction after photon absorption of MIL was photosensitization of COX, to inhibit enzymatic activity of COX in situ and cause respiratory chain reactive oxygen species (ROS) burst. Horvát-Karajz et al. [37] found that the effects of one time MIL irradiation, MIL induced stresses, were successful or self-limited at low dose but chronic at high dose according to our homeostasis theory [3, 4, 8], and cytostatic drugs such as cytarabine, paclitaxel, and vincristine may change the successful stress of MIL at low dose into chronic stress. In this context, LLL cannot increase COX activity if COX was the primary photoacceptor.

As Wu et al. [36] have demonstrated, MPBM is indeed mediated by COX-mediated ROS [4, 38]. According to our homeostasis theory [3, 4, 8], we have suggested that the membrane receptors of cells or organelles were the primary photoreceptors of LIL, and LPBM was mediated by receptor-activated signal transduction pathways [4, 9, 38]. Several signaling pathways have been identified that target COX including protein kinase A and C, receptor tyrosine kinase, and inflammatory signaling [30]. In addition, four phosphorylation sites have been mapped on cytochrome c with potentially large implications due to its multiple functions including apoptosis, a pathway that is overactive in stressed cells but inactive in cancer. In other words, LIL-activated pathways may modulate COX activity so that it can explain LIL increased COX activity.

The LLL promotion of the normalization of a dysfunctional function may be mediated by the promotion of the activation of partially activated NSP or/and its rNSP. Miyata et al. [17] found that MIL promoted the phosphorylation of ERK 1/2 between 5 and 30 min after MIL irradiation but did not affect p38 MAPK or c-Jun N-terminal kinase (JNK) phosphorylation. In our experiments [9, 10], the C2C12 myoblast proliferation in its nPlSM is normal, but the one in 10% FBS and hG at 90 mmol/L is dysfunctional. We found that hG increased IGF-1 mRNA expression of C2C12 myoblasts; LIL further increased the IGF-1 mRNA expression until the IGF-1 pathway is fully activated so that the hPlSH was established.

5. Photobiomodulation

There are many cellular functions. Generally, a cellular microenvironment only allows one function to be performed. If the allowed function is dysfunctional, LPBM may promote the activation of its partially activated NSP until it is fully activated so that the dysfunctional function becomes normal. If the allowed function is normal, for example, it is the $(n-1)$th-order normal function ($n = 2, 3, \ldots, N$) if the normal function has N possible NSPs, which is maintained by the synergistic full activation of one NSP and its $n-2$ rNSPs in its NSM; LPBM may promote the activation of its partially activated $(n-1)$th rNSP until it is fully activated so that the $(n-1)$th-order normal function is upgraded to be the nth-order normal function. The former and latter PBM are called direct and indirect PBM (dPBM and iPBM), respectively. The dPBM induces the second-order functional phase transition from a dysfunctional function to the first-order normal function, but the iPBM induces a first-order functional phase transition from the $(n-1)$th-order normal function to the nth-order normal function ($n = 2, 3, \ldots, N$) if the normal function has N possible NSPs.

5.1. Direct Photobiomodulation. There have been many studies of dPBM on proliferation of cells, but few ones on the other cellular functions. There may be differentiation-specific homeostasis (DiSH). Zhu et al. [20] have found that the differentiation-mediated apoptosis inhibition of dPBM was mediated by brain-derived neurotrophic factor (BDNF). Saygun et al. [39] have found that the dPBM promotion of the osteoblast differentiation of human mesenchymal stem cells (MSCs) was mediated by basic fibroblast growth factor (bFGF).

Amyloid β (Aβ) [19, 40] or 6-hydroxy dopamine [41] may decrease the proliferation rate by inducing apoptosis, and LIL [19, 40] or the insect antibacterial peptide [41], CopA3 (a D-type disulfide dimer peptide, LLCIALRKK), may inhibit the apoptosis by promoting proliferation. In Meng et al.'s paper [40], the neuron proliferation resisted LIL. It indicated that the neuron proliferation may be a normal proliferation. For the human neuroblastoma cell line SH-SY5Y in its PlSH, Aβ decreased the proliferation rate, but LIL promoted the dysfunctional proliferation until it became normal [40] so that the PlSH in Aβ (aPlSH) was established. BDNF can stimulate neuronal proliferation [42]. Meng et al. [40] found that LIL increased BDNF level. LIL increased BDNF level of neurons and then promoted dysfunctional proliferation until the aPlSH was established.

Huang et al. [43] exposed primary cultured murine cortical neurons to oxidative stressors: hydrogen peroxide, cobalt chloride, and rotenone in the presence or the absence of LIL at 810 nm. They found that the LIL increased both MMP and ROS in nonoxidative neurons and increased MMP but reduced high ROS levels and protected cultured cortical neurons from death in oxidative cells. Huang et al. [34] further studied the effects of LIL at 810 nm on glutamate, N-methyl-D-aspartate (NMDA), or kainate induced excitotoxicity of primary murine cultured cortical neurons. They found that the measurements can be divided into two groups: those in which the effect of the LIL is similar in direction (both increased) regardless of whether the neurons are nonexcitotoxic or excitotoxic (these are viability, adenosine triphosphate (ATP), and mitochondrial membrane potential (MMP)) and those measurements in which the direction of the LIL effect is opposite, raised for nonexcitotoxic neurons

and decreased for excitoxic neurons (these are intracellular Ca^{2+}, ROS, and NO). Their explanation based on the COX theory was very complicated [34, 43], but the one based on NSPs is very simple. Either oxidative/excitoxic or nonoxidative/nonexcitoxic neurons are dysfunctional so that their viability, ATP, and MMP have been promoted by LIL, but their mediated NSPs may be different from each other so that their intracellular Ca^{2+}, ROS, and NO have been oppositely modulated by LIL although the NSPs may be redundant with each other.

Esmaeelinejad and Bayat [44] have studied LPBM on human skin fibroblasts in lG and 10% FBS and found that LIL promoted the activation of interleukin-6 (IL-6)/bFGF mediated pathway. Jee et al. [45] found that IL-6 induced bFGF-dependent angiogenesis in basal cell carcinoma cell line via JAK/STAT3 and PI3K/Akt pathways.

5.2. Indirect Photobiomodulation. The most studied normal functions of cells are normal proliferation. LLL can upgrade the normal proliferation by promoting the activation of its partially activated rNSP.

In our experiments [9, 10], the LIL at 640 nm was found to induce the first-order phase transition from the first-order normal proliferation of C2C12 myoblasts in a PlSM to the second-order normal proliferation and then to the higher-order normal proliferation. For the first phase transition, the NSP and the first rNSP were found to be the nNSP and hNSP, respectively. The normal proliferation was maintained by the full activation of nNSP. LLL promoted hNSP activation. The synergistic action of nNSP and hNSP inhibited FOXO3a so that the normal proliferation was upgraded. FOXO3a inhibits breast cancer cell proliferation. The second phase transition from the second-order normal proliferation to the higher-order normal proliferation has been left to be solved.

For the iPBM on the normal proliferation of NIH3T3 fibroblasts in a PlSM in 10% FBS [9, 46], the rNSP is the PDGF-C pathway. Komine et al. [46] have studied LPBM on mRNA expression of PDGF-A, PDGF-B, PDGF-C, transforming growth factor-beta (TGF-beta), bFGF, PDGF-alpha receptor, and TGF-beta receptor and found that LPBM only increased PDGF-C mRNA expression but could not affect the mRNA expression of other genes.

For the iPBM on the normal proliferation of a human osteoblast-like cell line (Saos-2 cell line) in a PlSM in 10% FBS [47], the rNSP is one differentiation-mediated pathway. Bloise et al. [47] found that multiple doses of LIL increased extracellular matrix constituents such as alkaline phosphatase (ALP), decorin, fibronectin, and type-III collagen but did not affect extracellular matrix constituents such as osteocalcin, osteopontin, osteonectin, and type-I collagen. Moreover, multiple doses of LIL decreased the bone sialoprotein mRNA expression. On the other hand, the proliferation enhancement of titanium bioglass-coated scaffolds for Saos-2 human osteoblasts enhanced the deposition of extracellular matrix components such as ALP, decorin, fibronectin, osteocalcin, osteonectin, osteopontin, and type-I and -III collagens [48].

For the iPBM of the MIL at 532 nm on the normal proliferation of the human-derived glioblastoma cells (A-172) in a PlSM in 10% FBS [49] and the MIL at 660 or 780 nm on the normal proliferation of oral dysplastic cells in a PlSM in 10% FBS [50], the rNSP is AKT-mediated pathway. The γ-secretase inhibitor (GSI) inhibits AKT activity and then A-172 proliferation. Fukuzaki et al. [49] found that the MIL at 532 nm can promote GSI inhibited proliferation far from its PlSH. For the MIL at 660 or 780 nm on oral dysplastic cells [50], the heat shock protein 90 level increased at 12 h but completely recovered at 48 and 72 h.

For the iPBM on the normal proliferation of mouse bone marrow MSCs (D1 cells) in a PlSM [51], the rNSP is IGF-1/bone morphogenetic protein-2 (BMP-2)/ALP mediated pathway. IGF-1 can upregulate BMP-2 [52] and then ALP [53] expression. ALP is essential for proliferation [54]. Wu et al. [51] have studied LPBM on the mRNA expression of IGF-1, ALP, BMP-2, osteocalcin, runt-related transcription factor 2, and receptor-activated nuclear factor kappa B ligand/osteoprotegerin on days 3 and 5 from the first LIL irradiation on and found that LPBM increased the mRNA expression of IGF-1 on days 3 and 5 and ALP on day 5 but could not affect the mRNA expression of other proteins. The iPBM promoted the proliferation from day 5 on. They directly found the mediation of IGF-1 and BMP-2 on LPBM although they cannot found LPBM effects on BIM-2 mRNA expression on days 3 and 5.

The iPBM may be observed during the first irradiation [55] or just after the first irradiation [10] or some days after the first irradiation [46, 47, 51, 56]. In other words, the iPBM may not be observed during the first irradiation [57] or just after the first irradiation [58]. The duration may be wavelength-dependent. Szymanska et al. [59] observed the iPBM of LIL at 635 nm but not 830 nm on the normal proliferation of vascular endothelial cells in 20% FBS at day 4.

Cellular factors may promote iPBM. Mvula et al. [60] have studied the LPBM on adipose-derived stem cells (ADSCs) in a PlSM. Either epidermal growth factor (EGF) or one time LIL irradiation alone cannot affect ADSC proliferation, but their integration upgraded the normal proliferation at 48 h after the irradiation. For the iPBM on ADSCs in a PlSM [61], the rNSP is beta1-integrin mediated pathway. There is indeed an integration of IGF-1 and beta1-integrin [62].

One time irradiation may be self-limited. Bloise et al. [47] observed the iPBM of multiple doses of LIL on the normal proliferation of the Saos-2 cell line in a PlSM, but they found that the effects of single dose were self-limited.

6. Discussions

As it has been pointed out in this paper, which function of a cell may be perfectly performed depends on the microenvironment in which cells live. The dependence may be thermodynamic. A PSM allowed proliferation may be a direct proliferation through its NSP or a differentiation-mediated proliferation through its rNSP for dPBM or their synergistic integration for iPBM. For an iPBM in a PlSM, the differentiation was first promoted [51], but the normal

proliferation was finally upgraded. A DSM allowed differentiation may also be a direct differentiation through its NSP or a proliferation-mediated differentiation through its rNSP. MSCs were collected from adult human bone marrow, isolated, and precultured in complete medium and cultured in osteogenic medium in three-dimensional collagen scaffolds and simultaneously irradiated with LIL. Leonida et al. [63] found that the LIL promoted both proliferation and differentiation at day 7 but only promoted differentiation at day 14. Obviously, the proliferation at day 7 was differentiation-mediated, but the differentiation at day 14 was proliferation-mediated.

One signal transduction pathway may directly mediate normal differentiation in a DSM as an NSP in a dPBM and may also indirectly mediate enhanced normal proliferation through differentiation in a PlSM as an rNSP of the NSP of the normal proliferation in an iPBM. It was found that the promotion of LIL at 685 nm on both the osteoblast differentiation of human MSCs in osteogenic medium which included 10% FBS and 100 nM DEX in its dPBM [39] and proliferation of human gingival fibroblasts in a PlSM in 10% FBS in its iPBM [64] was mediated by bFGF/IGF-1/IGFBP3 mediated pathway. Pons and Torres-Aleman [65] found that bFGF strongly modulates IGF-1, its receptors, and its binding proteins in the two major cell types of the hypothalamus.

DEX can inhibit proliferation. It might inhibit one NSP, but one of its rNSPs can be fully activated to maintain normal proliferation. Wu et al. [66] found that LPBM can promote DEX inhibited proliferation of human periodontal ligament cells through differentiation-mediated pathway which included BMP-2 and ALP. The pathway might include IGF-1 according to Wu et al. [51] as it has been discussed in Section 5.2.

7. Conclusions

One normal function may have N possible NSPs which are redundant with one another. The first-order normal function is maintained by the full activation of each NSP in its NSM, but its enhancement, for example, the nth-order normal function ($n = 2, 3, \ldots, N$), is maintained by the synergistic full activation of the NSP and its $n - 1$ rNSPs in its NSM. A LLL may promote the activation of partially activated NSP or/and its rNSP so that a dPBM may induce the second-order functional phase transition from a dysfunctional function to the first-order normal function in a function-specific microenvironment, and an iPBM may also induce the first-order functional phase transition from the $(n - 1)$th-order normal function to the nth-order normal function in its NSM.

Conflict of Interests

The authors declare that there is no conflict of interests regarding the publication of this paper.

Authors' Contribution

T. C.-Y. Liu and D.-F. Wu contributed equally to this work.

Acknowledgments

This work was supported by National Science Foundation of China (60878061, 10974061, and 11374107), Doctoral Fund of Ministry of Education of China (20124407110013), and Guangdong Scientific Project (2012B031600004).

References

[1] E. S. Valchinov and N. E. Pallikarakis, "Design and testing of low intensity laser biostimulator," *BioMedical Engineering Online*, vol. 4, article 5, 2005.

[2] H. Chung, T. Dai, S. K. Sharma, Y. Y. Huang, J. D. Carroll, and M. R. Hamblin, "The nuts and bolts of low-level laser (light) therapy," *Annals of Biomedical Engineering*, vol. 40, no. 2, pp. 516–533, 2012.

[3] C. Y. Liu and P. Zhu, *Intranasal Low Intensity Laser Therapy*, People's Military Medical Press, Beijing, China, 2009.

[4] T. C. Y. Liu, R. Liu, L. Zhu, J. Q. Yuan, M. Wu, and S. H. Liu, "Homeostatic photobiomodulation," *Front Optoelectron China*, vol. 2, no. 1, pp. 1–8, 2009.

[5] T. C. Y. Liu, D. F. Wu, Z. Q. Gu, and M. Wu, "Applications of intranasal low intensity laser therapy in sports medicine," *Journal of Innovative Optical Health Sciences*, vol. 3, no. 1, pp. 1–16, 2010.

[6] L. Baratto, L. Calzà, R. Capra et al., "Ultra-low-level laser therapy," *Lasers in Medical Science*, vol. 26, no. 1, pp. 103–112, 2011.

[7] J. L. Hartman IV, B. Garvik, and L. Hartwell, "Principles for the buffering of genetic variation," *Science*, vol. 291, no. 5506, pp. 1001–1004, 2001.

[8] T. C. Y. Liu, Y. Y. Liu, E. X. Wei, and F. H. Li, "Photobiomodulation on stress," *International Journal of Photoenergy*, vol. 2012, Article ID 628649, 11 pages, 2012.

[9] T. C. Y. Liu, L. Zhu, and X. B. Yang, "Photobiomodulation-mediated pathway diagnostics," *Journal of Innovation in Optical Health Science*, vol. 6, no. 1, Article ID 1330001, 11 pages, 2013.

[10] T. C. Y. Liu, F. H. Li, E. X. Wei, and L. Y. Deng, "Redundant pathway mediated photobiomodulation enhancement on a myoblast proliferation in its proliferation-specific homeostasis," *Lasers in Surgery and Medicine*, vol. 45, supplement 25, p. 53, 2013.

[11] D. F. Wu, *The cross talk between proliferation and clock gene expression of serum-shocked myoblasts and its mechanism [Ph.D. thesis]*, South China Normal University, 2014.

[12] L. Y. Deng, *Self-limited recovery of high glucose induced stress of mouse mesenchymal stem cells and its photobiomodulation [M.S. thesis]*, South China Normal University, 2013.

[13] R. Straussman, T. Morikawa, K. Shee et al., "Tumour micro-environment elicits innate resistance to RAF inhibitors through HGF secretion," *Nature*, vol. 487, no. 7408, pp. 500–504, 2012.

[14] B. Haibe-Kains, N. El-Hachem, N. J. Birkbak et al., "Inconsistency in large pharmacogenomic studies," *Nature*, vol. 504, no. 7480, pp. 389–393, 2013.

[15] M. Wu and T. C. Y. Liu, "Single-cell analysis of protein kinase C activation during anti-apoptosis and apoptosis induced by laser irradiation," *Photomedicine and Laser Surgery*, vol. 25, no. 2, pp. 129–130, 2007.

[16] M. A. Pogrel, J. W. Chen, and K. Zhang, "Effects of low-energy gallium-aluminum-arsenide laser irradiation on cultured fibroblasts and keratinocytes," *Lasers in Surgery and Medicine*, vol. 20, no. 4, pp. 426–432, 1997.

[17] H. Miyata, T. Genma, M. Ohshima et al., "Mitogen-activated protein kinase/extracellular signal-regulated protein kinase activation of cultured human dental pulp cells by low-power gallium-aluminium-arsenic laser irradiation," *International Endodontic Journal*, vol. 39, no. 3, pp. 238–244, 2006.

[18] F. D. P. Eduardo, D. F. Bueno, P. M. de Freitas et al., "Stem cell proliferation under low intensity laser irradiation: A Preliminary Study," *Lasers in Surgery and Medicine*, vol. 40, no. 6, pp. 433–438, 2008.

[19] R. Duan, L. Zhu, T. C. Y. Liu et al., "Light emitting diode irradiation protect against the amyloid beta 25–35 induced apoptosis of PC12 cell *in vitro*," *Lasers in Surgery and Medicine*, vol. 33, no. 3, pp. 199–203, 2003.

[20] L. Zhu, X. Y. Li, T. C. Y. Liu, and S. H. Liu, "Protective effects of red light on differentiated PC12 cells against hydrogen peroxide induced oxidative stress," *Lasers in Surgery and Medicine*, vol. 41, supplement 21, p. 60, 2009.

[21] P. C. Davies, L. Demetrius, and J. A. Tuszynski, "Cancer as a dynamical phase transition," *Theoretical Biology and Medical Modelling*, vol. 8, article 30, 2011.

[22] E. D. Levy, C. R. Landry, and S. W. Michnick, "Cell signaling: signaling through cooperation," *Science*, vol. 328, no. 5981, pp. 983–984, 2010.

[23] D. Chrysis, A. Chagin, and L. Sävendahl, "Insulin-like growth factor-1 restores dexamethasone-induced heart growth arrest in rats: the role of the ubiquitin pathway," *Hormones*, vol. 10, no. 1, pp. 46–56, 2011.

[24] F. Giorgino and R. J. Smith, "Dexamethasone enhances insulin-like growth factor-I effects on skeletal muscle cell proliferation. Role of specific intracellular signaling pathways," *Journal of Clinical Investigation*, vol. 96, no. 3, pp. 1473–1483, 1995.

[25] Y. Uchijima, A. Takenaka, S. Takahashi, and T. Noguchi, "Dexamethasone stabilizes IGFBP-1 mRNA in primary cultures of rat hepatocytes," *Endocrine Journal*, vol. 46, no. 3, pp. 471–476, 1999.

[26] M. A. Nowak, M. C. Boerlijst, J. Cooke, and J. M. Smith, "Evolution of genetic redundancy," *Nature*, vol. 388, no. 6638, pp. 167–171, 1997.

[27] D. A. Linseman, R. A. Phelps, R. J. Bouchard et al., "Insulin-like growth factor-I blocks Bcl-2 interacting mediator of cell death (Bim) induction and intrinsic death signaling in cerebellar granule neurons," *Journal of Neuroscience*, vol. 22, no. 21, pp. 9287–9297, 2002.

[28] E. de Bruyne, T. J. Bos, F. Schuit et al., "IGF-1 suppresses Bim expression in multiple myeloma via epigenetic and posttranslational mechanisms," *Blood*, vol. 115, no. 12, pp. 2430–2440, 2010.

[29] N. Lane, "Cell biology: power games," *Nature*, vol. 443, no. 7114, pp. 901–903, 2006.

[30] M. Hüttemann, I. Lee, L. I. Grossman, J. W. Doan, and T. H. Sanderson, "Phosphorylation of mammalian cytochrome *c* and cytochrome *c* oxidase in the regulation of cell destiny: respiration, apoptosis, and human disease," *Advances in Experimental Medicine and Biology*, vol. 748, pp. 237–264, 2012.

[31] T. I. Karu and N. I. Afanas'eva, "Cytochrome *c* oxidase as the primary photoacceptor upon laser exposure of cultured cells to visible and near IR-range light," *Doklady Akademii Nauk*, vol. 342, no. 5, pp. 693–695, 1995.

[32] T. Karu, *The Science of Low-Power Laser Therapy*, Gordon and Breach Science Publishers, Amsterdam, The Netherlands, 1998.

[33] S. Song, F. Zhou, and W. R. Chen, "Low-level laser therapy regulates microglial function through Src-mediated signaling pathways: implications for neurodegenerative diseases," *Journal of Neuroinflammation*, vol. 9, article 219, 2012.

[34] Y. Y. Huang, K. Nagata, C. E. Tedford, and M. R. Hamblin, "Low-level laser therapy (810 nm) protects primary cortical neurons against excitotoxicity *in vitro*," *Journal of Biophotonics*, 2014.

[35] L. A. Montoro, A. P. Turrioni, F. G. Basso, C. A. de Souza Costa, and J. Hebling, "Infrared LED irradiation photobiomodulation of oxidative stress in human dental pulp cells," *International Endodontic Journal*, 2014.

[36] S. Wu, F. Zhou, Y. Wei, W. R. Chen, Q. Chen, and D. Xing, "Cancer phototherapy via selective photoinactivation of respiratory chain oxidase to trigger a fatal superoxide anion burst," *Antioxidants & Redox Signaling*, 2014.

[37] K. Horvát-Karajz, Z. Balogh, V. Kovács, A. H. Drrernat, L. Sréter, and F. Uher, "*In vitro* effect of carboplatin, cytarabine, paclitaxel, vincristine, and low-power laser irradiation on murine mesenchymal stem cells," *Lasers in Surgery and Medicine*, vol. 41, no. 6, pp. 463–469, 2009.

[38] Y. Y. Xu, T. C. Y. Liu, and L. Cheng, "Photobiomodulation process," *International Journal of Photoenergy*, vol. 2012, Article ID 374861, 7 pages, 2012.

[39] I. Saygun, N. Nizam, A. U. Ural, M. A. Serdar, F. Avcu, and T. F. Tözüm, "Low-level laser irradiation affects the release of basic fibroblast growth factor (bFGF), insulin-like growth factor-I (IGF-I), and receptor of IGF-I (IGFBP3) from osteoblasts," *Photomedicine and Laser Surgery*, vol. 30, no. 3, pp. 149–154, 2012.

[40] C. Meng, Z. He, and D. Xing, "Low-level laser therapy rescues dendrite atrophy via upregulating BDNF expression: implications for Alzheimer's disease," *Journal of Neuroscience*, vol. 33, no. 33, pp. 13505–13517, 2013.

[41] S. T. Nam, D. H. Kim, M. B. Lee et al., "Insect peptide CopA3-induced protein degradation of p27Kip1 stimulates proliferation and protects neuronal cells from apoptosis," *Biochemical and Biophysical Research Communications*, vol. 437, no. 1, pp. 35–40, 2013.

[42] B. Y. Chen, X. Wang, Z. Y. Wang, Y. Z. Wang, L. W. Chen, and Z. J. Luo, "Brain-derived neurotrophic factor stimulates proliferation and differentiation of neural stem cells, possibly by triggering the Wnt/β-catenin signaling pathway," *Journal of Neuroscience Research*, vol. 91, no. 1, pp. 30–41, 2013.

[43] Y. Y. Huang, K. Nagata, C. E. Tedford, T. McCarthy, and M. R. Hamblin, "Low-level laser therapy (LLLT) reduces oxidative stress in primary cortical neurons *in vitro*," *Journal of Biophotonics*, vol. 6, no. 10, pp. 829–838, 2013.

[44] M. Esmaeelinejad and M. Bayat, "Effect of low-level laser therapy on the release of interleukin-6 and basic fibroblast growth factor from cultured human skin fibroblasts in normal and high glucose mediums," *Journal of Cosmetic and Laser Therapy*, vol. 15, no. 6, pp. 310–317, 2013.

[45] S. H. Jee, C. Y. Chu, H. C. Chiu et al., "Interleukin-6 induced basic fibroblast growth factor-dependent angiogenesis in basal cell carcinoma cell line via JAK/STAT3 and PI3-kinase/Akt pathways," *Journal of Investigative Dermatology*, vol. 123, no. 6, pp. 1169–1175, 2004.

[46] N. Komine, K. Ikeda, K. Tada, N. Hashimoto, N. Sugimoto, and K. Tomita, "Activation of the extracellular signal-regulated kinase signal pathway by light emitting diode irradiation," *Lasers in Medical Science*, vol. 25, no. 4, pp. 531–537, 2010.

[47] N. Bloise, G. Ceccarelli, P. Minzioni et al., "Investigation of low-level laser therapy potentiality on proliferation and differentiation of human osteoblast-like cells in the absence/presence of

osteogenic factors," *Journal of Biomedical Optics*, vol. 18, no. 12, Article ID 128006, 2013.

[48] E. Saino, V. Maliardi, E. Quartarone et al., "*In vitro* enhancement of SAOS-2 cell calcified matrix deposition onto radio frequency magnetron sputtered bioglass-coated titanium scaffolds," *Tissue Engineering A*, vol. 16, no. 3, pp. 995–1008, 2010.

[49] Y. Fukuzaki, H. Sugawara, B. Yamanoha, and S. Kogure, "532 nm low-power laser irradiation recovers γ-secretase inhibitor-mediated cell growth suppression and promotes cell proliferation via Akt signaling," *PLoS ONE*, vol. 8, no. 8, Article ID e70737, 2013.

[50] F. F. Sperandio, F. S. Giudice, L. Corrêa, D. S. Pinto Jr., M. R. Hamblin, and S. C. de Sousa, "Low-level laser therapy can produce increased aggressiveness of dysplastic and oral cancer cell lines by modulation of Akt/mTOR signaling pathway," *Journal of Biophotonics*, vol. 6, no. 10, pp. 839–847, 2013.

[51] J. Y. Wu, Y. H. Wang, G. J. Wang et al., "Low-power GaAlAs laser irradiation promotes the proliferation and osteogenic differentiation of stem cells via IGF1 and BMP2," *PLoS ONE*, vol. 7, no. 9, Article ID e44027, 2012.

[52] G. J. Xu, S. Cai, and J. B. Wu, "Effect of insulin-like growth factor-1 on bone morphogenetic protein-2 expression in hepatic carcinoma SMMC7721 cells through the p38 MAPK signaling pathway," *Asian Pacific Journal of Cancer Prevention*, vol. 13, no. 4, pp. 1183–1186, 2012.

[53] Y. J. Kim, M. H. Lee, J. M. Wozney, J. Y. Cho, and H. M. Ryoo, "Bone morphogenetic protein-2-induced alkaline phosphatase expression is stimulated by Dlx5 and repressed by Msx2," *Journal of Biological Chemistry*, vol. 279, no. 49, pp. 50773–50780, 2004.

[54] V. Kermer, M. Ritter, B. Albuquerque, C. Leib, M. Stanke, and H. Zimmermann, "Knockdown of tissue nonspecific alkaline phosphatase impairs neural stem cell proliferation and differentiation," *Neuroscience Letters*, vol. 485, no. 3, pp. 208–211, 2010.

[55] T. Kantermann, S. Forstner, M. Halle, L. Schlangen, T. Roenneberg, and A. Schmidt-Trucksäss, "The stimulating effect of bright light on physical performance depends on internal time," *PLoS ONE*, vol. 7, no. 7, Article ID e40655, 2012.

[56] W. P. Hu, J. J. Wang, C. L. Yu, C. C. E. Lan, G. S. Chen, and H. S. Yu, "Helium-neon laser irradiation stimulates cell proliferation through photostimulatory effects in mitochondria," *Journal of Investigative Dermatology*, vol. 127, no. 8, pp. 2048–2057, 2007.

[57] P. M. O'Brien and P. J. O'Connor, "Effect of bright light on cycling performance," *Medicine and Science in Sports and Exercise*, vol. 32, no. 2, pp. 439–447, 2000.

[58] S. Incerti Parenti, S. Panseri, A. Gracco, M. Sandri, A. Tampieri, and G. A. Bonetti, "Effect of low-level laser irradiation on osteoblast-like cells cultured on porous hydroxyapatite scaffolds," *Annali dell'Istituto Superiore di Sanità*, vol. 49, no. 3, pp. 255–260, 2013.

[59] J. Szymanska, K. Goralczyk, J. J. Klawe et al., "Phototherapy with low-level laser influences the proliferation of endothelial cells and vascular endothelial growth factor and transforming growth factor-beta secretion," *Journal of Physiology and Pharmacology*, vol. 64, no. 3, pp. 387–391, 2013.

[60] B. Mvula, T. J. Moore, and H. Abrahamse, "Effect of low-level laser irradiation and epidermal growth factor on adult human adipose-derived stem cells," *Lasers in Medical Science*, vol. 25, no. 1, pp. 33–39, 2010.

[61] B. Mvula, T. Mathope, T. Moore, and H. Abrahamse, "The effect of low level laser irradiation on adult human adipose derived stem cells," *Lasers in Medical Science*, vol. 23, no. 3, pp. 277–282, 2008.

[62] Y. Suzuki, M. Yanagisawa, H. Yagi, Y. Nakatani, and R. K. Yu, "Involvement of β1-integrin up-regulation in basic fibroblast growth factor- and epidermal growth factor-induced proliferation of mouse neuroepithelial cells," *Journal of Biological Chemistry*, vol. 285, no. 24, pp. 18443–18451, 2010.

[63] A. Leonida, A. Paiusco, G. Rossi, F. Carini, M. Baldoni, and G. Caccianiga, "Effects of low-level laser irradiation on proliferation and osteoblastic differentiation of human mesenchymal stem cells seeded on a three-dimensional biomatrix: *in vitro* pilot study," *Lasers in Medical Science*, vol. 28, no. 1, pp. 125–132, 2013.

[64] I. Saygun, S. Karacay, M. Serdar, A. U. Ural, M. Sencimen, and B. Kurtis, "Effects of laser irradiation on the release of basic fibroblast growth factor (bFGF), insulin like growth factor-1 (IGF-1), and receptor of IGF-1 (IGFBP3) from gingival fibroblasts," *Lasers in Medical Science*, vol. 23, no. 2, pp. 211–215, 2008.

[65] S. Pons and I. Torres-Aleman, "Basic fibroblast growth factor modulates insulin-like growth factor-I, its receptor, and its binding proteins in hypothalamic cell cultures," *Endocrinology*, vol. 131, no. 5, pp. 2271–2278, 1992.

[66] J. Y. Wu, C. H. Chen, L. Y. Yeh, M. L. Yeh, C. C. Ting, and Y. H. Wang, "Low-power laser irradiation promotes the proliferation and osteogenic differentiation of human periodontal ligament cells via cyclic adenosine monophosphate," *International Journal of Oral Science*, vol. 5, no. 2, pp. 85–91, 2013.